Spectroscopic and Kinetic Investigation of Two Unusual Structural Features Found in Eukaryotic Cysteine Dioxygenase

by

Erin M. Imsand

A dissertation submitted to the Graduate Faculty of
Auburn University
in partial fulfillment of the
requirements for the Degree of
Doctor of Philosophy

Auburn, Alabama
May 14, 2010

Approved by

Holly R. Ellis, Chair, Professor of Chemistry and Biochemistry
Mark E. Byrne, Associate Professor of Chemical Engineering
Douglas C. Goodwin, Associate Professor of Chemistry and Biochemistry
David M. Stanbury, Professor of Chemistry and Biochemistry
Susanne Striegler, Associate Professor of Chemistry and Biochemistry
Russell B. Muntifering, Professor of Animal Sciences

Abstract

Cysteine dioxygenase (CDO) is a mononuclear ferrous enzyme located at a branch-point in cysteine metabolism and catalyzes the oxidation of L-cysteine using both atoms of dioxygen. Although several studies have attempted to characterize the enzyme kinetically, efforts have been thwarted by the apparent inactivation of the purified protein. Publication of the three-dimensional structure of several mammalian CDO enzymes revealed two unusual structural attributes that had previously not been identified in other mononuclear ferrous-dependent enzymes. The metal center of CDO is bound by a facial triad composed entirely of histidine residues in contrast to the previously ubiquitous 2-His/1-carboxylate facial triad found in other ferrous-dependent enzymes. Interestingly, a covalent linkage between Cys93 and Tyr157 was found near the metal center in the active site. The purpose of these studies is to probe the cause of inactivation of purified CDO and to determine how the 3-His facial triad and Cys-Tyr crosslink affect the catalytic properties of the enzyme.

Other ferrous-dependent enzymes stabilize the active oxidation state of their metal centers using a variety of strategies. To determine if inactivation of CDO occurring during purification is the result of an inability of the enzyme to protect its metal center from oxidation, EPR spectra and activity measurements were made of CDO expressed in

cell lysate and following purification. The spectrum of CDO expressed in cell lysate was consistent with Fe(II) and the lysate displayed considerable catalytic activity for cysteine oxidation. Following purification, the EPR spectrum of CDO indicated that greater than 99% of the iron center had been oxidized to the inactive Fe(III) form. Consistent with the oxidation, purified CDO displayed no activity beyond the background oxidation of L-cysteine. Activity was recoverable by the addition of L-ascorbate to assays and this corresponded to reduction of the metal center as observed by EPR. Necessity of including an external reductant for the metal center was extended to substrate binding studies using nitric oxide as a spectrally active analog of dioxygen. Purified CDO in the resting state was capable of binding L-cysteine but incapable of binding nitric oxide; however, when preincubated with an external reductant, the metal center was reactive to both substrates.

Typical purifications of CDO yield a mixture of crosslinked and non-crosslinked isoforms of the enzyme. Previous studies have shown that a single isoform is responsible for all observable activity. To determine which isoform represented the physiologically active enzyme, a two-fold approach was taken. Site-directed mutagenesis was used to replace Cys93 and Tyr157 with serine and phenylalanine, respectively, in order to study CDO in the absence of the thioether linkage. Both variant CDO enzymes were capable of binding substrates and retained catalytic efficiencies comparable to the wild-type enzyme, suggesting that the crosslink was not necessary for catalysis. To study CDO containing the thioether linkage, a method was developed to isolate the enzyme in the homogenously crosslinked isoform. The resulting homogenously crosslinked enzyme

was capable of binding both substrates but was catalytically inactive. This confirms the previous observation that only one isoform of CDO is catalytically active and demonstrates that the active isoform is non-crosslinked CDO. EPR spectroscopy was used to show that the metal center of homogenously crosslinked CDO has an altered metal coordination environment compared to wild-type, C93S, or Y157F CDO proteins, and this results in release of the metal center from the active site. The activity of CDO *in vivo* has been shown to be tightly regulated. The combined sensitivity of CDO to inactivation by oxidation of the metal center and crosslink formation may be linked physiologically and represent a redox sensitive regulation of CDO activity.

Acknowledgments

I would first like to thank my advisor, Dr. Holly R. Ellis, for mentoring me during my time at Auburn. She has truly helped me, not only with understanding experimental set-up, but to be able to think analytically about data as it relates to physiological relevance by selflessly volunteering her time to many lengthy discussions. I would also like to thank my committee members, Dr. Byrne, Dr. Goodwin, Dr. Stanbury, and Dr. Striegler, and my outside reader Dr. Muntifering, for helping me throughout my graduate career. Dr. Byrne has been an advisor to me since before I began the Ph.D. program and has always been supportive by taking the time to talk with me and offering critical career advice. Dr. Goodwin has been helped me to grow as a biochemist by giving me insight into enzymology both in the classroom and in seminars. Dr. Stanbury has always offered helpful advice and taken the time to bring particularly interesting and relevant papers to my attention. Dr. Striegler also has been instrumental in strengthening my understanding of chemical principles and has been extremely helpful when I have needed unexpected supplies or favors. Dr. Muntifering has been exceptionally helpful as my outside on short notice and is filled with interesting facts about the physiological relevance of my research topic. Additionally, I would like to thank Dr. Evert Duin for the use of his anaerobic tent and for assisting me in obtaining and understanding EPR spectra and Dr. Paul Cobine for the use of his ICP-AES. I would like to thank my friends and family, including present

and former lab members, for their unconditional support and love and for providing a stable shoulder for me during trying times in both research and personal life.

Table of Contents

List of Tables

List of Schemes

List of Figures

Chapter One

Literature Review

A primary focus of biochemical research is to elucidate how the chemical structure of an enzyme dictates its functional role in biology. Cysteine dioxygenase is a metalloprotein located at the intersection of several newly emerging trends in the research of structure-function relationships. Proper cysteine flux in eukaryotic systems has been shown to be paramount in the maintenance of crucial cellular functions including protein synthesis, respiration, defense against oxidative stress, immune responses, and ionic potential equilibrium (*1*-*3*). Over forty years ago it was discovered that the enzyme responsible for the majority of the regulation of cellular cysteine concentrations (cysteine dioxygenase or CDO) contained a mononuclear iron center (*4*). Mononuclear non-heme ferrous enzymes have gained momentum as a research focus in the last twenty years. Regardless of the reactions catalyzed by these enzymes, most known examples bind their iron centers using a facial triad composed of two histidine ligands and one carboxylate-donating ligand (*5*). Recent publication of the three-dimensional structure of CDO showed that the enzyme not only deviated from the previously conserved metal binding motif, but contained a covalent linkage between two non-adjacent amino acids in the primary sequence (*6*-*8*). With the exception of CDO, crosslinked amino acid structures had only been identified in enzymes that utilized a copper ion or heme cofactor. In order to understand the possible evolutionary advantage for the unique structural attributes of

CDO and how they affect its role in maintaining cellular cysteine concentrations, this chapter focuses on the characteristics of other mononuclear ferrous enzymes, the physiological relevance of cysteine metabolism, and the formation of amino acid crosslinks in enzymes.

1.1 Enzymes containing a 2-His/1-carboxylate facial triad

Although the reduction potential of molecular oxygen makes it essential for the synthesis of energetic molecules in aerobic organisms, the highly reactive species that result from activation of dioxygen are detrimental to several structural aspects in the cell. A challenge that faces all aerobic organisms is tapping into the reduction potential of molecular oxygen without compromising the integrity of the enzymes that accomplish the activation. Evolution has yielded enzymes that utilize a variety of cofactors such as copper, iron, and organic molecules like flavins that donate either one or two electrons to dioxygen. Many enzymes that utilize iron specifically use ferrous iron and incorporate the metal into either heme or iron-sulfur clusters. Several enzymes that utilize ferrous iron as a cofactor coordinate the metal center using only protein-derived ligands. Among these enzymes, a nearly conserved iron coordination has emerged consisting of two histidine residues and either a glutamate or aspartate residue (*5*). These residues are arranged in a facial triad and provide one face of an octahedron. The remaining three coordination sites are occupied by solvent molecules in the resting-state enzyme. This coordination motif is shown in Figure 1.1.1. The electronic environment of the 2-His/1-carboxylate facial triad in many proteins has been characterized by a combination of

Mossbauer, EPR, and magnetic circular dichroism spectroscopies. The combined results from these studies show several characteristics shared among this class of enzymes. In the reduced state, the metal center is EPR silent with S = 2. When oxidized to the Fe(III) form, these enzymes display characteristic S = 5/2 EPR signals at g = 4.3. These signals are also consistent for non-heme ferric iron enzymes that do not utilize a 2-His/1-carboxylate facial triad for metal coordination (*9-11)*.

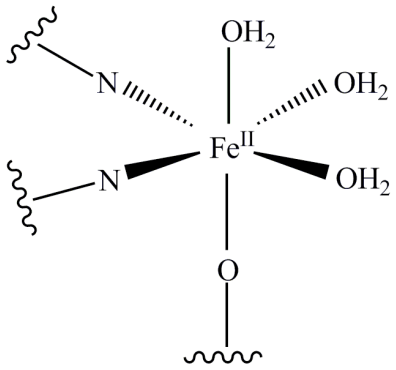

Figure 1.1.1 The 2-His/1-carboxylate metal-binding motif found in several ferrous-dependent oxygenases (*5*).

1.1.1 Metabolic functions of 2-His/1-carboxylate containing enzymes

Among the known 2-His/1-carboxylate oxygen-activating enzymes, several major classes have emerged, particularly the extradiol dioxygenases, the Rieske dioxygenases, the α-ketoglutarate-dependent oxidases, and the pterin-dependent hydroxylases. Additionally, there are several other enzymes that do no fit into any of these particular classes but also activate dioxygen using ferrous iron. The 2-His/1-carboxylate containing enzymes catalyze a wide variety of reactions that serve diverse metabolic and regulatory functions.

Much of the carbon derived from plant-life is in the form of unreactive aromatic compounds. Extradiol and intradiol dioxygenases are responsible for freeing up this available carbon in the soil by breaking the aromatic ring and incorporating an atom of oxygen to each resulting accessible carbon atom (Scheme 1.1.1) (*5*). The intradiol dioxygenases rely on the presence of Fe(III) in their active sites, while the extradiol dioxygenases rely on Fe(II) for activity (*5,12,13*). Unlike the intradiol dioxygenases, the ferrous iron of the extradiol dioxygenases has limited spectroscopic properties and so mechanistic knowledge of this family has lagged behind that of other metalloenzymes. Many of the techniques developed to study the extradiol dioxygenases (specifically 2,3-dihydroxybiphenyl 1,2-dioxygenase and homoprotocatechuate 2,3-dioxygenase) have been instrumental in understanding the catalytic mechanism of other 2-His/1-carboxylate-containing enzymes.

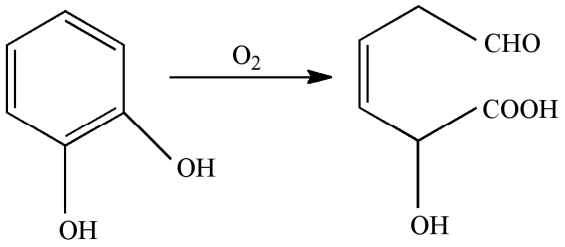

Scheme 1.1.1 The overall reaction catalyzed by the family of extradiol dioxygenases (*5*).

In contrast to the intradiol and extradiol dioxygenases, the Rieske dioxygenases catalyze the preliminary step in the breakdown of aromatic compounds and are responsible for forming the catecholic compounds that later become substrates for the intradiol and extradiol dioxygenases. This is accomplished by adding both atoms of dioxygen to unactivated carbons in an intact aromatic ring (Scheme 1.1.2). The Rieske dioxygenases are structurally similar to the extradiol dioxygenases because they coordinate their ferrous metal center using the 2-His/1-carboxylate facial triad. These two families of enzymes differ structurally because the Rieske dioxygenases contain a Rieske-type [2Fe-2S] cluster approximately 12 Å from the active site iron that acts as an electron supply during catalytic turnover (*5,12,13*).

Two other enzymes that use 2-His/1-carboxylate facial triads to coordinate a ferrous metal center that do not belong to a larger class have been characterized and provide insight into the structure and mechanism of these oxygenases. These enzymes differ from those in other classes because they accomplish full reduction of dioxygen into two water molecules. These two enzymes are 1-aminocyclopropane-1-carboxylate

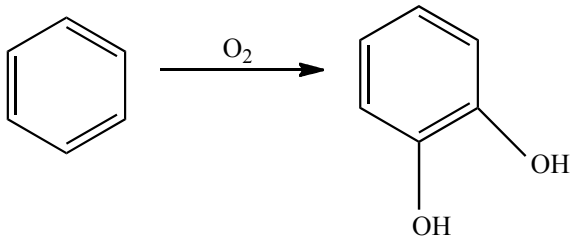

Scheme 1.1.2 The overall reaction catalyzed by the Rieske family of dioxygenases (*13*).

oxidase (ACCO) and isopenicillin N-synthase (IPNS). ACCO catalyzes the formation of the plant hormone ethylene using the co-substrate L-ascorbate (Scheme 1.1.3) (*13-15*). During catalysis, ascorbate (Figure 1.1.2) is converted to dehydroascorbate (Figure 1.1.3). IPNS catalyzes the second step in the biosynthesis of penicillin and cephalosporin antibiotics by forming two closed rings in the substrate δ-(L-α-aminoadipoyl)-L-cysteinyl-D-valine (ACV) (Scheme 1.1.4). Although IPNS coordinates its metal center using a 2-His/1-carboxylate facial triad, it also uses a transient protein-derived glutamine ligand that binds and releases the metal center through the catalytic cycle (*63*).

Several 2-His/1-carboxylate containing enzymes rely on the presence of α-ketoglutarate as a co-substrate for activity. This class of ferrous-dependent oxygen-activating enzymes has been identified in bacterial, plant, and animal systems. They catalyze a wide variety of reactions serving diverse metabolic functions. Some bacterial examples include taurine dioxygenase that functions to release sulfur from taurine under sulfur-starvation conditions, clavaminate synthase that functions to synthesize inhibitors for β-lactamase, and AlkB that is involved in the repair of single-stranded RNA and

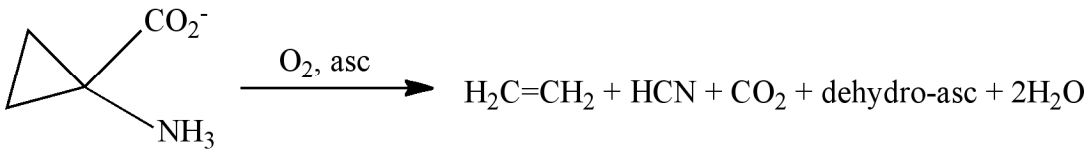

Scheme 1.1.3 The overall reaction catalyzed by the enzyme 1-aminocyclopropane-1-carboxylate oxidase. Asc denotes the co-substrate L-ascorbate (*15*).

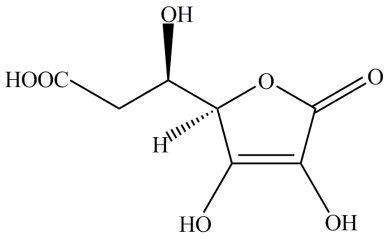

Figure 1.1.2 The chemical structure of L-ascorbate.

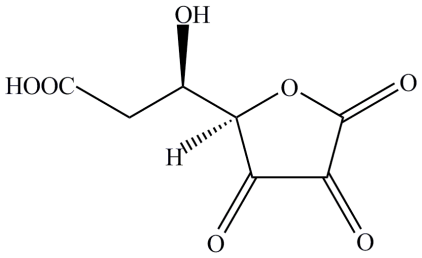

Figure 1.1.3 The chemical structure of L-dehydroascobate.

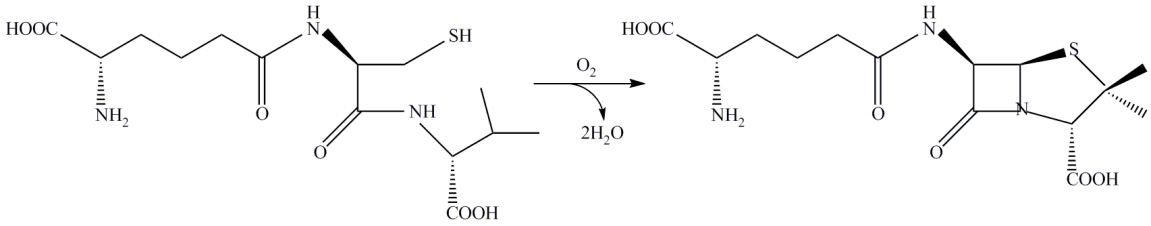

Scheme 1.1.4 The overall reaction catalyzed by the enzyme isopenicillin N-synthase (*16*).

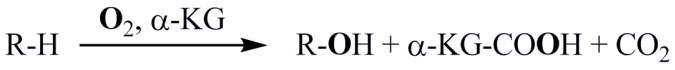

Scheme 1.1.5 Overall reaction catalyzed by the α-ketoglutarate-dependent family of oxygenases. The oxygen atoms in bold print derive from dioxygen (*12*).

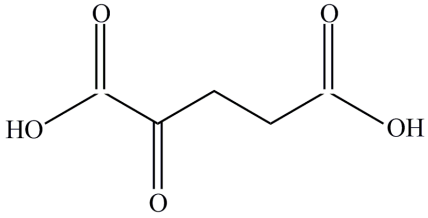

Figure 1.1.4 The chemical structure of α-ketoglutarate.

DNA (*5,9*). This class of enzymes couples decarboxylation of a 2-oxo-acid (usually α-ketoglutarate shown in Figure 1.1.4) with dioxygen activation, incorporating one atom from dioxygen into the product molecule and the other into the decarboxylated α-keto acid (Scheme 1.1.5).

In mammalian systems, some neurotransmitters and amino acids are synthesized by hydroxylases containing non-heme ferrous iron. Phenylalanine hydroxylase catalyzes the biosynthesis of tyrosine. Tyrosine hydroxylase catalyzes the biosynthesis of 3,4-dihydroxylphenylalanine (DOPA), which is the precursor for all catecholamine neurotransmitters. Tryptophan hydroxylases catalyzes the formation of 5-hydroxytryptophan which is the initial step in the biosynthesis of the neurotransmitter seratonin. Each enzyme is a monooxygenase and is responsible for the addition of a single hydroxyl group to an aromatic amino acid. The remaining atom of dioxygen is then reduced and released as water (Scheme 1.1.6). Although these enzymes contain 2-His/1-carboxylate facial triads, they differ from the extradiol dioxygenases and Rieske dioxygenases in two ways: the carboxylate-donating ligand coordinates the metal center as a bidendate leaving room for only two solvent molecules in the resting state and these enzymes also bind a tetrahydropterin co-substrate near the metal ion in the active site (Figure 1.1.5). Although tetrahydropterins are similar to flavins in both structure and catalytic function, most flavins are tightly bound in the enzyme active sites, while tetrahydropterins diffuse in and out of the active site during the catalytic cycle (*17*).

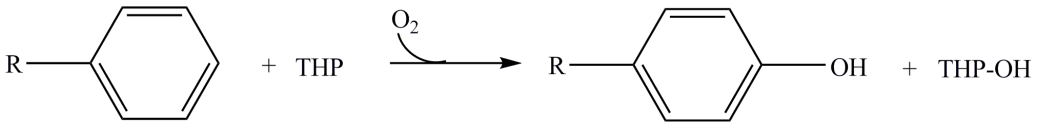

Scheme 1.1.6 The overall reaction catalyzed by the pterin-dependent family of hydroxylases (*17*).

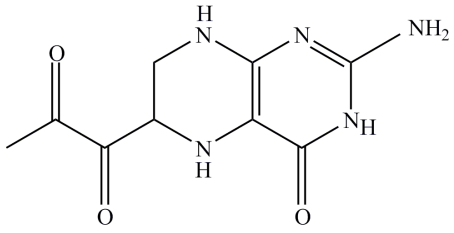

Figure 1.1.5 The chemical structure of tetrahydropterin.

1.1.2 Substrate binding in 2-His/1-carboxylate containing enzymes

In each of the classes of non-heme ferrous-dependent oxygenases, the substrate binding order has been shown to play a critical role in forming a proper metal coordination environment for oxygen activation. Typically these enzymes utilize an ordered-substrate binding mechanism and all substrates must be present before catalysis occurs. If a co-substrate is necessary for catalysis, the co-substrate binds first, followed by the non-oxygen substrate and finally dioxygen. Binding of each substrate induces a change in the coordination environment of the metal center. The trends in substrate binding exhibited by each of these classes of enzymes are detailed in Table 1.1 (*5,12,13*).

The first insight into the substrate binding order of ferrous-dependent oxygenases was provided through the use of nitric oxide as a spectrally active but catalytically inactive surrogate for dioxygen to study the extradiol dioxygenases, and consequently the most is known about substrate binding in this class of enzymes (*18*). Complexation between ferrous iron and nitric oxide results in a distinct spectral signal from dioxygen and Fe(II), and this species also results in distinct S = 3/2 electron paramagnetic resonance (EPR) spectra with *g* values occurring at 4, 4, and 2. Using nitric oxide as a dioxygen analog it was shown that the resting metal center of the extradiol dioxygenases was unreactive towards nitric oxide. Pre-complexation of the enzyme with the non-oxygen substrate increases the affinity of the metal center to nitric oxide. This indicates that this class of enzymes utilizes an ordered-binding mechanism. The three-dimensional

Table 1.1 Relathionships between substrate binding and the valence and coordination number of the metal center in several classes of 2-His/1-carboxylate containing enzymes (*5,9,10*).

		oxidation state and coordination number			
enzyme family	co-substrate	resting	+ co-substrate	+ non-oxygen	+ dioxygen
dioxygenases	none	Fe(II) or (III) 6C	—	Fe(II) 5C	Fe(II) 6C
dioxygenases	none	Fe(II) 6C	—	Fe(II) 5C	Fe(III) 6C
α-ketoglutarate-dependent oxidases	α-ketoglutarate	Fe(II) or (III) 6C	Fe(II) 5C	Fe(II) 5C	Fe(III) 6C
pterin-dependent hydroxylases	tetrahydropterin	Fe(III) 6C	Fe(II) 6C	Fe(II) 5C	Fe(II) 6C
ACCO	L-ascorbate	Fe(III) 6C	Fe(II) 6C	Fe(II) 5C	Fe(III) 6C
IPNS	none	Fe(II) 6C	—	Fe(II) 5C	Fe(III)

structures provided by X-ray crystallography with the non-oxygen substrate and nitric oxide (as a surrogate for dioxygen) indicated that the catecholic substrate coordinated the metal center in a bidentate manner (Scheme 1.1.7 complex II) and that nitric oxide bound in an end-on manner. Binding of the catechol substrate in the extradiol dioxygenases would result in increased electron density on the metal center, thus stabilizing the active ferrous state of this family of enzymes (*12,13*). Because of these earlier structures with nitric oxide, it was originally believed that dioxygen bound to the metal center of the extradiol dioxygenases in an end-on configuration as well. Recent evidence provided by the X-ray crystal structure of homoprotocatechuate 2,3-dioxygenase with dioxygen bound has shown that this substrate likely binds to the metal center in a side-on configuration (complex III) rather than the end-on configuration previously assumed (*19*).

The extradiol dioxygenases have provided insight not only into the order of substrate binding in some ferrous-dependent dioxygenases, but also into the mechanism of substrate binding. While the metal center of these enzymes is relatively spectroscopically silent, several of the extradiol dioxygenases have been studied using non-physiologically relevant alternative substrates of the non-oxygen substrate. This provides two benefits in studying the extradiol dioxygenase family of enzymes. Reaction with the physiological substrate occurs rapidly and the use of an alternative substrate depresses the reaction rate, thus stabilizing intermediates formed. Additionally, the intermediates formed have independent, unique spectroscopic properties. For example, homoprotocatechuate 2,3-dioxygenase has been studied using 4-nitrocatechol. This alternative substrate displays differing UV spectroscopic signatures depending on

ionization and polarization of the molecule within the active site. Studies with this enzyme show three unique rates involved in binding of the non-oxygen substrate. Based on the spectroscopic species formed, the proposed events involved in substrate binding are binding of the substrate in the active site of the resting enzyme (Scheme 1.1.7 complex I), coordination of the substrate to the active site metal (complex II), and then a rate-limiting rearrangement of ligands around the metal center (complex III). Evidence for the proposed rate-limiting rearrangement step is also provided by the three-dimensional crystal structure of these enzymes with the non-oxygen substrate bound. The resting state metal center is hexa-coordinate (complex II); however, the structure of the metal center coordinated by the non-oxygen substrate is penta-coordinate (complex III). This suggests that the binding event results in desolvation of the metal center and frees a metal binding site for dioxgen (*12,13,19*).

In the Rieske dioxygenases, dioxygen binds directly to the metal center and transfers electrons to the non-oxygen substrates through the active site metal (Scheme 1.1.8 complex III-IV) (*12,13*). The three-dimensional structure of naphthalene 1,2-dioxygenase with dioxygen bound shows the substrate binding in a side-on configuration, congruent to the reaction of dioxygen with the metal center of the extradiol dioxygenases (complex III) (*19*). The intermediate formed from reaction of dioxygen with the non-oxygen substrate subsequently coordinates the metal center as a bi-dentate ligand (complex V). Studies have suggested that binding of dioxygen to the mononuclear iron center is dependent on the oxidation state of the Rieske [2Fe-2S] cluster. EPR studies of naphthalene dioxygense using nitric oxide as a surrogate for dioxygen showed that the

analog could not bind to the metal center when the Rieske cluster was in the reduced state; however, the dioxygen analog could bind to the metal center when the Rieske cluster was in the oxidized state. Mossbauer studies using dioxgen suggested that the nitric oxide was not a physiologically relevant probe for dioxygen because no evidence of dioxygen coordination could be detected regardless of the oxidation state of the Rieske cluster. When the enzyme was pre-incubated with the non-oxygen substrate and the Rieske cluster was oxidized, the metal center became penta-coordinate (complex II) and both nitric oxide and dioxygen were able to bind properly (*12,13,19*).

Although the substrate for IPNS is chemically dissimilar to the catechol substrates of the extradiol dioxygenases, this enzyme has also been shown to coordinate its substrates directly to the iron center. The substrate ACV binds to the metal center of IPNS, creating a penta-coordinate environment more susceptible to reaction with dioxygen, although dioxygen can bind to the active site either prior to or after the complexation with ACV (Scheme 1.1.9 complex II). Binding of ACV differs from binding of the catecholic substrates to the extradiol dioxygenases because ACV is less electron-donating and binds as a mono-dentate ligand. Binding of ACV and O_2 displaces the protein-derived glutamine ligand that is unique to this enzyme and the metal center remains penta-coordinate (*5,12-14*). Substrate binding in ACCO occurs similarily to

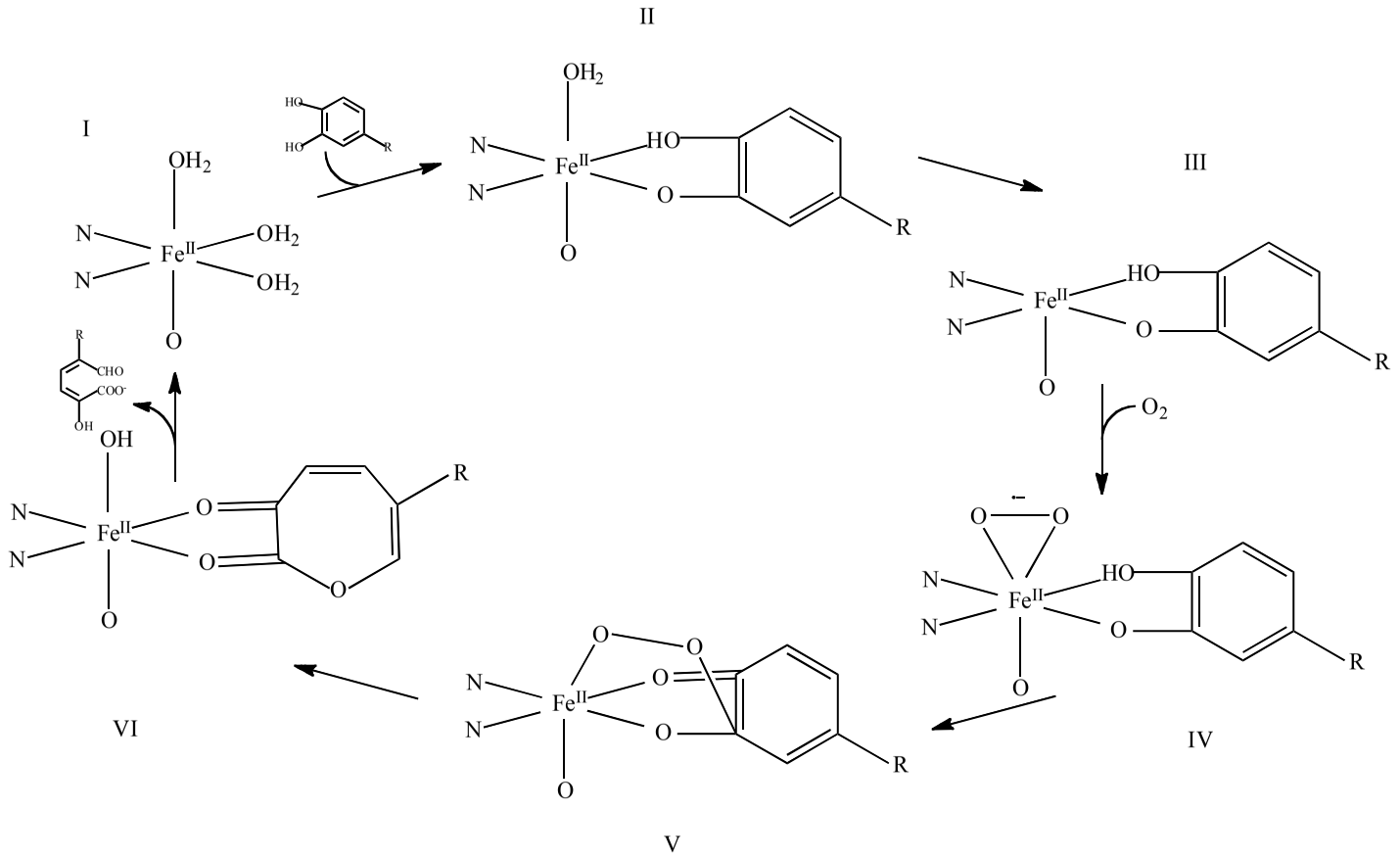

Scheme 1.1.7 The currently proposed mechanism for the family of extradiol dioxygenases (*19*).

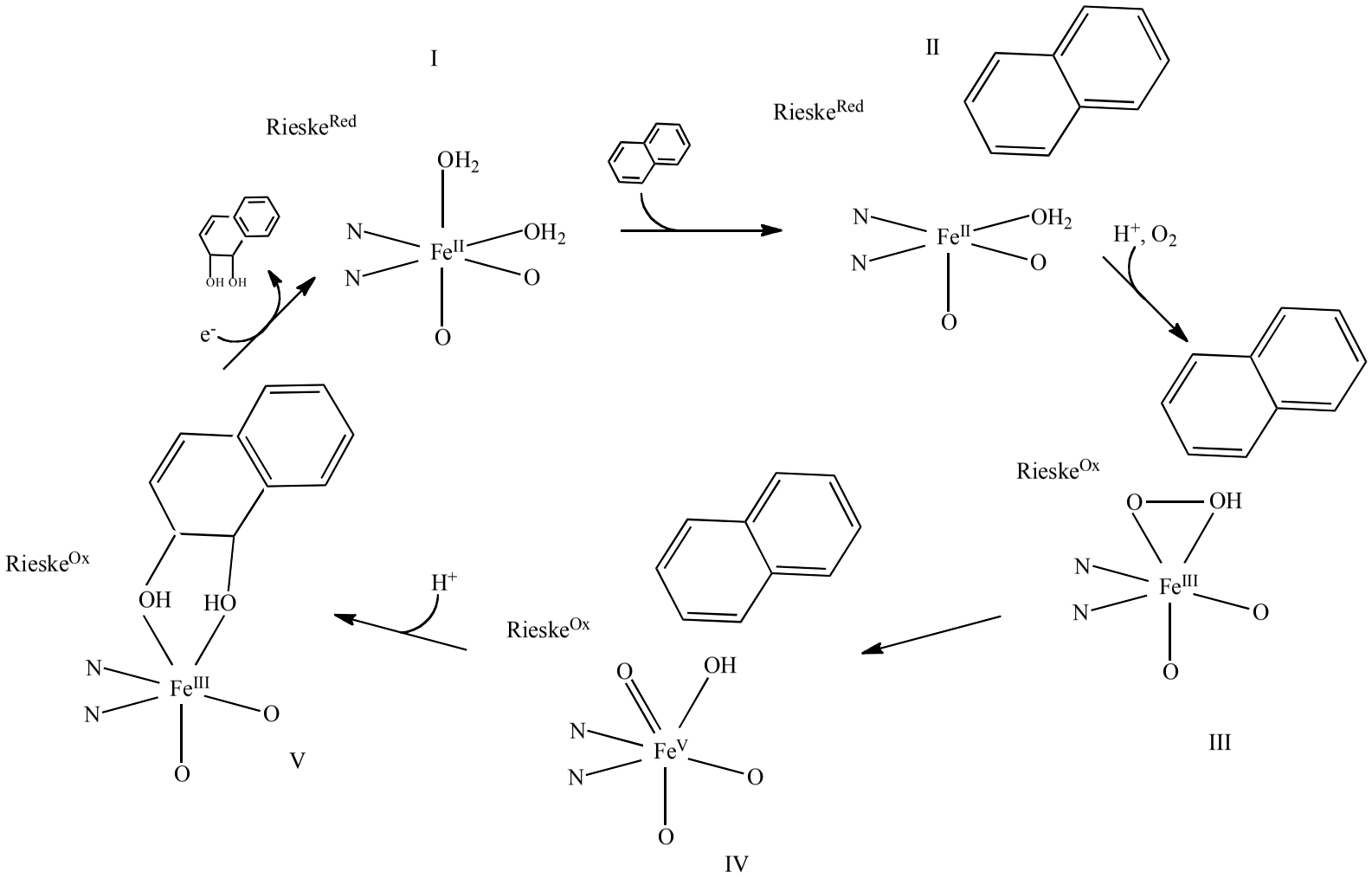

Scheme 1.1.8 The currently proposed catalytic mechanism for the Rieske family of dioxygenases (*19*).

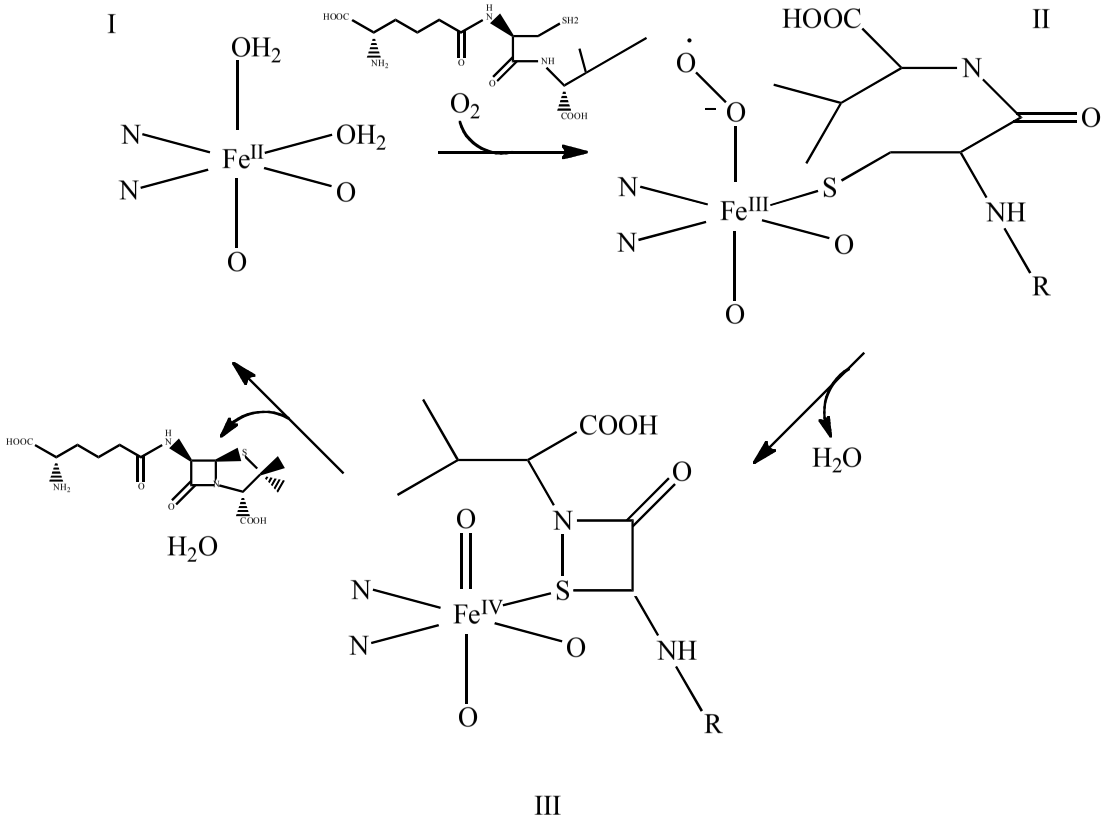

Scheme 1.1.9 The currently proposed mechanism for isopenicillin N-synthase (*19*).

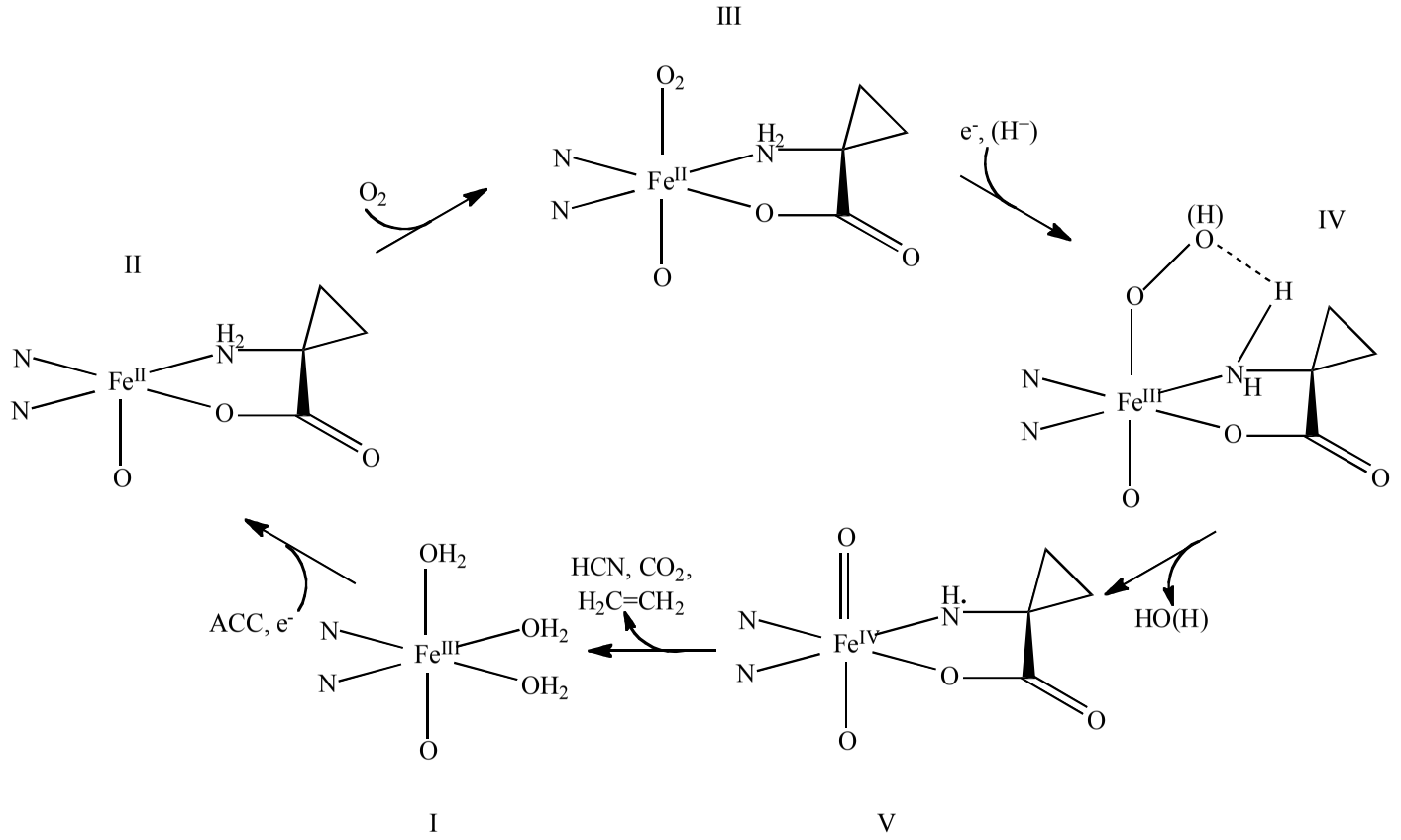

Scheme 1.1.10 The currently proposed mechanism for 1-aminocyclopropane-1-carboxylate oxidase (*14*).

IPNS. The co-substrate L-ascorbate binds first within the active site but does not coordinate the metal center. The substrate ACC binds to the metal center in a bidentate manner (Scheme 1.1.10 complex II) freeing a ligand site for dioxygen (complex III) (*13,19*).

Substrate binding in the α-ketoglutarate-dependent oxidases is unique because the non-oxygen substrate does not bind to the metal center. The α-ketoglutarate co-substrate binds first and coordinates the metal center analogous to the non-oxygen substrates in the extradiol and Rieske dioxygenases (Scheme 1.1.11 complex II). Subsequently, the non-oxygen substrate binds within the active site near the metal center (complex III). Similarly to the extradiol and Rieske dioxygenases, studies have shown that coordination of the metal center by α-ketoglutarate and binding of the non-oxygen substrate within the active site result in a penta-coordinate iron center and frees a coordination site for dioxygen (complex IV), and dioxygen binding does not occur unless both the co-substrate and non-oxygen substrate are bound within the active site (*12,13*).

Steady-state kinetic studies of phenylalanine and tyrosine hydroxylases indicate that these enzymes require the presence of all three substrates (tetrahydropterin, dioxygen, and the amino acid substrate) before any catalysis occurs. Interestingly, in contrast to the extradiol dioxygenases, Rieske dioxygenases, and IPNS, these enzymes do not coordinate their metal center with the amino acid substrate. In tyrosine and phenylalanine hydroxylases, a semi-ordered substrate-binding mechanism is used.

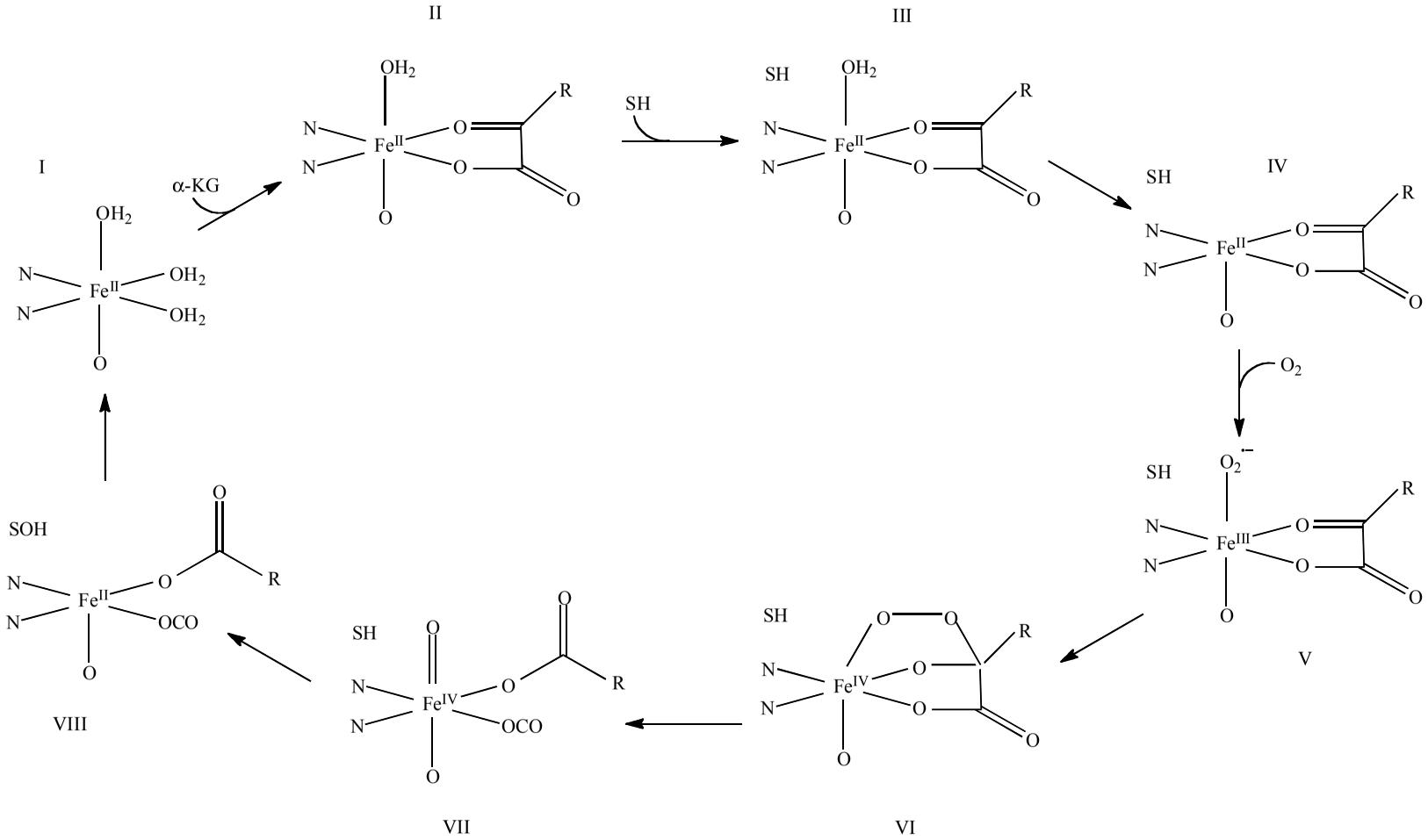

Scheme 1.1.11 The currently proposed catalytic mechanism for the α-ketoglutarate-dependent family of oxidases (*19*).

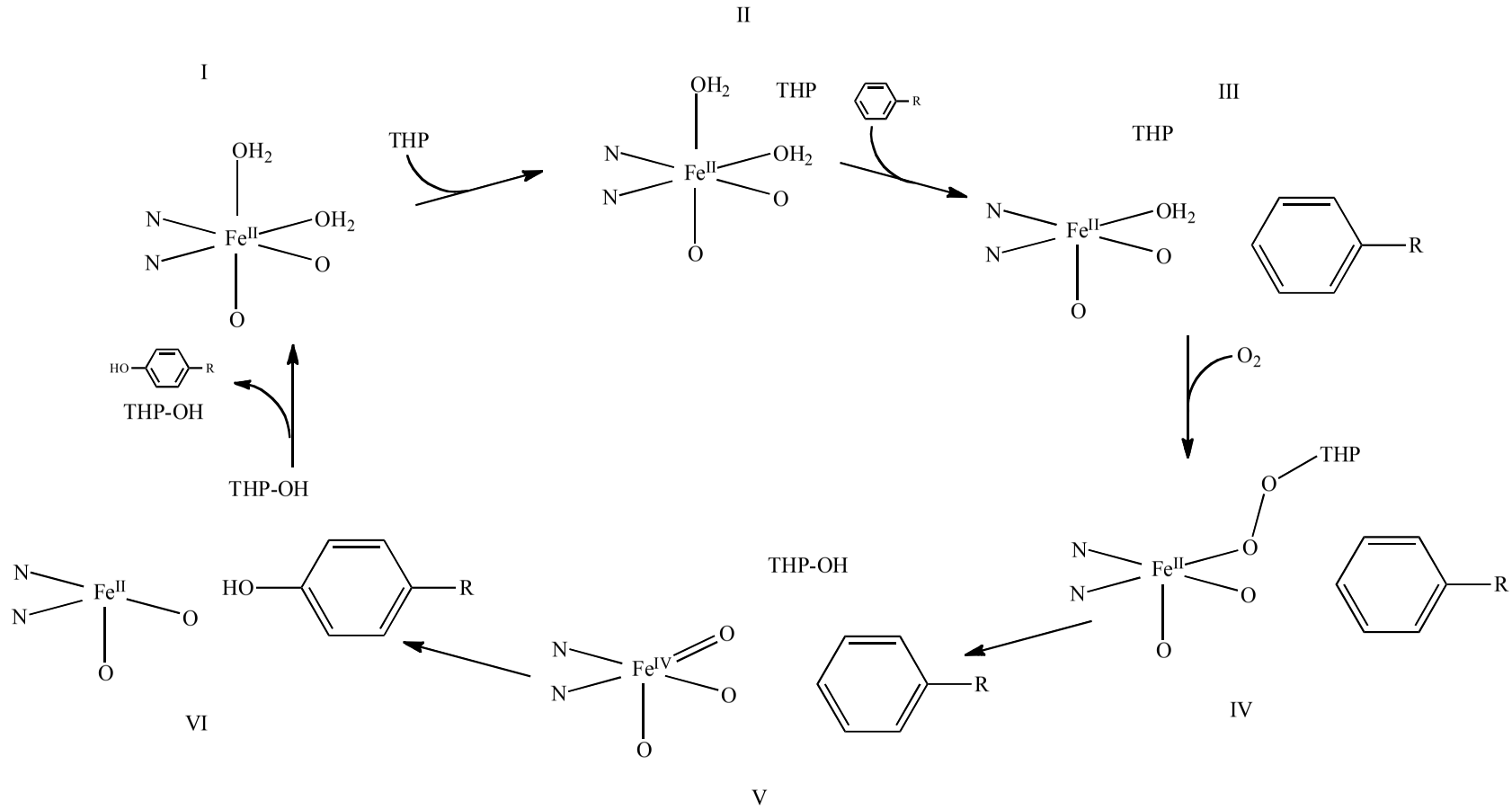

Scheme 1.1.12 The currently proposed catalytic mechanism for the pterin-dependent family of hydroxylases. THP denotes the pterin co-substrate (*19*).

Binding of the co-substrate pterin is required for coordination by dioxygen; however, the amino acid substrate can bind before or after dioxygen coordination. Some evidence has been presented that binding of the amino acid substrate within the active site increases the affinity of the enzyme for dioxygen (Scheme 1.1.12 complex III). In either case, dioxygen binds to the pterin co-substrate and then forms a bridge to the mononuclear metal center (complex IV) (*17*).

1.1.3 Oxygen activation and catalytic strategies in 2-His/1-carboxylate containing enzymes.

While proper coordination of dioxygen within the active sites of 2-His/1-carboxylate-containing enzymes has been shown to depend on binding of the non-oxygen substrates and co-substrates, the source of electrons needed to break the dioxygen double bond and the incorporation of oxygen atoms into the catalytic products vary between these classes of enzymes. In addition to the variability of the electron source and oxygen utilization, the valence state of the metal center upon reaction with dioxygen also differs from class to class. The trends in catalytic electron sources and catalytic intermediates in these classes of enzymes are detailed in Table 1.2 (*12,13,19*).

Many ferrous-dependent oxygenases rely on the use of electrons derived from the non-oxygen substrate in order to activate dioxygen. The simplest mechanism of oxygen activation is accomplished by the extradiol dioxygenases. The electronegativity of the catecholic substrates donates electron density to the metal center and stabilizes the reduced form of the iron. Electrons can then be donated to dioxygen by electronic

Table 1.2 Relathionships between the electron source for dioxygen bond cleavage and the iron-oxygen catalytic intermediate formed in several classes of 2-His/1-carboxylate containing enzymes (*12,13,19*).

class of enzyme	source of electrons for reducing O=O	iron-oxygen intermediate
extradiol dioxygenases	non-oxygen substrate	Fe(II)-$O_2^{\bullet}$
Rieske Rieske dioxygenases	Rieske [2Fe-2S] cluster	Fe(V)-O-OH
α-ketoglutarate-dependent α-ketoglutarate-dependent oxidases	co-substrate	Fe(IV)=O
pterin-dependent pterin-dependent hydroxylases	co-substrate	Fe(IV)=O
ACCO	co-substrate	Fe(IV)=O
IPNS	non-oxygen substrate	Fe(IV)=O

communication through the metal center. When oxygen binds to the metal center, a single electron from the iron is used to activate dioxygen, and this activation likely results in an Fe(III)-superoxide intermediate. No evidence for this intermediate has ever been detected, and so a valence change of the metal center may not be required (Scheme 1.1.7 complex II-V). Ultimately, the bound oxygen makes a nucleophic attack on the aromatic ring of the catecholic substrate, forming a radical on the aromatic ring. The resulting electron density on the non-oxygen substrate is donated to break the sigma bond of dioxygen (complex V). It has been proposed that a general base in the active site of the extradiol dioxygenases then donates a proton to the oxygen atom coordinated to the metal center. This would prevent an oxo-ferryl species from forming and maintain the valence state of the substrate-bound metal center. The bound hydroxyl group would then be transferred to the catecholic substrate resulting in ring cleavage and product release (complex VI) (*12,13,19,20*).

Oxygen activation occurs in a similar manner in the Rieske dioxygenases. In contrast to the extradiol dioxygenases, the non-oxygen substrates for this class are not functionalized with electron-donating groups, so an additional electron source must be provided. Reduction of the metal center from the ferric to the ferrous form is accomplished by the Rieske cluster. Reduction of the Rieske cluster to the active form is then coupled to NADH oxidation by another protein. Because there are no electron-donating groups to allow direct communication between the substrates through the metal center, a formal change in the valence state of the metal center is likely. Single-turnover experiments of naphthalene 1,2-dioxygenase show that, after one catalytic cycle, the

metal center and Rieske cluster have each been oxidized by one electron. This indicates that the ferrous iron of the Rieske dioxygenases donates a single electron to activate dioxygen resulting in the formation of an Fe(III)-peroxo intermediate (Scheme 1.1.8 complex III). The next step in dioxygen chemistry is not as well understood. Single-turnover and peroxide studies have provided evidence that another electron provided by the iron results in the formation of an Fe(V)-oxo-hydroxo intermediate (complex IV). Single-turnover studies have indicated that one electron is supplied by the active-site iron and one is supplied by the Rieske cluster; however, dioxygen never binds to the Rieske cluster, indicating that an electron transfer event must happen subsequent to the binding of dioxygen. An electron transfer between the metal center and the Rieske cluster would be similar to electron transfer processes that have been identified in other dioxygenase enzymes that have di-iron or di-heme centers. The Fe(V)-oxo-hydroxo species then binds to the non-oxygen substrate through both the oxo- and hydroxo-groups, followed by product release and a return to the resting valence state of the metal center (complex V) (*12,13,19*).

IPNS and ACCO are unique among the classes of 2-His/1-carboxylate containing enzymes because they accomplish the complete reduction of dioxygen into two molecules of water. The catalytic mechanism of IPNS is similar to that observed for the extradiol and Rieske dioxygenases. Both the non-oxygen and dioxygen substrates directly coordinate to the ferrous metal center allowing for transfer of electrons between the non-oxygen substrate and dioxygen (Scheme 1.1.9 complex II). Like the Rieske dioxygenases, ACV does not donate considerable electron density to the metal center.

Initial activation of molecular oxygen occurs by transferring an electron from the metal center, creating an Fe(III)-O_2 species (complex II). Instead of a nucleophilic attack that would result in oxygen incorporation, the radical formed from the binding of dioxygen with the metal center abstracts two hydrogen atoms from the non-oxygen substrate, breaking the remaining bond of dioxygen and leading to the formation of an Fe(IV)=O species (complex III). This also leads to the first ring closure of the catalytic process. The remaining ring closure occurs when two additional hydrogen atoms are abstracted from the non-oxygen substrate, followed by product release and a return to the resting state enzyme (complex III-I). The mechanism of ACCO is similar to both the extradiol and Rieske dioxygenases and to the α-ketoglutarate-dependent oxidases. ACCO also uses a co-substrate as an electron source. Activation of molecular oxygen is accomplished using two electrons derived from L-ascorbate through electronic communication with the metal center, although the co-substrate does not directly bind to the metal center. Instead, the non-oxygen substrate directly coordinates the metal center in a bidentate manner (Scheme 1.1.10 complex II). The rest of the mechanism follows similarly to that of IPNS, with hydrogen abstractions from the substrate resulting in an Fe(III)-O_2 (complex III) then an Fe(IV)=O (complex IV) (*12,13,19*).

In the α-ketoglutarate-dependent oxidases, the pterin-dependent hydroxylases, and ACCO, the electrons required for activation of dioxygen are provided by the co-substrate. In the case of the α-ketoglutarate-dependent oxygenases, the initial steps in the catalytic mechanism are similar to the extradiol and Rieske dioxygenases. α-

ketoglutarate replaces the role of the non-oxygen substrates in priming the metal center for reaction with dioxygen (Scheme 1.1.11 complex IV). After complexation between α-ketoglutarate and the metal center, activation of dioxygen occurs when dioxygen binds to the metal center (complex V). Like the Rieske dioxygenases, α-ketoglutarate does not donate as much electron density as the catecholic substrates of the extradiol dioxygenases, and so direct electronic communication through the metal center is not favored. Instead, a electron from the metal center is donated when dioxygen binds and causes the formation of an Fe(III)-O_2 radical (complex V). A peroxo bridge is formed between the metal center and the co-substrate, followed by cleavage of the sigma O-O bond using an electron provided by α-ketoglutarate (complex VI). An additional electron donated by the co-substrate leads to formation of an Fe(IV)=O species (complex VII). Hydride transfer from the non-oxygen substrate to the Fe(IV)=O results in hydroxylation of the substrate and release of both products (complex VII-I) (*12,13,19*).

The pterin-dependent oxidases are unique because the electrons supplied for dioxygen bond cleavage come from a co-substrate that is not directly bound to the metal center. Binding of dioxygen to the metal center is facilitated by the co-substrate and amino acid substrate, but the initial electrons required to activate molecular oxygen come from the ferrous metal center. Isolation of enzymes from this family has been shown to result in oxidation of the majority of the metal center, and so the facilitation of dioxygen binding by the presence of the co-substrate is likely due to reduction of the metal center by the pterin (Scheme 1.1.12 complex II). Activation of dioxygen leads to formation of a

peroxo bridge between the metal center and the pterin (complex IV). The electron required for the initial activation of dioxygen comes from the pterin allowing the metal center to remain in its ferrous state. Following formation of the peroxo bridge, an additional electron transfer is coupled with hydride transfer to form a C4a-hydroperoxy intermediate (Figure 1.1.6, Scheme 1.1.12 complex V). Two electrons are donated by the metal center to break the remaining O-O bond. This leads to the formation of a hydroxytetrahydropterin and an Fe(IV)=O species (complex V). Recently, the high-valent iron has been trapped and detected directly (*13*). The final step in the catalytic cycle is donation of a hydride from the amino acid substrate, causing hydroxylation of the aromatic ring (complex VI) (*12,13,17,19*).

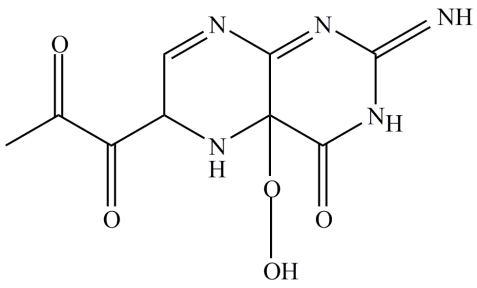

Figure 1.1.6 The C4a-hydroperoxy intermediate species formed from reaction of tetrahydropterin with dioxygen (*17*).

1.2 Physiological relevance of cysteine

Sulfur is one of the six most abundantly found elements in living organisms, and thiol-containing compounds are used in a variety of ways to accomplish cellular needs. In addition to providing key functional groups for methionine and cysteine, sulfur-containing compounds also serve as cofactors, redox-active signaling molecules, and protection for aerobic cells exposed to reactive oxygen species. The use of sulfur is particularly important for redox chemistry. The most commonly used form of sulfur for redox chemistry is the thiol, with the majority of thiols in biology existing in two major forms: as a cysteine residue incorporated into the primary structure of a protein or as the functional group of small soluble molecules.

In eukaryotic organisms, cysteine is at the hub of sulfur metabolism. Products from each branch of cysteine metabolism play key roles in forming signaling molecules, cofactors, and proteins vital for normal cellular function. The concentration of cysteine must be tightly regulated because large concentrations of oxidation products of the amino acid can be cytotoxic. Formation of cysteine disulfides results in insoluble cystine stones that result in cell death. Formation of free cysteine sulfinic and sulfonic acids are also toxic to cells and can react adversely with other small molecular weight species in the cell. Despite the negative effects of elevated cysteine concentrations, cells also need a sufficient supply of free cysteine for protein synthesis, the synthesis of coenzyme A, and the production of inorganic sulfate (*21*).

1.2.1 Cysteine biosynthesis and hydrogen sulfide producton

Cysteine biosynthesis and formation of the gaseous molecule hydrogen sulfide overlap metabolically in eukaryotic organisms through the enzymes cystathionine β-synthase and cystathionine γ-lyase. Cysteine is the precursor for a variety of important sulfur-containing molecules that will be discussed in the remainder of the section. Knowledge of the physiological relevance of hydrogen sulfide is a recent biological research focus. The implications of nitric oxide as a gaseous signaling molecule are well documented, and emerging evidence suggests that hydrogen sulfide may play just as important of a role in signaling of vascular smooth-muscle contractions. It has been shown that two key enzymes in cysteine biosynthesis (cystathione β-synthase and cystathionine γ-lyase) catalyze the reversible reactions to produce hydrogen sulfide in addition to the previously determined physiologically relevant products (*3,21,22*).

The thiol of cysteine derives from methionine, which is converted into homocysteine by several enzymes that also function to catalyze the initial steps of the transsulfuration pathway. Methionine adenosyltransferase catalyzes the formation of S-adenosylmethionine (SAM). SAM is critical for many processes in the cell because it is the substrate utilized in methylation of nucleic acids, proteins, and membrane phospholipids. In cysteine biosynthesis, SAM is then converted to S-adenosylhomocysteine by a methyl transferase, and then to homocysteine by the enzyme S-adenosylhomocysteine hydrolase. The next step in mammalian cysteine synthesis is a condensation reaction combining homocysteine with another amino acid, serine. This

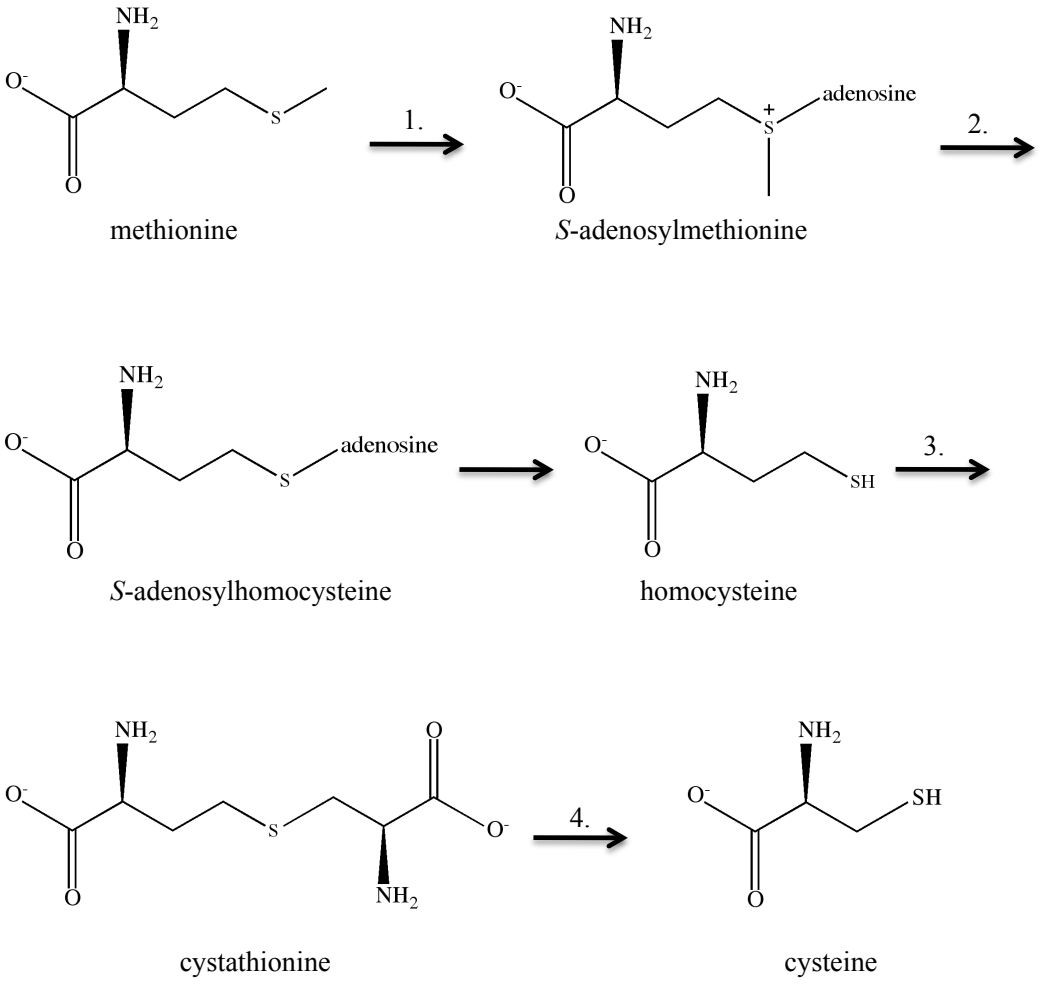

1. methionine adenosyl transferase
2. *S*-adenosylhomocysteine hydrolase
3. cystathionine β-synthase, + serine
4. cystathionine γ-lyase, - α-ketobutyrate

Scheme 1.2.1 The cysteine biosynthetic pathway (*4*).

step is dependent on pyridoxal-5-phosphate (PLP) and is catalyzed by the enzyme cystathione β-synthase. The product of this reaction (cystathionine) is then hydrolyzed in another PLP-dependent reaction by the enzyme cystathionine γ-lyase. This enzyme releases one molecule of ammonium, one molecule of α-ketobutyrate, and one molecule of cysteine. The cysteine biosynthetic pathway is shown in Scheme 1.2.1 (*4,21,23*).

1.2.2 Incorporation of cysteine into proteins

One of the most important physiological roles of cysteine is its incorporation into the primary structure of enzymes. The pK_a of cysteine is dependent on the microenvironment of the protein that it is incorporated into, and this redox sensitivity allows cysteine to be used for a variety of purposes within a protein (*2,24*). The thiol group of a cysteine molecule can undergo a one-electron oxidation and form a covalent bond with another single-electron oxidized thiol molecule to form cystine (Figure 1.2.1). This covalent crosslinking between the two non-adjacent cysteine residues has a considerable impact on the overall architecture of the enzyme, and the disulfide linkage has added thermostability over protein structures typically dependent on noncovalent interactions (*25*). Cysteine residues can also serve as an anchor to stabilize cofactors within enzyme active sites. In metalloproteins, the thiols from cysteine residues are used to bind iron-sulfur clusters and also provide protein-derived metal binding ligands in many mono- and dinuclear iron, copper, manganese, and zinc containing proteins. Additionally, many flavin cofactors are covalently bound to protein derived thiols (*26*). Although thiols are chemically similar to alcohols, the sulfur atom of a thiol is less

electronegative than the oxgen atom of an alcohol and so they often exist as thiolates at physiological pH. Because of this reactivity, cysteines often act as general acids or bases in the catalytic mechanism of many enzymes. This also affords cysteine residues the ability to stabilize both cationic and anionic intermediates formed during catalytic cycles, depending on the relative pK_a of the thiol (*4,21*).

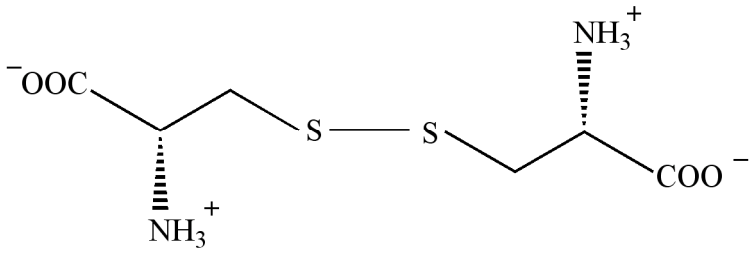

Figure 1.2.1 The chemical structure of cystine.

One of the most important functions of thiols in proteins is their role as redox signals that mediate cellular processes. Oxidation of thiols incorporated into a peptide can serve reversible and irreversible regulatory functions. Oxidation of a protein thiol to a sulfonic acid is biologically irreversible and targets the protein for proteolytic degradation. All other oxidations of protein thiols are reversible and these are the targets for redox signaling in response to oxidative stress (*2*). The proteins that are responsible for most of the redox signaling are the thioredoxins, thioredoxin reductases, peroxiredoxins, and glutaredoxins (*25*).

Thioredoxin proteins act to reduce disulfide bonds in target molecules to the constituent thiols. Several different thioredoxin proteins have been identified in both prokaryotic and eukaryotic organisms. The majority of thioredoxins have two cysteine residues located in their active site that are susceptible to disulfide bond formation. The redox chemistry between the two active site thiols is primarily involved in signaling and catalytic oxidoreductase activity. The thiols in the active site of the thioredoxin are often involved in disulfide interchange reactions with a diverse group of substrate molecules. These enzymes have evolved to serve a role similar to chaperones by reversing disulfide formation in misfolded proteins. Thioredoxins contribute to cellular defense against oxidative stress by reactivating proteins involved in detoxification of peroxides and by reducing hydrogen peroxide and dimers of glutathione (*27*). Thioredoxins can also serve as cofactors for the enzymes ribonucleotide reductases and methionine sulfoxide, reductases and are known to play an integral role in DNA repair processes (*28*). Additionally, maintenance of the active reduced state of the thiols of many transcription factors involved in the oxidative stress response is accomplished by thioredoxin proteins (*25*).

Thioredoxin reductases are a homologous class of enzymes that act on a diverse group of substrate molecules. They have two cysteine residues in their active center capable of being oxidized and reduced for disulfide interchange reactions with substrate molecules (*29-31*). While the thioredoxin reductases all share high sequence homology, they are active over a wide pH range and act on a larger group of substrate molecules than the thioredoxins. This diversity is partly the result of a conserved selenocysteine in

the active sites of many mammalian thioredoxin reductases. The selenocysteine replaces one of the conserved active-site cysteine residues and is hypothesized to lower the reduction potential of the remaining conserved cysteine residue in the active site, making it more reactive at a larger pH range (*32*). Thioredoxin reductases act to reduce the oxidized form of thioredoxin and can also act on oxidized glutathione dimers, restoring them to their active state. In addition to reducing thioredoxins and glutathione, another regulatory role for the thioredoxin reductases is their ability to convert dehydroascorbate to ascorbate, thus reactivating another important cellular antioxidant (*25,33*).

Glutaredoxins are also small-molecular weight proteins that have two redox-sensitive cysteine residues in their active site (*34*). The substrates for glutaredoxins are typically proteins containing disulfide bonds. Most proteins that regulate disulfide bond formation act only on linkages between cysteine residues; however, glutaredoxins can also target mixed disulfides formed from reaction of protein-derived cysteine residues with glutathione (glutathionylation). The redox-sensitive thiols in glutaredoxins can donate either one reducing equivalent to the substrate protein (to remove glutathione from a target cysteine residue) or two reducing equivalents (in order to break a disulfide linkage between two cysteine residues) to the target protein. Glutathionylation is an important process for the regulation of transcription factors involved in the signaling of cellular defense towards oxidative stress, and so glutaredoxins act to restore transcription factors and target proteins to their active states (*25,35,36*).

In contrast to thioredoxins, thioredoxin reductases, and glutaredoxins, peroxiredoxins are mammalian proteins that contain redox-active cysteine residues involved in formation of intersubunit disulfide bonds. These enzymes receive electrons from either glutathione or thioredoxin to catalytically degrade hydrogen peroxide. Splitting of the oxygen-oxygen bond of hydrogen peroxide results in formation of cysteine sulfenic acid from an active-site cysteine residue, and the sulfenic acid is subsequently glutathionylated. Peroxiredoxins play an important regulatory role because of the dual physiological roles of hydrogen peroxide. In high concentrations, hydrogen peroxide leads to the formation of reactive oxygen species and cellular damage. In low concentrations, hydrogen peroxide is imperative for proper signaling for the cellular defense against oxidative stress. It is hypothesized that the conserved cysteine residues in the peroxiredoxins act as redox sensors for the cell to regulate consumption of hydrogen peroxide based on signaling needs (*25,37*).

1.2.3 Equilibrium between cysteine and glutathione

Glutathione and free cysteine are the two small-molecular-weight thiols that constitute the majority of relief from oxidative stress. The pK_a of thiols differs considerably depending on if it is incorporated into a peptide or as part of a lower-molecular-weight compound. While thiols incorporated into proteins are redox-sensitive targets for signaling the cellular response to oxidative stress, low-molecular-weight thiols remove redox active agents in the cellular environment. Several different small molecules are known to react with low molecular weight thiols under biological settings

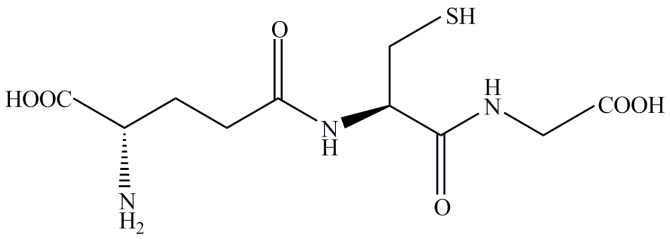

Figure 1.2.2 The chemical structure of reduced glutathione.

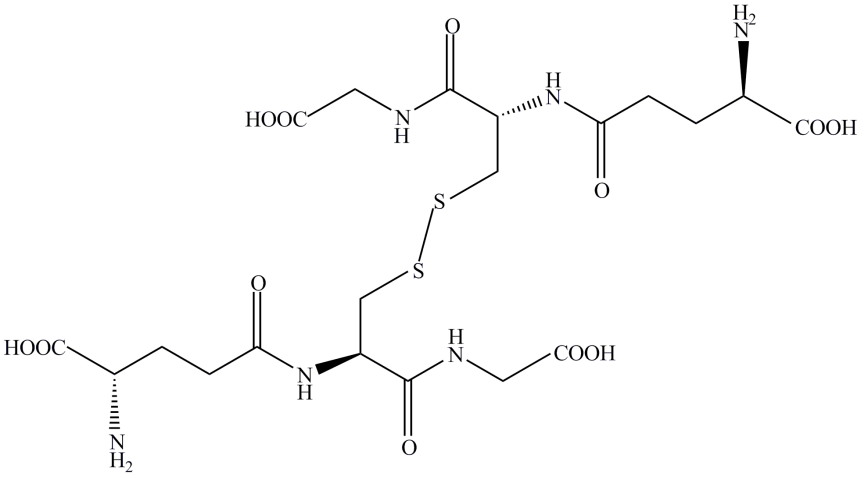

Figure 1.2.3 The chemical structure of oxidized glutathione.

including hydrogen peroxide, superoxide, peroxynitrite, hypochlorous acids, and haloamines. Glutathione is the predominating thiol in intracellular environments and reacts with a variety of small reactive species associated with oxidative stress including peroxides and peroxynitrite. Glutathione is a tripeptide composed of a glutamate, cysteine, and glycine residue. Within a cellular environment, glutathione exists either in a one-electron reduced or oxidized state. One-electron reduced glutathione exists as a thiol (Figure 1.2.2), while one-electron oxidized glutathione exists as a dimer with another glutathione molecule (Figure 1.2.3). Free cysteine is the predominating free thiol in extracellular environments. Free cysteine can also form cystine molecules, and this dimer is insoluble in cellular environments, leading to cytotoxicity. Because of this, the concentration of cysteine is heavily regulated (*2,38*).

The concentration of free cysteine in the cell is in equilibrium with the cellular concentration of glutathione and the concentration of these thiols is regulated *via* two metabolic processes (*23,38*). When mammals are fed a diet with enough sulfur-containing amino acids to sustain protein synthesis, glutathione pools become depleted while the incorporation of cysteine into proteins is unaffected. This indicates that protein synthesis takes priority and suggests that cysteine metabolism is critical in regulating the concentration of glutathione available for removal of reactive oxygen species. Synthesis of glutathione from cysteine is accomplished by glutamate-cysteine ligase which couples condensation of the two amino acids (glutamate and cysteine) with energy provided by ATP (Scheme 1.2.2). This results in the formation of L-γ-glutamyl cysteine. An additional molecule of ATP is hydrolyzed to condense the product molecule with glycine

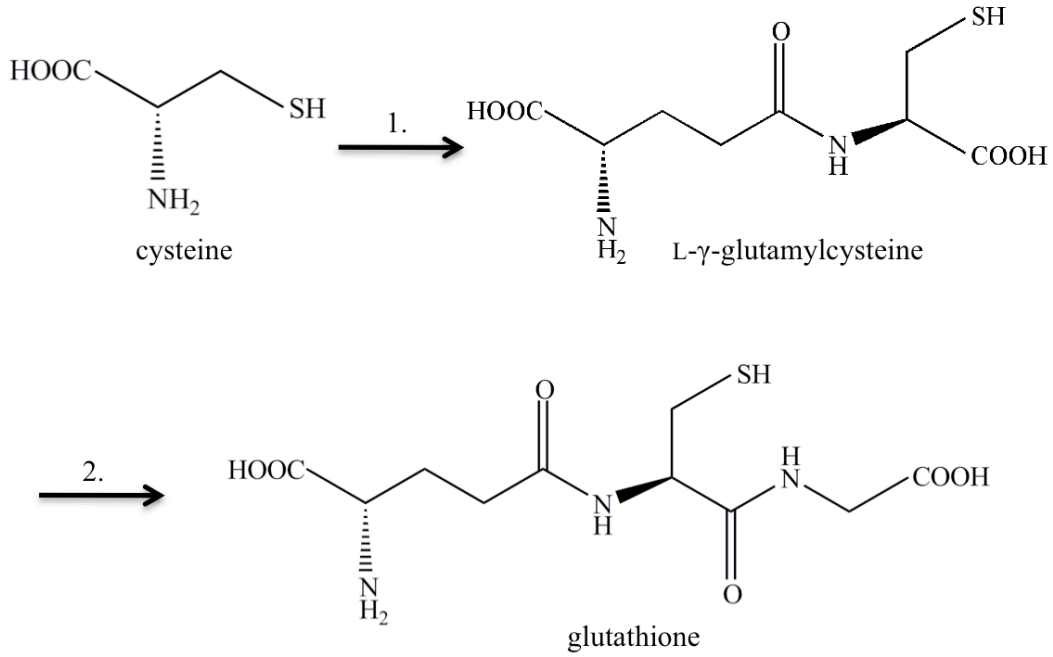

1. glutamate-cysteine ligase, + glutamate
2. glutathione synthase, + glycine

Scheme 1.2.2 The glutathione biosynthetic pathway (*4,38*).

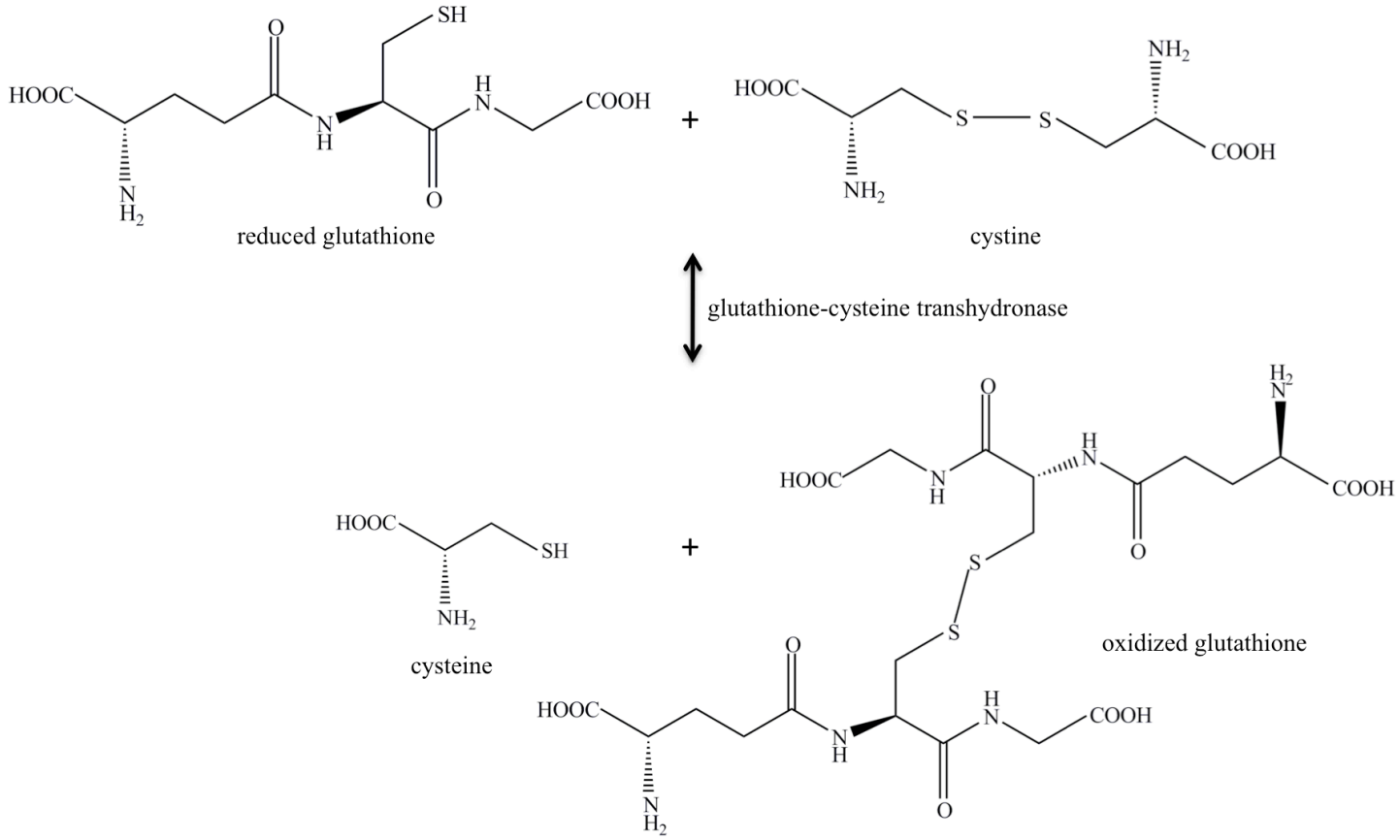

Scheme 1.2.3 The enzymatic relationship between cysteine and glutathione (*4*).

by the enzyme glutathione synthase. The cellular concentrations of glutathione and cysteine are also linked metabolically by the enzyme glutathione-cysteine transhydrogenase, which catalyzes disulfide exchange reactions between molecules of cystine and oxidized glutathione and helps to regulate the cellular redox potential (Scheme 1.2.3) (*1-3,23,38*).

1.2.4 Biosynthesis of sulfur-containing cofactors

Cysteine residues in a protein can provide the sulfur ligands in iron-sulfur cluster cofactors; however, the sulfur in free cysteine can also be metabolized for the formation of coenzyme A. Coenzyme A is involved in a variety of necessary metabolic processes, most notably for its integral role in the biochemical reaction linking glycolysis with the TCA cycle in cellular respiration. The first step in the biosynthesis of coenzyme A is the point of regulation and is the phosphorylation of pantothenate by the enzyme pantothenate kinase (*23,38*). After phosphorylation of pantothenate, the molecule is condensed with cysteine by the enzyme phosphopantothenate-cysteine ligase to form 4-phosphopantothenoylcysteine. The carboxylic acid of the cysteine is removed by 4-phosphopantothenoylcysteine decarboxylase, forming 4-phosphopantetheine. If coenzyme A is not needed in the cell, this product can be dephosphorylated and decomposed to release pantothenate and cysteamine. The cysteamine can be converted into taurine by cysteamine dioxygenase. If coenzyme A synthesis is needed, ATP hydrolysis is catalyzed by 4-phosphopantetheine adenylyl-transferase to form dephospho-coenzyme A. An additional ATP is hydrolyzed to form coenzyme A in a reversible step

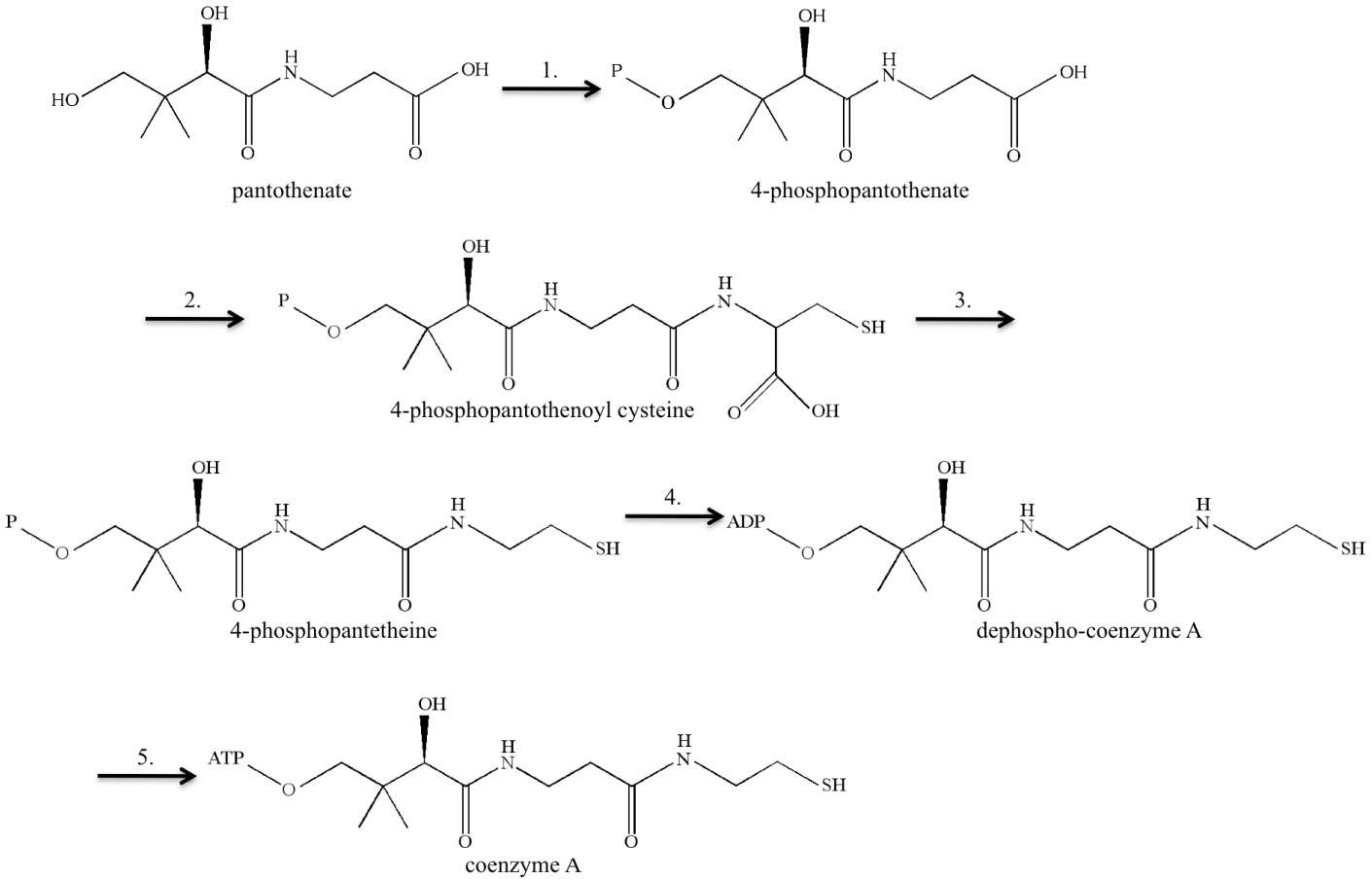

1. pantothenate kinase, + ATP
2. 4-phosphopantothenate-cysteine ligase, + cysteine
3. phosphopantothenate-cysteine decarboxylase, - CO_2
4. 4-phosphopantotheneine adenylyl transferase, + ATP
5. dephospho-coenzyme A kinase, + ATP

Scheme 1.2.4 The coenzyme A biosynthetic pathway (*4,38*).

catalyzed by the enzyme dephospho-coenzyme A kinase. The biosynthesis of coenzyme A is detailed in Scheme 1.2.4 (*4,38*).

1.2.5 Role of taurine in eukaryotic organisms

The predominant metabolic process that regulates cellular concentrations of cysteine is the oxidation of its thiol to form cysteine sulfinic acid. Cysteine sulfinic acid is located at a branch-point in cysteine metabolism, with one branch leading to the biosynthesis of taurine and the other leading towards the production of pyruvate and inorganic sulfate. The formation of cysteine sulfinic acid is catalyzed by the mononuclear iron enzyme cysteine dioxygenase (CDO). Cysteine sulfinate decarboxylase is a PLP-dependent enzyme that catalyzes the removal of the carboxylic acid group to form hypotaurine. This is the committed step in the taurine biosynthetic pathway. The final step in taurine biosynthesis is catalyzed by the enzyme hypotaurine dehydrogenase, which is dependent on NAD^+. Cysteine sulfinic acid is also a substrate for aspartate aminotransferase, which transforms α-ketoglutarate into glutamate. The other product from this reaction is 3-sulfinylpyruvate, which is decomposed to pyruvate and sulfite by the enzyme 3-sulfinylpyruvate sulfurtransferase. Pyruvate is fed into the TCA cycle and sulfite is further oxidized to form sulfate for use in varying biochemical processes. The taurine biosynthetic pathway is shown in Scheme 1.2.5 (*4,38*).

Although taurine is not a thiol, it has been directly correlated with the maintenance of cellular redox equilibrium, and its biosynthesis constitutes a major branch of eukaryotic thiol metabolism. Taurine is the most abundant free amino acid found in

mammalian systems, reaching a concentration of 50 mM in leukocytes, and it has recently been shown to be incorporated into some tRNAs. All mammals with the exception of felines have the capability of synthesizing taurine. Taurine is also obtained through dietary sources, and is transferred from mother to offspring during nursing in many mammals. Taurine is considered an amino acid because it has a sulfonic acid functional group, although the carboxylic acid group characteristic of most amino acids has been removed. Because of this, taurine is incapable of being incorporated into proteins, and due to the hydrophilicity of the molecule it is incapable of diffusing through cellular membranes (*39,40*). A taurine transporter (TauT) has been identified that regulates the cellular concentration of taurine. This transporter is regulated by the internal ionic environment, electrochemical charge, and transcriptional and translational factors (*41*).

First noted to protect against several optical disorders, taurine has been shown to have an impact on many mammalian diseases. Taurine is known to act on cationic channels, including sodium channels. Taurine has been shown to be especially important in regulating calcium ion concentrations in the cell and thus in maintenance of cellular osmotic pressure. It is unclear whether the effects of taurine on calcium concentrations are the result of direct interaction with calcium transporters or a cooperative effect between the concentration of calcium and sodium ions in the cell. Proper maintenance of calcium ion concentrations is critical for prevention of cardiac and vascular diseases and also for cellular protection against neurotoxicity due to over-stimulation. Dietary supplementation with taurine has been shown to decrease the rate of heart failure in

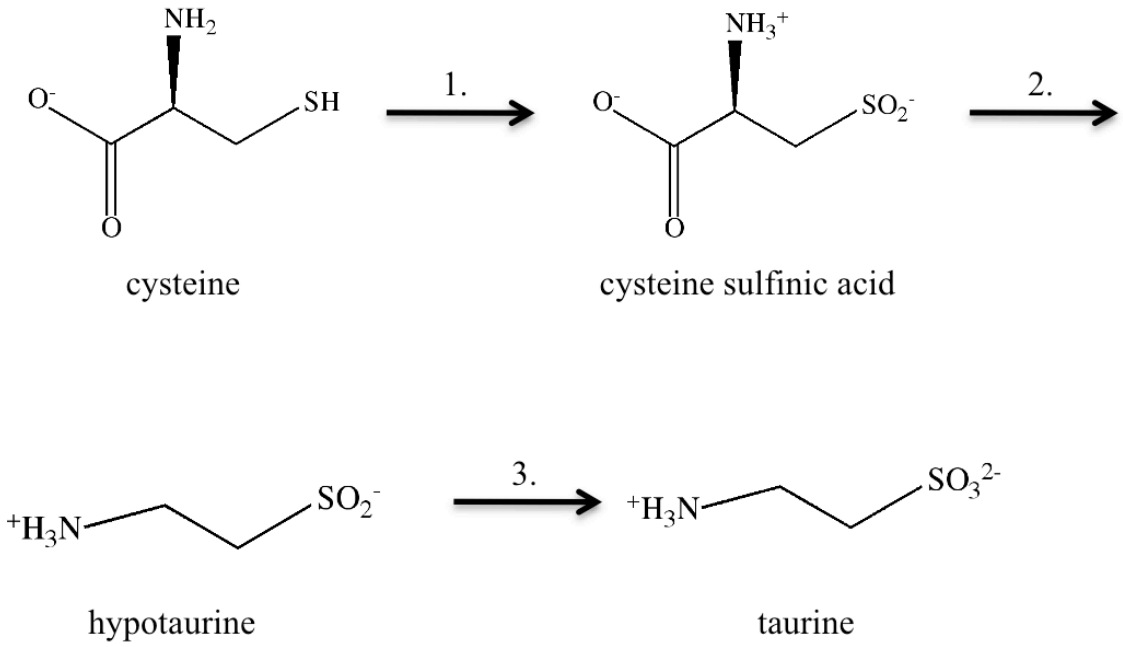

1. cysteine dioxygenase, + O_2
2. cysteine sulfinic acid decarboxylase, - CO_2
3. hypotaurine dehydrogenase, + ½ O_2

Scheme 1.2.5 The taurine biosynthetic pathway (*4,38*).

patients and also to decrease to rate of nerve cell death. In addition to regulating the concentrations of monovalent metals in the cell, taurine has been shown to affect cholesterol metabolism. Taurine and glycine are two amino acids that work to emulsify fatty acids by forming bile salts. These bile acids are a key step in cholesterol metabolism. It has been shown through lab studies that mammals that are deficient in taurine have elevated levels of cholesterol; conversely, mammals being fed a diet rich in taurine have decreased cholesterol levels. Patients with cystic fibrosis that suffer from the build up of fecal fatty acids experienced a decrease in this build-up when admistered taurine supplements, which suggests that taurine also plays a role not only in emulsifying fatty acids but also in their absorption. This behavior is also believed to account for the positive effects of taurine on cardiac diseases and diabetes (*39,40*).

A major research focus of taurine and its effects on the human body is the role of taurine in alleviating symptoms of recovering alcoholics. Acamprosate is a drug that was developed to increase cellular absorption of taurine. It is the salt of homotaurine and readily diffuses across cellular membranes. Evidence suggests that Acamprosate works on glutamate/N-methyl-D-aspartate and γ-aminobutyric acid receptors. The physical symptoms of alcohol addiction include cell toxicity by increased calcium ion intake and decreased glutamate neurotransmitter action (called glutaminergic activity) (*40*). This depletion is regulated by a series of counter-measures that restore the homeostatic balance. When ethanol intake is eliminated, the counter-measures are no longer balanced by the depressing effect of the alcohol and the result is hyper-glutaminergic activity. The hyper-glutaminergic activity results in the restlessness and relapse urges observed in

patients. In human and animal studies, the physical symptoms of alcohol withdrawal were alleviated by doses of Acamprosate. Interestingly, Acamprosate also had an effect on the patient relapse behavior. Patients being administered the drug had no relapse urges compared with patients being given a placebo. These effects have made Acamprosate a leading medication in the treatment of alcohol addiction (*39,40,42*).

One of the most potent oxidants to biological organisms is hypochlorous acid. Hypochlorous acid is produced in large amounts by neutrophils and monocytes as part of the immune response; however, none of the thiols that regulate the redox signaling for oxidative stress reacts with hypocholorous acid. Taurine reacts with hypochlorous acid to form a considerably less oxidative product, Tau-Cl. Tau-Cl directly inhibits the transciption factor involved in the formation of the mRNA for inducibile nitric oxide synthase and for cyclooxygenase. Nitric oxide synthase plays an intergral role in signaling the inflammation response by producing the gaseous signaling molecule nitric oxide. Cyclooxygenase also plays an important role in signaling the inflammation response by catalyzing the formation of signaling prostaglandin molecules. These effects have led to the development of the inflammation suppressant tauriline, which breaks down in the cellular environment to produce two molecules of taurine (*39,40,43*).

1.3 Characterization of cysteine dioxygenase

In the 1960s, an enzyme was discovered in crude liver extracts that produced L-cysteine sulfinic acid from L-cysteine (*44*). The resulting protein was called cysteine oxidase and it was shown through the use of $^{18}O_2$ and $H_2{}^{18}O$ that both atoms of oxygen

used by the enzyme were derived from a stoichiometric amount of dioxygen, making the enzyme a dioxygenase (*45*). The overall reaction catalyzed by this enzyme is shown in Scheme 1.3.1.

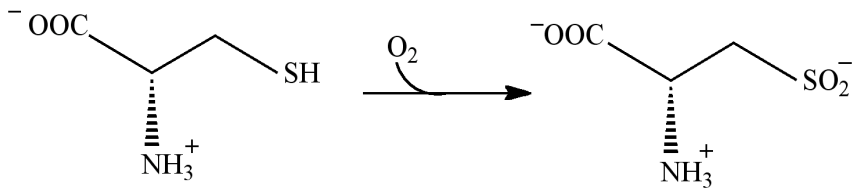

Scheme 1.3.1 The overall reaction catalyzed by CDO (*45*).

The product of this reaction is located at a branch-point in cysteine metabolism, with one branch leading to taurine biosynthesis and the other leading to the production of pyruvate and inorganic sulfate. The activity of CDO has been shown to directly regulate the cellular concentrations of these sulfur-containing compounds (*46*).

Because of the variety of medical disorders associated with an imbalance in the equilibrium of these small molecules, the catalytic mechanism of CDO has become particularly relevant. Both prokaryotic and eukaryotic CDO proteins have been identified and characterized structurally, although more is known about the metabolic function of eukaryotic CDO. Eukaryotic CDO is expressed in the highest concentration in the liver,

although large quantities of the protein can also be found in the kidneys and lungs, and smaller quantities in the brain and testis. Emerging evidence shows that CDO may be expressed ubiquitously throughout eukaryotic tissues (*47*).

1.3.1 Early isolation and recombinant expression of CDO

Although several mammalian CDO enzymes have been identified, the first isolation of CDO was from rat liver. The purified protein was analyzed by gel filtration and found to have an approximate molecular weight of 22,500 ± 1,200 Da. Atomic absorption analysis of the metal center showed that the enzyme contained 0.8 moles of iron per mole of enzyme, with the majority of the remaining active sites occupied by copper ions. To determine which metal represented the physiologically active center, copper- and iron-specific chelators were added to activity assays of CDO present in liver lysate. CDO activity was not diminished in the presence of copper-specific chelator bathocuproine sulfonate; however, the activity was diminished completely in the presence of several chelators selective for iron. This provided evidence that the active enzyme utilizes iron as a metal cofactor during catalysis. Following the purification procedure, CDO was found to be completely inactive. Anaerobic pre-incubation with the substrate L-cysteine was reported to recover some of the activity lost during purification. With this pre-incubation, a K_m of 670 μM for L-cysteine was estimated based on the initial velocity (*48*).

Other reports of CDO isolated from liver indicated that multiple isoforms of the enzyme might be present. Initial isolation of the enzyme showed a secondary protein

termed protein A that co-purified with CDO. These studies also reported that incubation with protein A during activity assays could re-activate purified CDO (*48*). A subsequent study reported that CDO migrated as a species of apparently 68 kDa when resolved on SDS-PAGE. It was hypothesized that this approximately 68 kDa species might represent CDO covalently bound to protein A or that CDO existed as a dimer (*49*). Later, this 68-kDa species was dismissed when it was shown that CDO existed as a monomer and protein A studies lacked reproducibility. It was repeatedly shown that resolution of CDO by SDS-PAGE yielded two separate species of approximately 23 and 25 kDa. The approximately 25-kDa species was observed in all samples of CDO, whereas the approximately 23-kDa species was sometimes absent (*50*).

The genes of several CDO proteins have been identified and cloned into expression vectors (*6,8,51,52*). These include human, mouse, rat, and *Cupriavidus necator* (a bacterium). Several purification schemes have been utilized, including immoblilized metal affinity chromatography. This was accomplished using a His-tag and a Ni-NTA affinity column, and the His-tag was removed using a cleavage factor after purification. Early analysis of the resulting protein indicated that there is a non-specific cleavage site for the enzyme between Arg17 and Gly18 (*51*). Purification schemes that did not include an affinity tag were lengthy and used more than three different, consecutive chromatographic steps to yield homogenously pure enzyme. Despite the diversity in purification strategies, all preparations of CDO showed the same two interesting characteristics. All recombinant samples of CDO resolved as two species on SDS-PAGE, and all bound significantly less iron than CDO isolated from liver. Metal

binding analysis indicated that purified recombinant CDO bound between 10 – 50% iron (*6,8,51,52*). Separation of the two isoforms of the enzyme was accomplished by immobilized metal affinity chromatography HPLC, and the resulting species were analyzed for activity. It was shown that the species of apparently lower molecular weight had no catalytic activity and all catalytic ability could be attributed to the species of apparently higher molecular weight (*52*). The presence of active and inactive isoforms suggests that a post-translational modification of the enzyme occurs as a form of regulation of the enzyme.

1.3.2 Spectroscopic characterization of the iron center

Early studies of CDO showed that activity was dependent on the presence of iron in the active site. Several spectroscopic techniques have been implemented to characterize this metal center and its redox properties in the presence and absence of both L-cysteine and analogs of dioxygen. Extended X-ray absorbance fine structure (EXAFS) studies waere performed to determine what the ligand environment of the metal center was in the resting enzyme and in the presence of L-cysteine. These studies showed six O/N donating ligands coordinating the resting enzyme, indicating that in the absence of substrates the enzyme is hexa-coordinate. This is consistent with the resting state of other non-heme ferrous enzymes including the extradiol dioxygenases. When CDO was pre-incubated with L-cysteine, results indicated that there were still six O/N donating ligands. These results indicated that if L-cysteine directly bound the metal center, it does

not bind as a bidentate or through the thiol. Based on the reaction catalyzed by CDO, the likely coordination would be through the amino group of the substrate (*53*).

Substrate binding in CDO was also investigated using nitric oxide as a spectrally active probe for dioxygen. These studies used EPR to investigate the environment of the metal center. Incubation of CDO with nitric oxide did not result in formation of an iron-nitrosyl species observed by EPR. When CDO was anaerobically preincubated with L-cysteine, the appearance of a doublet signal at $g = 2.0$ was observed. The lack of signal observed in the absence of L-cysteine indicated that CDO uses an ordered substrate-binding mechanism with L-cysteine binding to the metal center before dioxygen can be properly coordinated (*54*).

1.3.3 Reported steady-state assays and kinetic parameters

Several assay methods have been implemented to examine the kinetic properties of CDO. Despite demonstration of the reaction catalyzed by CDO, it has been proposed that the enzyme fulfills another physiological role due to the low activity observed for the enzyme. Because initial isolation of the enzyme from rat liver showed it to be catalytically inactive, a variety of approaches have been taken to restore the activity of the enzyme. Currently all assays utilize end-point analysis of the production of cysteine sulfinic acid.

The first assay of purified recombinant CDO was published in 2005 (*51*). This study measured the production of cysteine sulfinic acid using UV detection at 215 nm. Cysteine sulfinic acid was resolved from L-cysteine and other oxidation products using a

hydrophobic C18 HPLC column. To retain the polar substrate and product, the ion-pairing agent heptafluorobutyric acid was added to the mobile phase. Because of the low activity of CDO and the weak absorbance properties of L-cysteine and cysteine sulfinic acid, incubation of the reaction mixture for three hours was implemented before quenching the reaction and measuring the product by HPLC analysis. Using this assay method, a specific activity of 17.4 nmol·(min·mg)$^{-1}$ and an estimated K_m of 2.5 ± 0.4 mM was obtained based on the observed initial rate of reaction. This assay yielded an optimum pH for CDO of 7.5 (*51*). Two other groups implemented this assay method to determine steady-state kinetic parameters for mouse and human CDO and reported very different results (*6,8*). The group investigating mouse CDO reported a k_{cat} of 3.6 min^{-1} and a K_m of 2.1 mM (*6*), while the group investigating human CDO reported a k_{cat} of 102 min^{-1} and a K_m of 3.1 mM (*8*).

Another catalytic assay of purified recombinant rat CDO was published in 2006 (*52*). This method also employed a C18 HPLC column to resolve reaction components. The amino acid reaction components were labeled to increase fluorescence with *o*-phthalaldehyde. This increased the hydrophobicity of the components so that no ion-pairing agent was necessary in the mobile phase for retention by the C18 column. These studies included 0.3 mM exogenous ferrous iron to the assay to account for the substoichiometric amount of iron bound to the purified recombinant enzyme. Because of increased sensitivity of fluorescence detection and the addition of exogenous iron, this study used incubation times ranging from 10 – 20 minutes. This assay method yielded a specific activity of 1,870 nmol·(min· mg)$^{-1}$ and a K_m of 0.45 mM, representing an

increase in activity of over two orders of magnitude and a two and a half-fold decrease in the K_m value compared with previously determined values. This assay method yielded an optimum pH of 6.1 (*55*). The results from kinetic studies of purified recombinant CDO are summarized in Table 1.3.

Table 1.3 Published kinetic parameters for purified recombinant CDO proteins. ND indicates a value that was not determined in that particular study. A (+) sign in % iron bound indicates that 0.3 mM exogenous iron was included in that particular assay (*6,8,51,52*).

enzyme	specific activity nmol· (min· mg)$^{-1}$	K_m mM	k_{cat} min^{-1}	pH_{opt}	% iron bound
Rat CDO Chai *et al.* (2005)	17.4	2.5	ND	7.5	10
Rat CDO Simmons *et al.* (2006)	1,870	0.45	ND	6.1	(+) iron
Mouse CDO McCoy *et al.* (2006)	ND	2.1	3.6	ND	25
Human CDO Ye *et a.l* (2007)	ND	3.1	102	ND	68

1.3.4 The three-dimensional structure of CDO

The three-dimensional crystal structures of several prokaryotic and eukaryotic CDO proteins have been published (*6,7,8*). The first crystal structure was published in 2006 for mouse CDO using Ni(II) as a substitute for the active site iron (*6*). This structure revealed that CDO was a member of the cupin superfamily. Members of this superfamily have a characteristic β-barrel, jelly-roll fold topology and coordinate a mononuclear metal ion. The metal ion in the cupin superfamily is typically coordinated by two loosely conserved motifs: $G(X)_5HXH(X)_{3,4}E(X)_6G$ and $G(X)_5PXG(X)_2H(X)_3N$. The metal ion in characteristic cupin enzymes is coordinated by the two histidines and glutamate residue in the first motif and the histidine residue in the second motif. The metal center of mouse CDO is coordinated only by the three histidine residues (His86, His88, and His140), with the glutamate replaced by a cysteine residue that does not coordinate the metal center. The three histidine residues form one face of a facial triad, similar to the arrangement of ligands in the 2-His/1-carboxylate facial triad (Figure 1.3.1). Three solvent molecules occupy the other face of the octahedron resulting in a hexa-coordinate metal center, in agreement with results from EXAFS. Publication of this crystal structure also revealed an unusual thioether linkage formed between the thiol of Cys93 and the meta-carbon of Tyr157 near the active-site metal (Figure 1.3.2). The thioether is also observed in the copper-dependent enzyme galactose oxidase. Tyr157 was found to be conserved in all known CDO proteins while Cys93 is only conserved in CDO proteins found in mammalian organisms. In addition to Tyr157 and the metal-binding histidine residues, Tyr58, Arg60, Trp77, Ser153, and His155 were all shown to be conserved among CDO enzymes (*6*).

Shortly after publication of the structure of mouse CDO, the three-dimensional structures of rat (*7*) and human CDO (*8*) with iron bound in the active sites were also

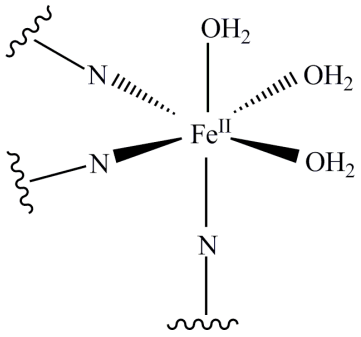

Figure 1.3.1 The 3-His facial triad that coordinates the metal center in CDO (*6*-*8*).

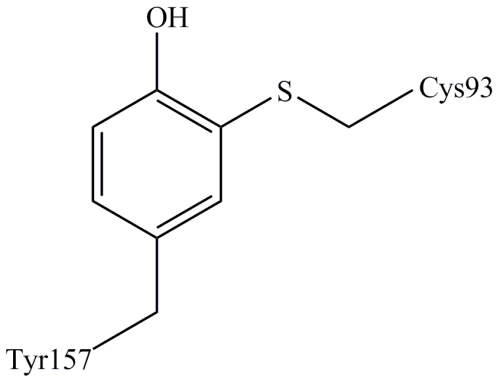

Figure 1.3.2 The thioether linkage formed from the primary sequence in CDO (*6*-*8*).

published and although the results were never formally published, a crystal structure for CDO from *C. necator* with iron bound was deposited in the Protein Data Bank. The crystal structures of rat and human CDO confirmed that all forms of mammalian CDO contained the thioether linkage within the active site. Interestingly, the three-dimensional structure of rat CDO showed a penta-coordinate resting state with only one solvent molecule coordinating the metal. It was proposed that CDO utilized a general base during catalysis and hypothesized from structural data that this could be the hydroxyl group of Tyr157. The catalytic mechanism proposed in this study is based on the catalytic mechanism of the extradiol dioxygenases and is illustrated in Scheme 1.3.2. L-cysteine was proposed to bind to the metal center first in as a bidentate ligand freeing a coordination site for dioxygen (complex II). Dioxygen was proposed to bind to the metal center next in an end-on orientation resulting in an Fe(III)-$O_2^{\bullet}$ (complex III). This orientation would prime the distal oxygen to make an attack on the thiol of L-cysteine forming a peroxo bridge prior to oxygen insertion (complex IV). The crystal structure of human CDO was obtained with L-cysteine bound in the active site (*8*). The structure indicated that Arg60 was in hydrogen-bonding contact with the carboxylic acid group of the substrate. Additionally, the structure showed that L-cysteine bound to the metal center in a bidentate coordination through the thiol and amine groups, confirming the initially proposed catalytic mechanism for the enzyme. Iron coordination by cysteine is in disagreement with data obtained from EXAFS. The three-dimensional structure of human CDO also showed that the metal center was penta-coordinate with the non-oxygen substrate bound similarly to what is observed for the extradiol dioxygenases

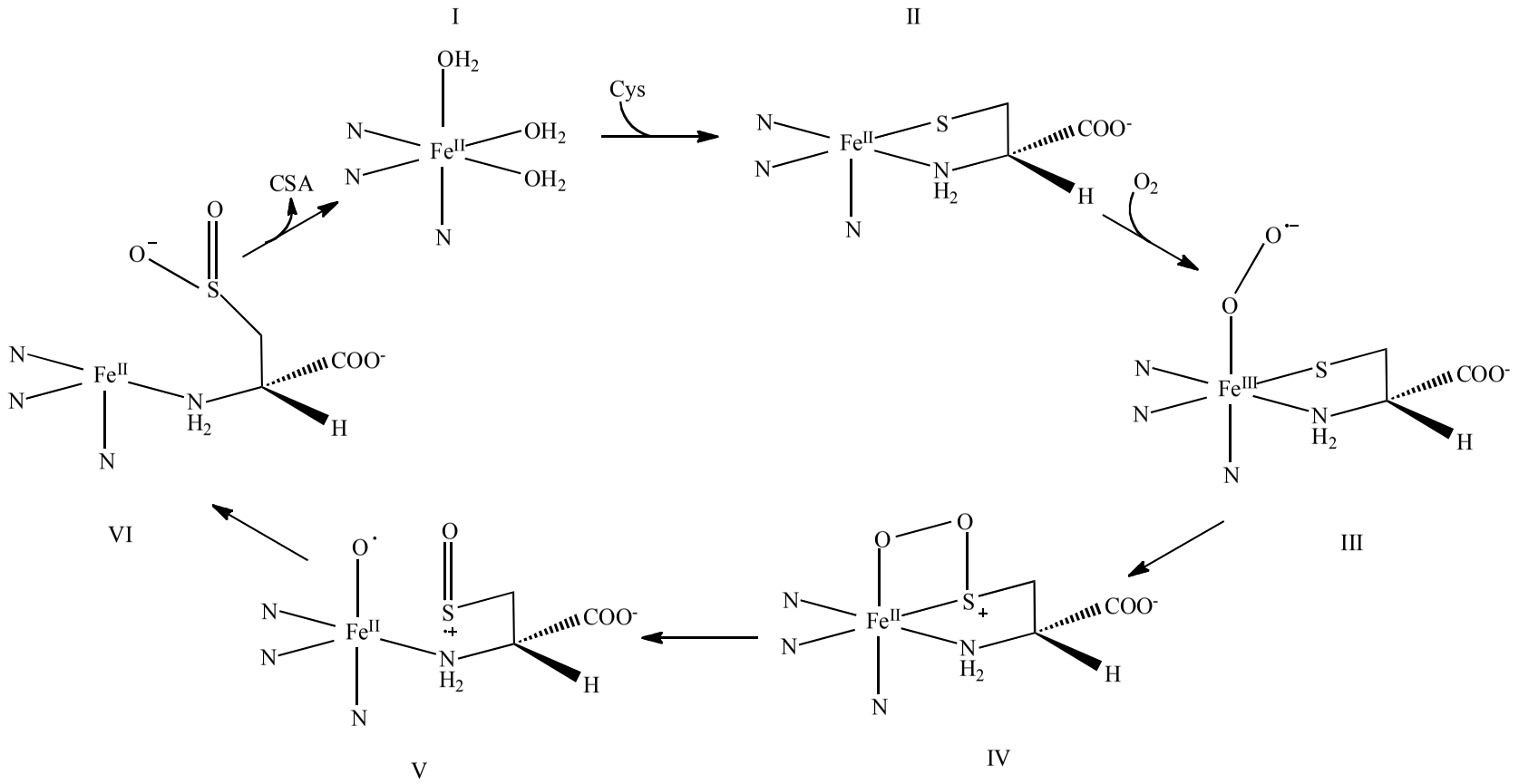

Scheme 1.3.2 The catalytic mechanism proposed for CDO based on the three-dimensional structure of the resting enzyme (*6*).

and isopenicillin N-synthase. The three-dimensional structure of CDO from *C. necator* revealed an interesting difference from mammalian CDO proteins. Although Cys93 is conserved throughout all mammalian CDO enzymes, in the bacterial structure it was replaced with a glycine residue, disabling prokaryotic CDO from forming the covalent crosslink.

Recently, the three-dimensional structure of CDO with L-cysteine and carbon monoxide bound was published (*56*). Carbon monoxide was used as a surrogate for dioxygen in order to obtain crystals with both substrates bound. This structure supported results of cysteine binding from human CDO which indicated that the cysteine substrate bound to the metal center in a bidentate manner and that the carboxylic acid group was stabilized by hydrogen bonding with Arg60 (Scheme 1.3.3 complex II). It also indicated that carbon monoxide bound to the metal center in an end-on manner, and so presumably dioxygen would bind in the same orientation (complex III). Interestingly, this structure showed that the hydroxyl group of Tyr157 was in hydrogen-bonding contact with the carbon atom of carbon monoxide that was bound to the metal center (complex III). If carbon monoxide is a suitable surrogate for dioxygen, this would indicate that incorporation of dioxygen into cysteine molecules proceeds along a similar reaction coordinate as is proposed for the extradiol dioxygenases. Incorporation of the oxygen atom hydrogen bonded to the hydroxyl group of Tyr157 into the cysteine thiol would occur first (complex IV). Incorporation of the distal oxygen atom would lead to a persulfonate intermediate (complex V) before product formation and release.

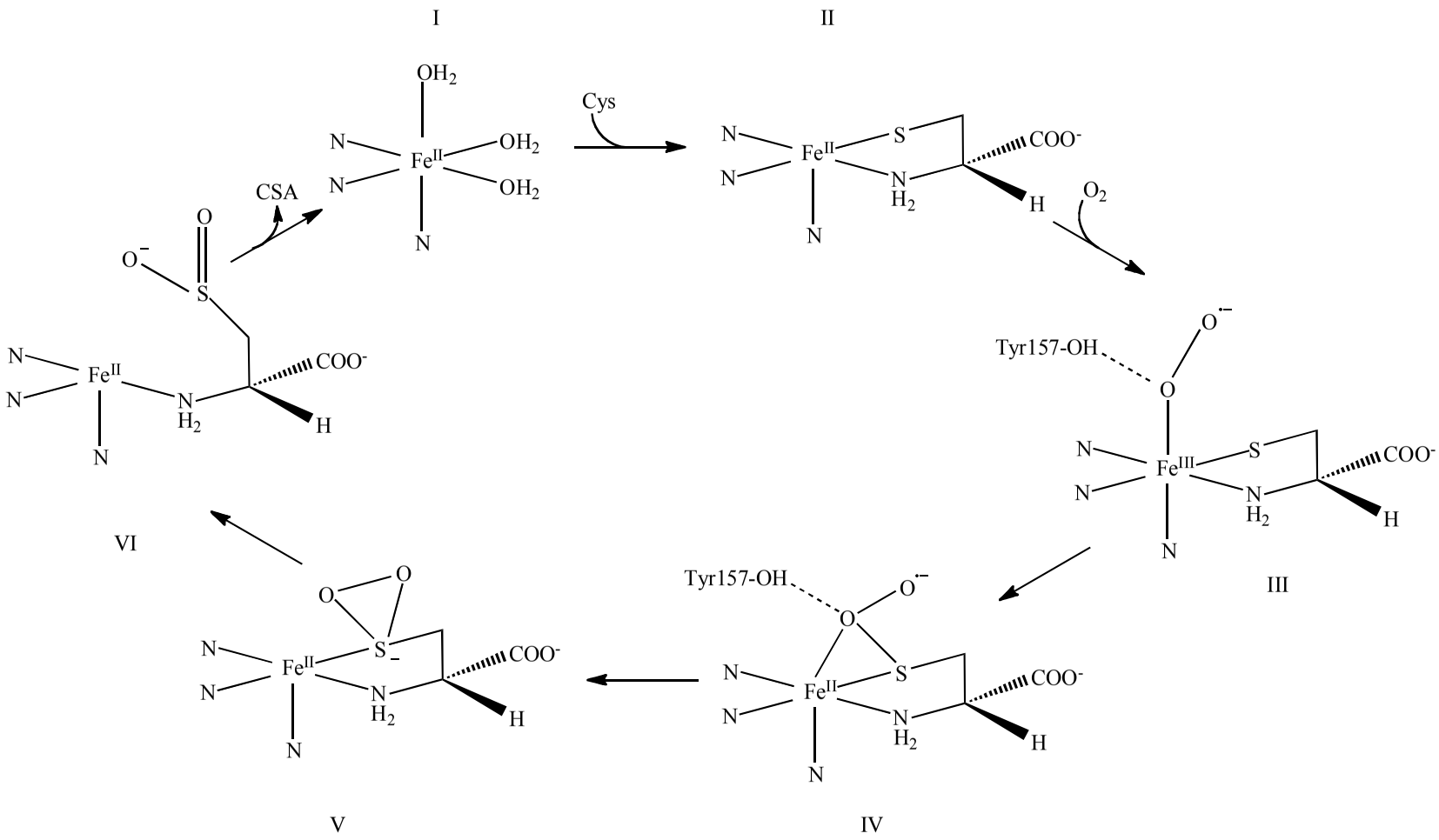

Figure 1.3.3 The catalytic mechanism of CDO proposed from the three-dimensional structure with substrates bound (*56*).

1.3.5 Regulation of CDO activity

Because of its metabolic significance, the activity of CDO has been shown to be tightly regulated. Currently two mechanisms have been identified by which CDO activity is regulated. It was shown early in studies of CDO that enzyme expression is increased in response to increased cellular cysteine concentrations (*57*). CDO is also regulated post-translationally through ubiquitination. Ubiquitin is a small protein that is covalently attached to specific lysine residues in eukaryotic target proteins. A preliminary ubiquitin molecule is attached to the target protein and then conjugated to form a poly-ubiquitin chain using a group of conjugating and ligating enzymes. The attachment of ubiquitin signals the target enzyme for proteolytic degradation. CDO has been shown to be ubiquitinated both *in vitro* and *in vivo*, suggesting that cellular levels of CDO can be controlled by the ubiquitin-proteasome (*58*).

Another post-translational modification of CDO may provide an additional mechanism of regulation. The physiological relevance of the thioether linkage between Cys93 and Tyr157 near the active-site metal in CDO has not been determined. Early isolation of the protein indicated that two isoforms of the enzyme exsisted when the purified protein is resolved by SDS-PAGE. Recently, mass-spectrometry of each band from SDS-PAGE has been reported identifying the two species as the crosslinked and non-crosslinked isoforms of CDO (*59*). Formation of the crosslinked isoform appears to occur more frequently in animals fed high protein diets. This study also showed that formation of the thioether crosslink is dependent on the presence of the active site iron

and L-cysteine. Removal of the thioether linkage by site-directed mutagenesis does not eliminate the activity of CDO, suggesting that the linkage may serve a regulatory function (*8,59*). Site-specific oxidation to the amino acid side chains of several proteins has been shown to target them for proteolytic degradation by the ubiquitin-proteasome system. Formation of the thioether linkage may be involved in ubiquitin regulation; however, no role for the thioether linkage has yet been investigated.

1.4 Crosslinked amino acids in enzymes

Early biochemical studies of enzymes focused on the direct interaction of primary sphere amino acids with substrates and cofactor molecules. Emerging research on enzymes and enzyme-mimics has shown that the entire enzyme architecture is important for the high specificity and rate accelerations accomplished by proteins. A growing branch of research on enzymes and how they effectively catalyze biochemical reactions is focused on the presence of intra-peptidyl crosslinkages. These linkages are formed from non-adjacent amino acids within the primary structure of the peptide that are covalently bound together. Amino acid crosslinkages can serve several different functions in an enzyme. An early example of amino acid crosslinking was the linkages formed between collagen fibrils (*60*). Two separate crosslinkages have been identified in collagen: a protein-mediated crosslinking involved in maturation of collagen fibrils and an unmediated one involved in the aging process that results in vascular disease. The functional crosslinks formed between collagen fibrils form in two stages: one enzyme mediated and the second occurring spontaneously. The linkages are intermolecular, in

contrast to most other identified amino acid crosslinkages, and occur most commonly between hydroxylysine residues that have been functionalized to aldehydes by the enzyme lysyl oxidase. Once the aldehyde has been formed by lysyl oxidase, crosslinking occurs spontaneously.

Several heme enzymes have been shown to have crosslinked amino acids within their active sites. A particularly interesting example is the bifunctional catalase-peroxidase KatG. Covalent bonding between a methionine, tyrosine, and tryptophan residue forms a crosslinked bridge between the two domains of the protein and is termed a covalent adduct (*61-64*). This linkage is shown in Figure 1.4.1. Interestingly, these catalase-peroxidases have active sites homologous to peroxidases, although monofunctional peroxidases do not contain a covalent adduct. This implies that the catalase activity of KatGs derives from the presence of the crosslink. Mutagenic studies have verified that removal of the linkage results in complete loss of catalase activity but not peroxidase activity (*62*). The covalent adduct acts to stabilize a protein-derived radical that participates in electron-transfer during catalysis (*63*). Formation of the covalent adduct in KatGs is not dependent on a processing enzyme and is a function of catalytic turnover. Binding of hydrogen peroxide in the active site leads to the formation of an oxoferryl porphyrin cation radical. Single mutation of each residue involved in the covalent adduct shows that a covalent bond is still formed between the tyrosine and tryptophan residues in the absence of the methionine residue; however, no linkage is formed in the absence of either the tyrosine or tryptophan residue. This suggested that the radical created by binding of hydrogen peroxide to the active site is transferred to the

tryptophan residue which then binds to the tyrosine residue, delocalizing the unpaired electron between the two residues. The radical would then be primed to react with the methionine residue to form the last bond in the covalent adduct (*61-64*).

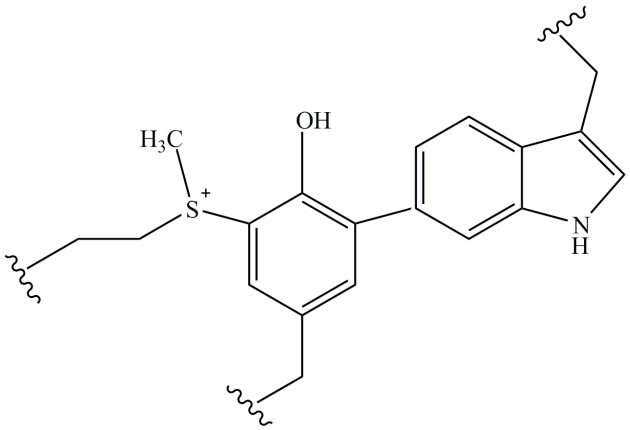

Figure 1.4.1 The structure of the peptidyl cofactor formed from crosslinking between a methionine, a tyrosine, and a tryptophan residue in the primary sequence of the bifunctional enzyme KatG (*61*).

An additional class of crosslinked cofactors have been identified in some amine-reactive enzymes. The cofactors are quinones derived from either a tyrosine or tryptophan residue that has been structurally modified and is sometimes covalently bound to a modified cysteine, lysine, or other tryptophan residue. The result is a quinone cofactor that functions as a Schiff base during catalysis converting the substrate amine into the corresponding aldehyde. Four different quino-cofactors have been identified:

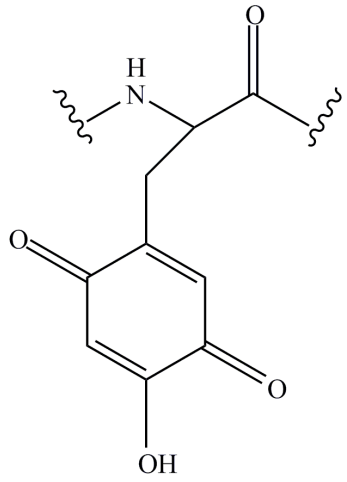

Figure 1.4.2 The structure of the cofactor TPQ formed from a tyrosine residue in enzyme primary structure (*65*).

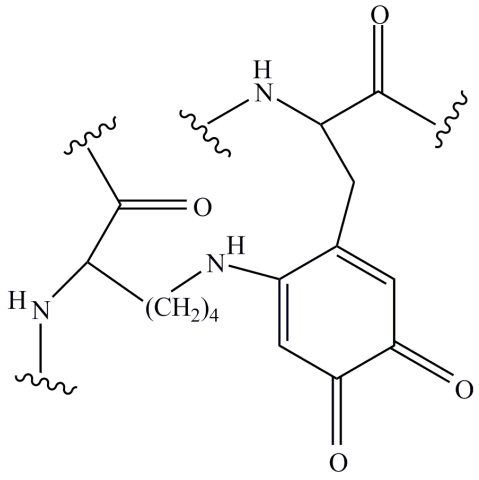

Figure 1.4.3 The structure of the cofactor LTQ formed from crosslinking between a lysine and a tyrosine residue in the enzyme primary structure (*65*).

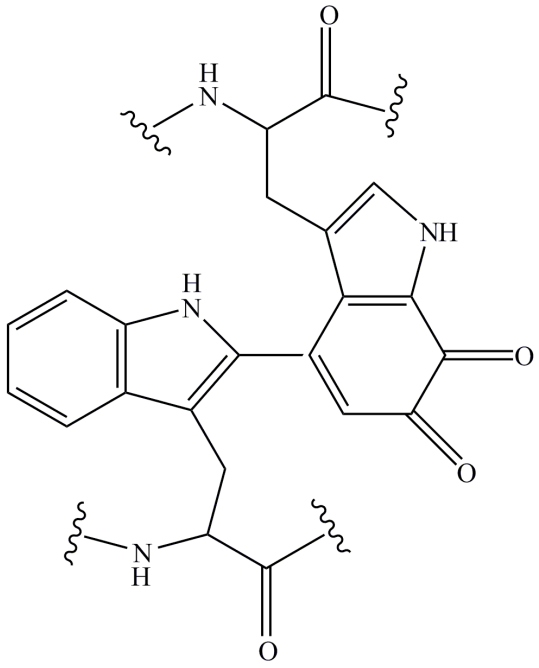

Figure 1.4.4 The structure of the cofactor TTQ formed from crosslinking between two tryptophan residues in the enzyme primary sequence (*65*).

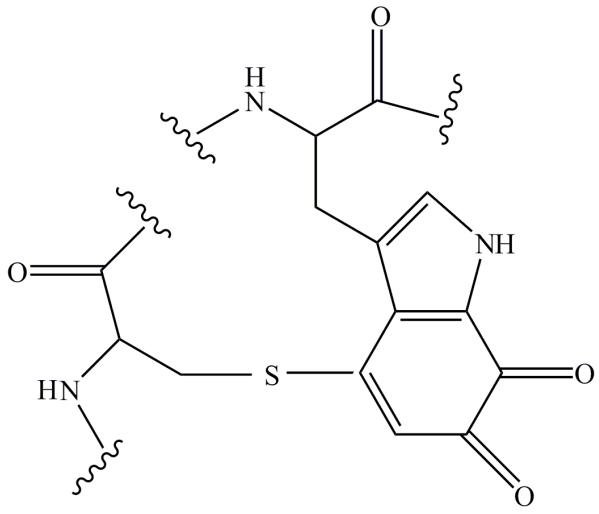

Figure 1.4.5 The structure of the cofactor CTQ formed from crosslinking between a cysteine and a tryptophan residue in the enzyme primary sequence (*65*).

TPQ (tyrosine-derived, not crosslinked), LTQ (from lysine and tyrosine crosslinkage), TTQ (from tryptophan and tryptophan crosslinkage) and CTQ (from cysteine and tryptophan crosslinkage). The structures of these linkages are shown in Figures 1.4.2-5. The linkages derived from tyrosine (TPQ and LTQ) have been identified in copper-dependent amine oxidases, while the linkages derived from crosslinked tryptophans (TTQ and CTQ) are present in enzymes lacking a metal cofactor. The mechanism of biogenesis of each quino cofactor varies. Both quino cofactors derived from tyrosine residues have been shown to require no external enzymatic processing. Formation of TPQ and LTQ depend only on the presence of the target enzyme's active-site copper in aerobic conditions. The biogenesis of TTQ and CTQ have been shown to depend on a series of processing enzymes. TTQ biogenesis is dependent on the activity of four other processing enzymes, some of which have yet to be characterized. One of the enzymes that has been shown to be critical in cofactor biogenesis is MauG which contains a di-heme active center. CTQ biogenesis has also been shown to depend on the activity of uncharacterized processing enzymes, including a putative iron-sulfur cluster-containing radical SAM enzyme. This indicates that the presence of metal ions is still necessary for amino acid crosslinking despite the lack of a metal cofactor in the target enzyme (*65-68*).

Another copper-dependent enzyme that contains a cofactor derived from crosslinked amino acids is found in galactose oxidase. A tyrosine residue that directly coordinates the mononuclear copper center is covalently attached to a cysteine residue (Figure 1.4.6). The linkage occurs between the thiol of the cysteine and the meta-carbon of the tyrosine residue. Mutagenic studies of galactose oxidase showed that the enzyme

was catalytically inactive when either residue was substituted, including a double mutant galactose oxidase where the primary structural location of the cysteine and tyrosine had been reversed. Spectroscopic studies have shown that the thioether linkage between these two residues functions to stabilize a tyrosyl radical during catalysis. Biogenesis of the thioether crosslinkage has been shown to depend on the presence of the active site copper in the reduced oxidation state. Originally it was proposed that formation of the crosslink was dependent on dioxygen, but it was recently shown that the linkage forms autocatalytically under anaerobic conditions in the copper-containing enzyme. These

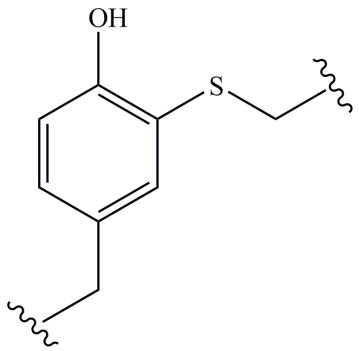

Figure 1.4.6 The structure of the thioether cofactor formed from crosslinking between a cysteine and a tyrosine residue in the primary sequence of galactose oxidase (*69*).

results combined with mutagenesis studies suggest that direct interaction between the tyrosine residue and the active-site copper leads to covalent bond formation with the cysteine residue (*69-72*).

The thioether linkage found in galactose oxidase is synonymous with the thioether linkage found in the previously described iron-dependent enzyme CDO. CDO contains a covalent crosslink between the thiol of a cysteine residue and the meta-carbon of a tyrosine residue located near the iron center in the active site. Similarly to galactose oxidase, formation of the crosslink in CDO is dependent on the presence of the active-site metal. Despite this similarity, three key differences exist between the thioether linkage identified in CDO and that found in galactose oxidase. The hydroxyl group of the tyrosine residue in CDO is not directly bound to the iron center. Instead, the hydroxyl group stabilizes a water ligand for the metal center in the resting state of the enzyme. Additionally, mutagenic studies of the thioether linkage in CDO revealed that the crosslink is not necessary for catalysis. The crosslink in CDO is not formed in the resting enzyme. Formation of the thioether linkage in CDO has been shown to be dependent on proper orientation of L-cysteine in the active site (*6-8,59*).

1.5 Summary

The reactivity of thiols, dioxygen, iron, and amino acid side chains are linked together in many biological processes. Molecular oxygen is necessary for most eukaryotic cells and mononuclear non-heme iron oxygenases containing a 2-His/1-carboxylate facial triad have been shown to play a critical role in activating molecular oxygen for a variety of metabolic purposes. Despite the increase in energy conversion achieved with the large reduction potential of dioxygen, activated oxygen causes many problems for biological architecture. Cellular defense against this oxidative damage is

triggered in eukaryotic organisms by a series of thiol redox reactions, and all of these reactions rely on cysteine metabolism to supply the necessary thiol. CDO is the enzyme responsible for regulating cellular cysteine concentrations and utilizes the reactivity of molecular oxygen, iron, thiols, and modified amino acid side chains to accomplish this role. Despite the central role of this enzyme in cellular maintenance, little is known about the enzyme mechanistically, and reported studies of the enzyme are contradictory.

Interestingly, this metabolically important enzyme has two unusual structural features that may aid in its regulatory role. CDO is one of only three enzymes identified to have a ferrous metal center coordinated by three histidines in contrast to the well-characterized 2-His/1-carboxylate facial triad found in most other ferrous-dependent enzymes. Little is known about the chemical reactivity of the 3-His facial triad and why an additional histidine ligand would be evolutionarily selected rather than a carboxylate ligand. This first half of the studies described in this work will focus on the redox stability of the 3-His coordinated iron in CDO and how this stability affects the kinetic properties of the enzyme following purification. The other unusual structural attribute of CDO is the presence of a thioether linkage near the active site metal formed from two non-adjacent amino acids in the primary structure. Removal of the linkage by site-directed mutagenesis does not abolish the catalytic ability of the enzyme. The second half of the studies described will focus on elucidating the effects of the thioether linkage on catalysis.

Chapter Two

Elucidating the Role of an External Reductant on Catalysis in the Metalloprotein Cysteine Dioxygenase

2.1 Introduction

Cysteine dioxygenase (CDO) is a mononuclear iron-containing enzyme that catalyzes the oxidation of L-cysteine to form cysteine sulfinic acid using both atoms of dioxygen (*45*). Cysteine sulfinic acid is located at a branch-point in eukaryotic cysteine metabolism, and is the starting material for the biosynthesis of either taurine or pyruvate and sulfate (*73*). Each of these products plays an important role in diverse metabolic processes. In addition, increased levels of cysteine have been shown to be both cytotoxic and neurotoxic. CDO plays a critical role in maintaining both cellular cysteine and taurine concentrations, and in the synthesis of sulfonated metabolites (*46*). Because CDO plays a central role in essential metabolic processes, determining the mechanistic properties of the enzyme is of current interest.

Early studies of CDO involved the characterization of the enzyme purified from rat liver. Gel filtration chromatography showed that CDO exists as a monomer of 22.5 kDa, and atomic absorption spectroscopy confirmed that there were 0.80 atoms of iron present per monomer of purified protein (*48*). Although cysteine dioxygenase was shown to be

ferrous-dependent, the role of the iron in catalysis was not determined in these early studies. The mechanistic function of the enzyme was shown through $^{18}O_2$ and $H_2{}^{18}O$ studies (*45*). Mass spectrometric analyses of the cysteine sulfinic acid product showed that both oxygen atoms originated from dioxygen. The physical and kinetic properties of recombinant CDO enzyme from several mammalian sources have also been evaluated (*6,8,51,52*). Recombinant CDO typically has appreciably less iron incorporated (approximately 10 – 70%) than native CDO, which may be caused by the expression and purification conditions (*6,8,51,52*). To account for the lack of iron, exogenous ferrous iron is often added to kinetic assays of CDO. Due to the different reaction conditions and methods used to monitor activity, the reported kinetic parameters for recombinant CDO vary considerably (K_m: 0.45 mM – 8.4 mM; k_{cat}: 0.19 s^{-1} – 0.72 s^{-1}) (*6,8,51,52*).

Interest in the mechanism of CDO has arisen from the unique metal coordination of the enzyme. In contrast to enzymes that contain a 2-His/1-carboxylate facial triad, the iron center of CDO is coordinated by a facial triad composed of three histidine residues (*6-8*). Different coordination states of the metal have been reported for CDO based on three-dimensional structural information and extended x-ray absorption fine-structure (EXAFS) data (*6,7,53*). Amino acid sequence analysis and structural determination of several eukaryotic and prokaryotic CDO proteins revealed that the enzyme is a member of the cupin superfamily (*6-8*). Currently, the cupin superfamily contains several enzymes that utilize a 3-His facial triad for iron coordination (*74*). Comparison of the spatial arrangement of 2-His/1-carboxylate and the known 3-His facial triads shows a negligible difference in the positioning of the three protein-derived ligands around the

metal center (*75*). Although the positioning of the metal-binding ligands is congruent, mutational analysis of enzymes containing a 2-His/1-carboxylate facial triad has shown that substitution of the carboxylate-donating ligand with a histidine residue results in the loss of dioxygenase activity (*76-78*). Similarly, substitution of the histidine residues to glutamate or aspartate in the 3-His β-diketone-cleaving enzyme (Dke1) led to inactivation of the enzyme (*79*). The increasing number of enzymes identified to carry out oxygen activation chemistry and known to contain a 3-His facial triad suggests that the chemical reactivity of the iron with dioxygen may differ from the 2-His/1-carboxylate containing enzymes.

It has been proposed that the resting state of the purified protein is the ferrous form of the enzyme or that the bidentate coordination of L-cysteine to the metal center is the necessary reductant for catalysis (*6,51,53*). In the studies described herein, the oxidation state of the metal center of recombinant CDO was evaluated through spectroscopic and kinetic approaches to definitively determine the resting and active forms of the iron center. These studies provide the first plausible explanation for the low activity observed for the enzyme and demonstrate the importance of including an external reductant in CDO assays for maximal catalytic activity.

2.2 Materials and Methods

2.2.1 Materials

Potassium phosphate (monobasic anhydrous and dibasic anhydrous), 4-(2-hydroxyethyl)-1-piperazineethanesulfonic acid (HEPES), 2-(*N*-morpholino)ethanesulfonic acid (MES), 3-(*N*-morpholino)propanesulfonic acid (MOPS), *N*-cyclohexyl-3-aminopropanesulfonic acid (CAPS), tris(hydroxymethyl)aminomethane hydrocloride (Tris-HCl), ammonium acetate, sodium chloride, ampicillin, diethylamine nitric oxide (DEANO), sodium hydrosulfite (dithionite), streptomycin sulfate, L-ascorbate, ammonium sulfate, ferrous ammonium sulfate, sodium ferricyanide, trifluoroacetic acid, sodium cyanide, and L-cysteine were purchased from Sigma (St. Louis, MO). Isopropyl-β-D-thiogalactoside (IPTG), glycerol, hydrogen peroxide, boric acid, lysozyme, acetonitrile, and sodium phosphate (monobasic anhydrous and dibasic anhydrous) were purchased from Fischer Biotech (Pittsburg, PA). Difco-brand Luria-Bertani (LB) media was purchased from VWR (West Chester, PA). Napthalene dicarboxaldehyde (NDA) was purchased from Invitrogen (Carlsbad, CA).

2.2.2 Construction of the expression vector

The vector containing cDNA for rat CDO was obtained from the American Type Culture Collection (ATCC 3803501). The cloning of the cDNA gene into an expression vector was performed utilizing the Seamless Cloning System (Stratagene, La Jolla, CA). The T7 RNA polymerase-dependent expression vector pET21a (Novagen, Madison, WI) was amplified using the primers (5' CAG TCA CTC TTC CCA TAT GTA TAT CTC CTT CTT) and (5' GCT TGC CTC TTC ACT CGA GCA CCA CCA CCA CCA) and included the *Eam*1104 I restriction sites to produce *Nde* I and *Xho* I overhangs following digestion with the enzyme. The vector containing cDNA for rat CDO was PCR-amplified using the primers (5' ATA AGG CTC TTC GAT GAA CGG ACC GAG CTG CTG) and (5' CAG TTT CTC TTC CGA GTT AGT TGT TCT CCA GTG AAC C) which included the *Eam*1104 I restriction sites and engineered to produce *Nde* I and *Xho* I overhangs following digestion by *Eam*1104 I for ligation into the pET21a expression vector. DNA vectors containing representative clones were submitted for sequence analysis at Davis Sequencing (University of California, Davis).

2.2.3 Protein expression and purification

Plasmids containing the CDO gene were transformed into competent *E. coli* BL21(DE3) cells and stored as glycerol stocks at -80 °C. Cells from these stocks were isolated on LB-agar plates containing 0.1 mg/mL ampicillin (LB-amp). A single colony was selected for growth in 5 mL LB-amp media at 37 °C. A 1% inoculum from the 5-mL culture was used to inoculate a 100-mL flask of LB-amp media for growth overnight. A

2% inoculum of the overnight culture was used to inoculate each of four 1 L flasks that were incubated at 37 °C until the A_{600} value reached 0.4 – 0.5. The culture was induced with 0.4 mM IPTG and incubated at 25 °C for 6 hours. Purification of CDO was carried out using a standard buffer of 25 mM potassium phosphate buffer, pH 7.5 with 10% glycerol. Cells were harvested by centrifugation and resuspended in 100 mL standard potassium phosphate buffer containing 0.2 mg/mL lysozyme. The cell suspension was lysed by sonification followed by the addition of 1.5% streptomycin sulfate to the resulting supernatant to precipitate nucleic acids. The mixture was gently stirred at 4 °C for 1 hour, and the precipitated nucleotides were removed by centrifugation. The supernatant was applied to a Macro-Prep® High Q Support (Bio-Rad Laboratories, Hercules, CA) and eluted using a linear gradient from 0 – 150 mM sodium chloride in 25 mM standard potassium phosphate buffer. The purest fractions were determined by SDS-PAGE and pooled. Because potassium phosphate was found to interfere with activity measurements, CDO was concentrated by precipitating with 75% ammonium sulfate and resuspended in the desired volume of 25 mM HEPES buffer, pH 7.5, with 10% glycerol and 100 mM sodium chloride before iron loading with a of 1.2:1 molar ratio ferrous ammonium sulfate to protein. All samples were dialyzed twice against one liter of the resuspension buffer. The samples were divided into aliquots, flash frozen, and stored at -80 °C. Final protein concentration was determined by absorption spectroscopy at 280 nm using a molar extinction coefficient of 25,440 $M^{-1} \cdot cm^{-1}$ (*80*).

The amount of iron present in each preparation of CDO was determined by inductively-coupled plasma atomic emission spectroscopy (ICP-AES). Protein samples

(20 – 80 μM) were diluted 50-fold with 25 mM HEPES buffer, pH 7.5, in a final volume of 600 μL and analyzed using a Perkin Elmer Optima 7300 DV ICP-AES (Perkin Elmer Life Sciences, Fremont, CA). A standard curve was generated with atomic absorption iron standard (2.4 – 7.2 μM) in a total volume of 600 μL 25 mM HEPES buffer, pH 7.5. The results were the average from three separate experiments. The specific activity and steady-state kinetic parameters were corrected for the concentration of iron bound to CDO determined for each enzyme preparation. Additionally, all EPR experiments were quantitated using the known concentration of iron bound.

2.2.4 Assays

Activity assays were conducted using a Clark-type oxygen electrode (Hansatech, Inc., Norfolk, United Kingdom). Initial assays were performed to monitor the non-enzymatic oxidation of L-cysteine by ferrous iron. The assays were initiated by the addition of L-cysteine (10 mM) to a solution of ferrous ammonium sulfate (1 mM) at 37 ˚C (1 mL total volume) in 25 mM HEPES buffer, pH 7.5, and the reaction was monitored over five minutes. The reaction was then quenched and analyzed for production of cysteine sulfinic acid. Additional assays were performed to investigate buffers suitable for measuring the activity of CDO. These assays utilized buffer concentrations of 25 mM at pH values ranging from 6.1 to 8.5. The following buffers were tested: HEPES, MES, ammonium acetate, Tris-HCl, potassium phosphate, MOPS, and CAPS. After identifying an optimal buffer, standard reactions were initiated by the addition of 2.0 nmol CDO to a mixture of 10 mM L-cysteine and 25 mM HEPES buffer, pH 7.5, at 37 °C (1 mL total

volume). Assays containing an external reductant included 1 mM L-ascorbate. The background rate of cysteine oxidation in buffer with or without L-ascorbate was recorded for each reaction to ensure that no significant product was formed from side reactions prior to the addition of enzyme. The initial rate was determined by monitoring the decrease in oxygen concentration over 30 s. For experiments involving cell lysate, a 1% inoculum from a 5-mL overnight culture was used to inoculate a 100-mL flask of LB-amp media. The culture was induced at an A_{600} value of approximately 0.4 with 0.4 mM IPTG and incubated for 6 hours at 25 °C. Cells were resuspended in 5 mL of 25 mM HEPES, pH 7.5 and lysed by sonification. When measuring the activity of cell lysate, a total protein concentration of 2 μM was used in the assay. The total protein concentration of the cell lysate was determined using a Bradford assay (Bio-Rad Laboratories, Hercules, CA) with a calibration curve of bovine serum albumin (0 – 10 $mg \cdot mL^{-1}$). Each specific activity was calculated as the average of three separate experiments.

Steady-state kinetic assays were also conducted using an oxygen electrode to measure the consumption of oxygen by CDO. Steady-state kinetic parameters were determined by incubating 2.0 nmol of protein with varying L-cysteine concentrations (50 μM – 10 mM) in the presence or absence of 1 mM L-ascorbate in 25 mM HEPES buffer, pH 7.5, at 37 °C (1 mL total volume). Data were fit to the Michaelis-Menten equation using Kaleidagraph™ software. Each rate was calculated as the average of three separate experiments.

In order to evaluate the coupling between dioxygen consumption and cysteine sulfinic acid production, L-cysteine and cysteine sulfinic acid were labeled with NDA and resolved using high-pressure liquid chromatography (HPLC) (*79,81*). Coupling was determined by continuously monitoring oxygen consumption over a five-minute period to ensure the reaction was still linear, followed by quenching a 40-μL aliquot of the reaction with 200 μL of 1 M sodium borate, pH 9.5. The sample was filtered through a 0.22-μm syringe filter and derivatized by adding equal volumes (30 μL) of 2 mM NDA in acetonitrile and 2 mM cyanide in water. The sample was incubated in the presence of the derivatization solution for 20 minutes before diluting with 1.7 mL of 0.5% trifluoroacetic acid in 12.5 mM sodium phosphate, pH 7.2, and then 50 μL of the solution was injected into the HPLC. Separation was accomplished using a C-18 Novapak column (Waters Corporation, Milford, MA) with a linear gradient from 0 – 22% acetonitrile in 12.5 mM sodium phosphate, pH 7.2, with 0.5% trifluoroacetic acid. The derivatized compounds were detected with a Shimadzu RF-10axl fluorimeter (Shimadzu Scientific, Columbia, MD) at an excitation wavelength of 380 nm and an emission wavelength of 520 nm. Quantification was performed using a calibration curve constructed with known concentrations of cysteine sulfinic acid (2.5 – 250 μM). All measured values were collected as the sum of three separate experiments.

2.2.5 EPR spectroscopic measurements

Electron paramagnetic resonance (EPR) experiments were performed with approximately 100 μM CDO in 25 mM HEPES buffer, pH 7.5, 100 mM sodium chloride,

and 10% glycerol at 6 – 10 K. Spectra were collected using a Bruker EMX spectrometer (Bruker Biospin Corporation, Billerica, MA) at 9 GHz with a field modulation frequency of 100 kHz and amplitude of 0.6 mT. Cooling was performed with an Oxford Instruments ESR 900 flow cryostat and an ITC4 temperature controller. The EPR spectra were normalized by subtracting the spectrum of HEPES buffer. EPR spectra of cell lysate were also normalized using the spectrum of cell lysate containing a vector control lacking the CDO gene. The spectra of CDO obtained under various conditions utilized the following final concentrations where applicable: 6 mM L-cysteine, 10 mM hydrogen peroxide, 5 mM ferricyanide, 15 mM dithionite, or 50 mM L-ascorbate. Samples containing ferricyanide were normalized using the spectrum of 5 mM ferricyanide in 25 mM HEPES buffer, pH 7.5, 100 mM sodium chloride, and 10% glycerol. All spectra were obtained at 30 dB with a time constant 20.48 ms as the sum of 4 accumulations.

Nitric oxide binding experiments were performed with 80 μM CDO in 25 mM HEPES buffer, pH 7.5 with 10% glycerol and 100 mM sodium chloride (400 μL total volume). Anaerobic protein solutions were prepared by repeated evacuation and flushing with high-purity argon in an anaerobic cuvette. Reduced protein samples were generated by anaerobically incubating CDO with 15 mM dithionite for 15 minutes prior to reaction with nitric oxide. This same method was also used to prepare samples containing 6 mM L-cysteine. Nitric oxide was introduced into samples in the form of diethylamine nitric oxide (DEANO), which is a stable molecule in solutions above pH 8.0 but decomposes releasing two moles of nitric oxide and one mole of diethylamine at pH 7.5 used in the experiments (*82*). A final concentration of 100 μM DEANO (from a 20 mM stock

solution in 0.1 M sodium hydroxide) was allowed to react with the sample for approximately 15 minutes before transferring the sample to an EPR tube inside an anaerobic tent, flash freezing, and immediately measuring the spectrum. All spectra were obtained at 20 dB with a time constant of 655.35 ms. Quantitation of each signal was determined by double integration using the WinEPR software (Bruker Biospin Corp., Billerica, MA) and normalizing for the amount of iron incorporated by each sample.

2.3 Results

2.3.1 Analysis of CDO activity

L-Cysteine is unstable in solution and readily oxidizes to form cystine, cysteine sulfinic acid, and cysteine sulfonic acid over time (*83*). To minimize the non-enzymatic oxidation of cysteine, the reaction of CDO was continuously measured using a Clark-type oxygen electrode and this value was correlated with the amount of product formed in the reaction. This method has been used successfully to measure the activity of other oxygen-activating metalloenzymes (*84-87*). Similar to previously reported results, analysis of CDO by ICP-AES showed that the purified enzyme contains only 25 – 35% bound iron depending on the preparation. Several research groups supplement the assay with exogenous ferrous iron due to the substoichiometric ratio of iron coordinated to purified CDO (*52,53*). To determine if the addition of exogenous iron would have an effect on the background rate of dioxygen consumption in the absence of CDO, L-cysteine was incubated with ferrous iron in solution. No consumption of dioxygen was detected for ferrous iron in solution; however, the concentration of dioxygen dropped rapidly in the presence of 1 mM Fe(II) following the addition of 10 mM L-cysteine. This yielded the formation of 34 ± 6 nmol·min^{-1} of cysteine sulfinic acid. Because incubation of L-cysteine with exogenous iron increased the rate of dioxygen being consumed and yielded non-enzymatic product formation, exogenous iron was not included in

subsequent assays. To determine the effect of pH on non-enzymatic L-cysteine oxidation, L-cysteine was incubated in buffers with pH values ranging from 6.1 to 8.5. There was no observable dioxygen consumption at pH values exceeding 6.8, but considerable oxygen consumption corresponding to L-cysteine oxidation was observed at lower pH values (data not shown). HEPES buffer at pH 7.5 was chosen for subsequent studies because this buffer and pH had no appreciable effect on L-cysteine oxidation.

CDO in the absence of exogenous iron is reported to have negligible activity (*48*). To determine if inactivation of CDO is an artifact of purification, specific activity measurements were made with cell lysate containing expressed CDO and compared with purified recombinant CDO. Assays continuously monitored the consumption of dioxygen, and the activity was correlated with product formation by HPLC analysis. As a control, specific activity measurements were also made to determine the rate of oxygen consumed by cell lysate containing vector only, and this value was subtracted from the rate of oxygen consumption measured in the presence of the enzyme. Cell lysate containing expressed CDO was found to consume 3,800 ± 500 $nmol \cdot (min \cdot mg)^{-1}$ of oxygen, demonstrating that the enzyme is considerably active in the cellular environment (Table 2.1). Conversely, consumption of dioxygen by purified recombinant CDO was found to be comparable to the background rate of L-cysteine oxidation in the absence of enzyme (3.6 ± 0.1 $nmol \cdot (min \cdot mg)^{-1}$), and no product formation was detected (Table 2.1).

Table 2.1. Specific activity of CDO. Consumption of the dioxygen substrate by CDO (2 μM) was continuously monitored over five minutes at which point the reaction was quenched. Cysteine sulfinic acid production was quantified by fluorescence labeling aliquots of the reaction and resolving by HPLC. Reactions were carried out in 25 mM HEPES, pH 7.5 and 10 mM L-cysteine at 37 °C. Values in parentheses have been corrected using the known concentration of iron-bound enzyme as determined by ICP-AES. Each activity was determined as the average of three separate experiments.

	specific activity dioxygen consumption (nmol·(min·mg)$^{-1}$)	specific activity cysteine sulfinic acid production (nmol·(min·mg)$^{-1}$)
CDO in cell lysate	3,800 ± 500	N/D
purified CDO	3.6 ± 0.1	ND*
purified CDO + L-ascorbate	535 ± 100 (1,900 ± 400)	440 ± 120 (1,500 ± 400)

* No activity detected.

N/D Value not determined. Quantification of cysteine sulfinic acid production by cell lysate was not measured due to non-specific labeling of other components in the cell lysate by the fluorescence tag.

The previous results suggest that inactivation of CDO occurs during removal of the protein from the cellular environment. To determine whether or not this inactivation was caused by oxidation of the metal center, assays of purified CDO were run with the addition of L-ascorbate. Because CDO contains substoichiometric amounts of bound iron, it was necessary to correct for the concentration of iron-bound enzyme present in assays. CDO in the presence of L-ascorbate was catalytically active, consuming 540 ± 100 nmol·(min·mg)$^{-1}$ or 1,900 ± 400 nmol·(min·mg)$^{-1}$ of dioxygen when the iron-bound enzyme concentration was used (Figure 2.1) (Table 2.1). Likewise, this corresponded to the production of 440 ± 120 nmol·(min·mg)$^{-1}$ or 1,500 ± 400 nmol·(min·mg)$^{-1}$ for the iron-bound enzyme of cysteine sulfinic acid. The activity of CDO in the presence of L-ascorbate displayed saturation behavior and gave a k_{cat} value of 9.48 ± 0.40 min^{-1} and a K_m value of 0.11 ± 0.03 mM, resulting in a k_{cat}/K_m value of 89 ± 25 mM^{-1}·min^{-1} (Figure 2.2, open circles). This demonstrates that L-ascorbate can act as an appropriate external reductant for CDO by increasing the catalytic efficiency of the enzyme. When the kinetic parameters were calculated using the iron-bound enzyme concentration, the k_{cat}/K_m value was 254 ± 72 mM^{-1}·min^{-1} (Figure 2.2, closed circles).

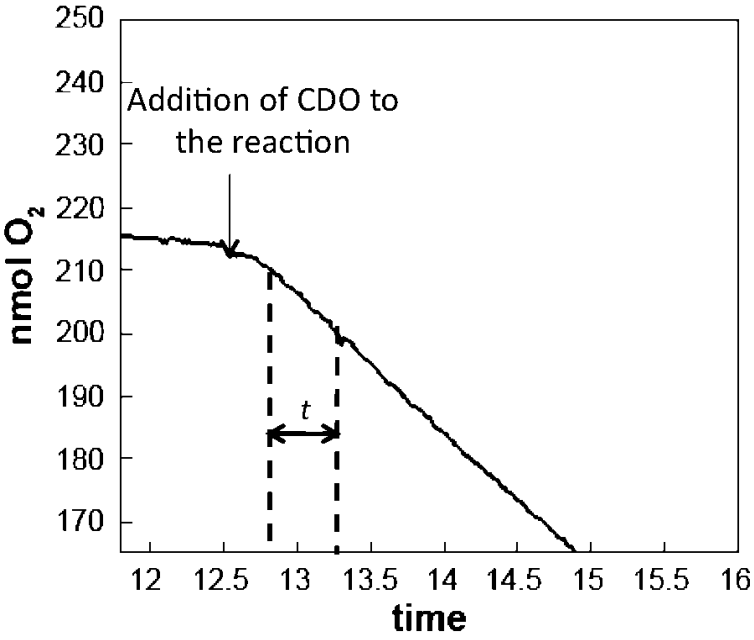

Figure 2.1 Consumption of dioxygen by CDO in the presence of 1 mM L-ascorbate. CDO activity was determined by measuring the rate of dioxygen consumption of 2.0 nmol of enzyme in the presence of varying concentrations of L-cysteine (50 μM – 10 mM) and 1 mM L-ascorbate in 25 mM HEPES, pH 7.5 at 37 °C over 30 s, denoted by the variable *t*.

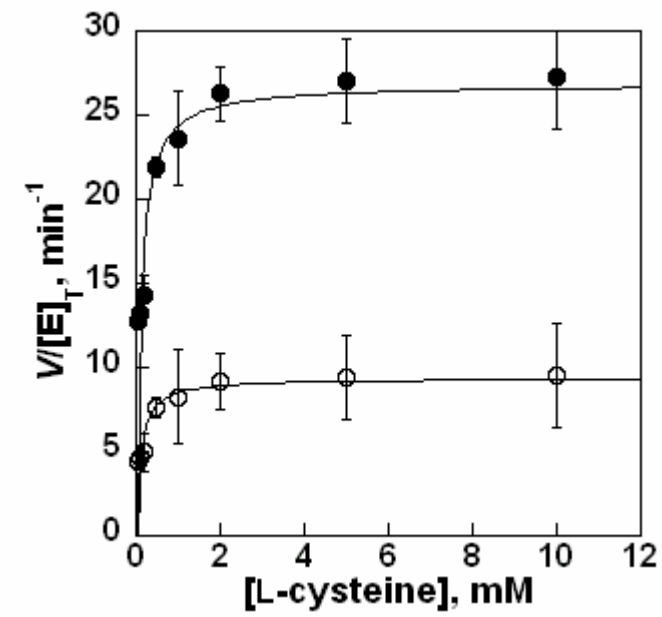

Figure 2.2 Apparent and corrected kinetic traces of wild-type CDO at varying concentrations of L-cysteine (50 μM – 10 mM). Steady-state kinetic parameters were determined by measuring the consumption of dioxygen by CDO in 25 mM HEPES, pH 7.5 and L-ascorbate (1 mM) at 37 °C. The initial concentration of dioxygen in air-saturated buffer was approximately constant between experiments at 220 μM. Each trace is the average of three separate experiments. Apparent rates (○) were calculated directly from the measured consumption of oxygen. Corrected rates (●) were calculated by adjusting the total enzyme concentration using the stoichiometric iron incorporation measured by ICP-AES.

2.3.2 EPR analysis of the CDO metal center

In order to determine if the increased activity observed for CDO in cell lysate was due to reduction of the metal center, EPR spectra of cell lysate containing expressed CDO were obtained. The EPR spectrum of cell lysate containing expressed CDO was normalized using the spectrum of cell lysate containing a vector-only control to correct for the presence of other metalloenzymes in the cell lysate. Spectra of cell lysate containing expressed CDO showed no observable EPR signal, suggesting that the majority of the enzyme was in the EPR silent Fe(II) form observed for enzymes containing a 2-His/1-carboxylate facial triad (Figure 2.3a). To determine if the lack of an observable signal was due to reduced CDO rather than an insufficient concentration of CDO, the cell lysate was incubated with ferricyanide. The spectra of cell lysate containing expressed CDO and ferricyanide showed a distinct Fe(III) signal representing oxidized enzyme that was not observed in the lysate of vector-only control with ferricyanide (Figure 2.3b). This Fe(III) signal at $g = 4.3$ is consistent with the oxidized signal obtained for enzymes containing a 2-His/1-carboxylate facial triad. This suggested that the lack of an EPR signal present in the cell lysate containing expressed CDO was due to a reduced iron center, and further suggested that reduced iron is the active oxidation state of the metal center.

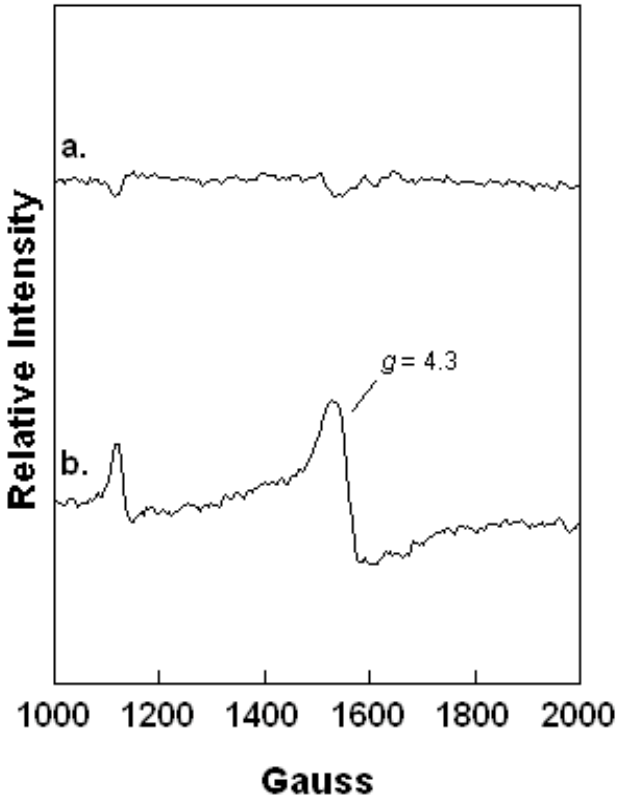

Figure 2.3 EPR spectra of CDO expressed in cell lysate. (*a*) Cell lysate containing expressed CDO. The spectrum of CDO in cell lysate was normalized with the spectrum of lysate containing a vector-only control. (*b*) Cell lysate containing expressed CDO in the presence of 5 mM ferricyanide. The spectrum of CDO in cell lysate with ferricyanide was normalized with the spectrum of vector-only lysate incubated with 5 mM ferricyanide. EPR spectra of cellular lysate utilized cells that had been incubated in the presence of 0.4 mM IPTG for three hours prior to lysing in 25 mM HEPES, pH 7.5, 100 mM sodium chloride and 10% glycerol. All spectra were obtained at 8 K.

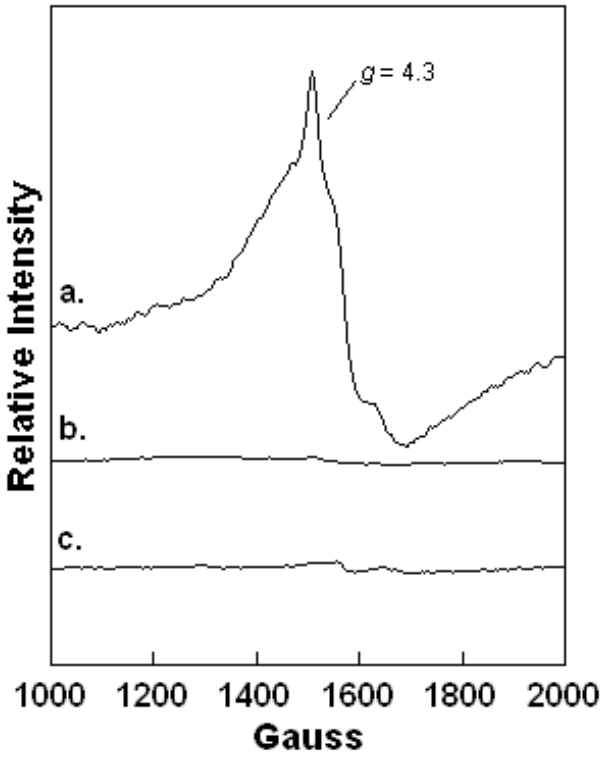

Figure 2.4 EPR spectra of CDO following purification. (*a*) Purified CDO. (*b*) Purified CDO in the presence of 15 mM dithionite. (*c*) Purified CDO in the presence of 50 mM L-ascorbate. EPR spectra of purified CDO were obtained using approximately 100 μM protein in 25 mM HEPES, pH 7.5, 100 mM sodium chloride, and 10% glycerol. All spectra were obtained at 8 K.

Because a decrease in activity is observed for purified CDO compared with CDO in cell lysate, EPR analysis was performed to determine if the metal center of CDO is oxidized following purification. The spectrum of purified CDO showed a high-spin Fe(III) signal (S = 5/2) that was not consistent with the oxidation state observed for CDO in cell lysate but rather the signal obtained for oxidized non-heme iron (Figure 2.4a). The addition of 15 mM dithionite reduced the signal to the EPR silent Fe(II) form (S = 2), confirming that the resting state observed for the purified enzyme was Fe(III) (Figure 2.4b). Oxidation of purified CDO in the resting state by either hydrogen peroxide or ferricyanide failed to induce an increase in the EPR signal (data not shown). Double integration of the resting state and oxidized EPR signals showed that the signal intensity varied by less than 0.01 indicating that the amount of Fe(III) present in purified CDO represents greater than 99% of the total spin count. Additionally, to correlate the increase in activity observed in the presence of L-ascorbate with the conversion of Fe(III) to Fe(II), a spectrum was obtained with a comparable molar ratio of L-ascorbate to CDO utilized in the activity assays. The iron center of CDO in the presence of reductant was found to be primarily Fe(II) (Figure 2.4c), confirming that the increase in activity observed in the presence of the reductant was attributable to a change in the oxidation state of the metal center. In addition, there was no apparent quenching of the ferric EPR signal with the addition of L-cysteine (up to 6 mM) to the sample, further confirming the inability of L-cysteine to reduce the iron center (Figure 2.5b). Addition of L-cysteine did result in a sharpening of the signal peak, indicating a change in the coordination environment of the metal induced by substrate binding (Figure 2.5b).

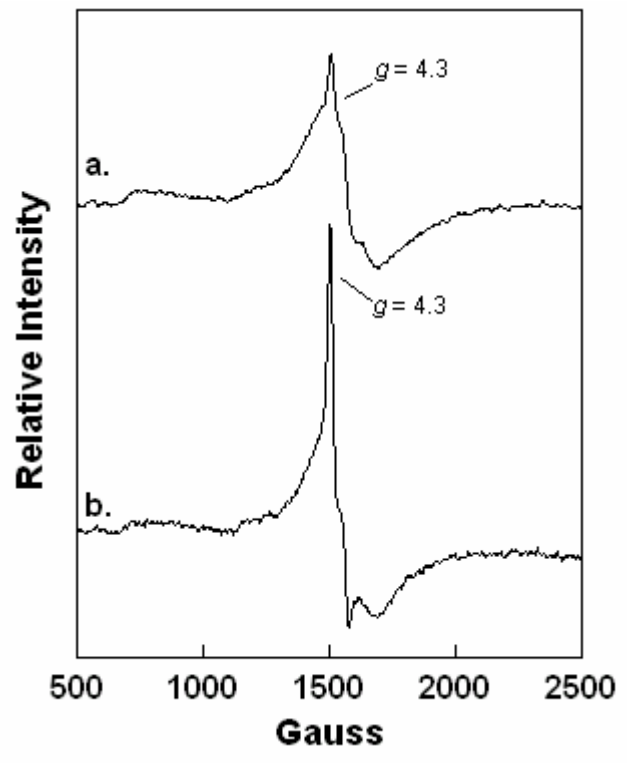

Figure 2.5 EPR spectra of CDO with and without L-cysteine. (*a*) CDO. (*b*) CDO in the presence of 6 mM L-cysteine. All EPR spectra were obtained using approximately 100 μM protein in 25 mM HEPES, pH 7.5, 100 mM sodium chloride, and 10% glycerol at 8 K.

2.3.3 Analysis of nitric oxide coordination

To probe the reactivity of the resting metal site in recombinant CDO, nitric oxide was utilized as a catalytically inactive yet spectrally active analog of dioxygen. Studies with the dioxygen analog nitric oxide have shown that the binding of substrate to CDO occurs by an ordered mechanism similar to several of the 2-His/1-carboxylate (*5,54,88,89*). The binding of L-cysteine to CDO likely frees a coordination site to the iron, allowing dioxygen to bind. Addition of nitric oxide into protein samples can introduce two molecules of nitric oxide per enzyme metal center, making analysis of the physiologically relevant signal problematic (*90*). In order to stoichiometrically control the concentration of nitric oxide reacted with CDO, a NONOate was used in place of pure nitric oxide gas. In order to avoid over occupation of the metal center, the ratio of nitric oxide to CDO was held at 2.2:1. The EPR signal observed at this ratio is consistent with previously reported signals for other non-heme ferrous centers (*76-78*). Samples of oxidized CDO were incubated with and without L-cysteine to evaluate the effects of L-cysteine binding on nitric oxide coordination. The spectrum of CDO in the presence of nitric oxide was indistinguishable from that of untreated purified CDO (Figure 2.6a). Similarly, when CDO was incubated with L-cysteine prior to reaction with nitric oxide, the spectrum was nearly indistinguishable from the spectrum for CDO incubated with L-cysteine with a small amount of signal at g = 4.0 detected (Figure 2.6b). To determine the effects of an external reductant on nitric oxide coordination, these experiments were repeated with anaerobic pre-incubation of CDO and dithionite. CDO in the presence of dithionite and nitric oxide showed trace complexation with nitric oxide (Figure 2.6c);

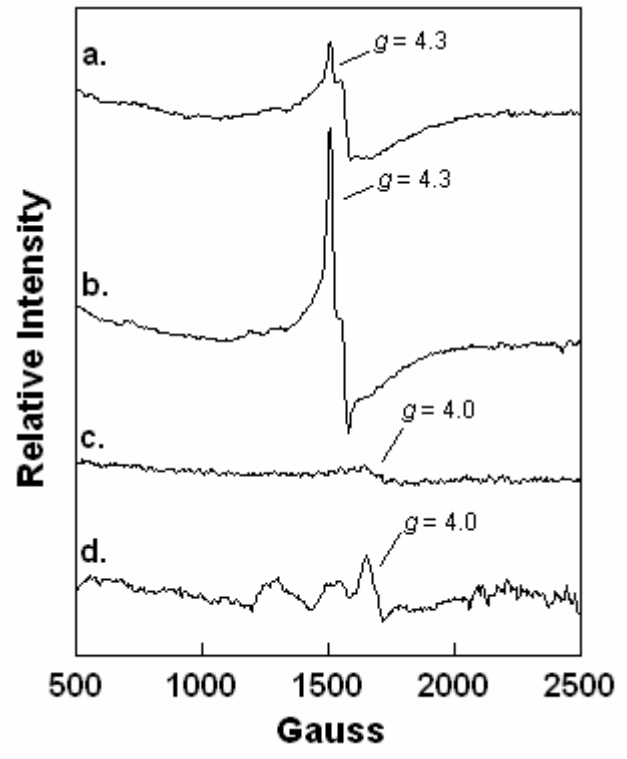

Figure 2.6 EPR spectra of CDO incubated with nitric oxide. (*a*) CDO in the presence of nitric oxide (*b*) CDO in the presence of nitric oxide and 6 mM L-cysteine. (*c*) CDO in the presence of nitric oxide and 15 mM dithionite. (*d*) CDO in the presence of nitric oxide, 6 mM L-cysteine, and 15 mM dithionite. All EPR spectra were obtained using approximately 80 μM protein and 100 μM DEANO in 25 mM HEPES, pH 7.5, 100 mM sodium chloride, and 10% glycerol at 8 K.

however, CDO in the presence of dithionite, L-cysteine, and nitric oxide showed a distinct signal at g = 4.0 (Figure 2.6d). Double integration of each spectrum at g = 4.0 showed that reduced CDO coordinates approximately 90% more nitric oxide when pre-incubated with L-cysteine. Results from the integration of the spectra of CDO and L-cysteine in the presence and absence of an external reductant showed that the enzyme coordinates greater than 99% more nitric acid when pre-incubated with dithionite. These results suggest that any complexation with nitric oxide observed in the absence of dithionite may be attributed to the trace amounts of ferrous iron in the purified enzyme (less than 1% of the total iron) and that the oxidized form of the enzyme in the presence of L-cysteine is unreactive with the dioxygen analog.

2.4 Discussion

Recombinant CDO has been expressed and purified by several groups, and the as-isolated protein typically exhibits low activity (*6,8,51,52*). Because of the low levels of iron bound (approximately 10 – 70%) to the recombinant enzyme, several CDO assays include exogenous ferrous iron (*51,52*). The studies reported herein show that product is produced non-enzymatically in the presence of ferrous iron and L-cysteine alone, and therefore the addition of exogenous iron to the assay may lead to erroneous results. Other groups that do not include exogenous iron utilize extended incubation times to obtain sufficient product formation for quantitation (*6,8,51*), but this also yields a large error associated with background oxidation of the L-cysteine substrate. Buffers used in assays of CDO range in pH values from 6.1 – 7.5; however, these studies indicate that L-cysteine is readily oxidized at pH values below 6.8 in the absence of enzyme. Based on these results, an assay to minimize the non-enzymatic oxidation of L-cysteine was developed in order to evaluate the activity of CDO.

The CDO enzyme from rat liver was catalytically active in liver supernatant, but was inactivated when removed from the cellular environment (*48*). It was speculated that the enzyme becomes inactivated by the oxidation of the metal center to Fe(III) (*48*);

however, this postulation was never tested. Indeed, the low activity consistently reported for CDO suggests that CDO is not in the correct oxidation state for catalysis. As shown in these studies, the low activity presumed to be due solely to substoichiometric amounts of bound iron cannot be alleviated simply by the addition of excess iron because of non-enzymatic oxidation of cysteine. In order to shed light on several inconsistencies reported in the literature, the active redox state of the metal center of CDO was evaluated by combining kinetic and spectroscopic approaches. An oxygen electrode was used to continuously measure the consumption of the dioxygen substrate, and this rate was correlated directly with product formation by HPLC analysis. Incubation of purified CDO with L-cysteine in oxygenated buffer consumed little dioxygen, yielding a specific activity of 3.6 ± 0.1 nmol·(min·mg)$^{-1}$. There was no measurable product formed, confirming the initial observation that purified recombinant CDO is catalytically inactive. Conversely, incubation of cell lysate containing expressed CDO with L-cysteine showed an increase in specific activity of over three orders of magnitude compared with purified CDO, also consistent with previous reports that the enzyme shows considerable activity in lysate (*48*). The difference between these two specific activities suggests that there is an inactivation of CDO occurring when the enzyme is removed from the reducing environment of the cell. To determine the susceptibility of the iron center of CDO to oxidation, EPR spectra of CDO still present in cell lysate and following purification were compared. The spectrum of purified CDO shows a distinct signal at $g = 4.3$ consistent with high-spin Fe(III) indicating that the metal center in the purified enzyme exists in a partially oxidized state. This signal was quenched to the EPR silent Fe(II) form of the

enzyme upon addition of reductant confirming that the observed signal in the resting enzyme was derived from oxidized iron. Double integration of the EPR signal was performed in order to determine what fraction of the total iron present in purified CDO contributes to the Fe(III) signal at $g = 4.3$. Samples of CDO were incubated with either hydrogen peroxide or ferricyanide in order to fully oxidize the protein, and these spectra were used as standards for comparison. Addition of various concentrations of either hydrogen peroxide or ferricyanide failed to induce an increase in the Fe(III) signal. Quantification of the signal indicated that greater than 99% of the spin count obtained for purified CDO contributed to the ferric signal observed (represented by a signal increase from 18.73 to 18.97). The EPR spectrum of cell lysate containing expressed CDO showed no signal corresponding to the ferric iron at $g = 4.3$; however, a strong signal at this g value was obtained when the sample was oxidized with ferricyanide. Absence of the $g = 4.3$ signal in the resting state shows that CDO is capable of stabilizing the ferrous state of its metal center in a cellular environment. The combined results from EPR and activity analyses further suggest that the resting iron in recombinant purified CDO is Fe(III).

To determine the effects of a reductant on the redox state of the metal center, the specific activity and EPR spectra of CDO were determined in the presence of L-ascorbate. A specific activity of 540 ± 100 nmol·(min·mg)$^{-1}$ was observed following the addition of L-ascorbate. While this activity is lower than that measured for CDO present in cell lysate, purified CDO contains substoichiometric amounts of iron. When the concentration of iron bound to CDO is taken into account, the specific activity increases

to 1,900 ± 400 nmol·(min·mg)$^{-1}$, comparable to the activity measured for CDO present in cell lysate. EPR analysis confirmed that the addition of L-ascorbate reduced the metal center to the EPR-silent ferrous form. These results suggest that the low activity measured for the purified protein is likely due to both the oxidation state of the iron and the low amount of iron incorporated into the recombinant enzyme. Addition of an external reductant had a direct impact on the kinetic parameters previously reported for recombinant CDO (*6,8,51,52)*. When the enzyme was assayed in the presence of an external reductant, the k_{cat}/K_m value of the enzyme increased 50-fold from the previously reported values (1.7 mM^{-1}·min^{-1} to 89 ± 25 mM^{-1}·min^{-1}) (*6*). Addition of L-ascorbate to steady-state assays reduced the K_m value from 2.1 to 0.11 ± 0.03 mM. The measured concentration of free cysteine in rat liver is approximately 0.1 mM, comparable to the K_m determined for CDO in the presence of a reductant (*59*). When the concentration of iron-bound enzyme is taken into account, the k_{cat}/K_m value for the enzyme is increased to 254 ± 72 mM^{-1}·min^{-1} suggesting that the activity observed for CDO using a continuous assay in the presence of an external reductant is a more reliable method to evaluate the kinetic parameters.

Several members of the 2-His/1-carboxylate family of enzymes utilize an ordered binding mechanism where coordination of the active site metal by the non-oxygen substrate frees a metal coordination site and lowers the reduction potential thus priming the metal to react with dioxygen (*5,12,13*). Many of the enzymes that belong to this family do not require the presence of an external reductant for this reaction to occur as

the metal center is stabilized in the reduced form. Nitric oxide experiments were performed in order to determine if the metal center of CDO was in the correct oxidation state for reaction with dioxygen. The resting form of the enzyme was unreactive with nitric oxide in the presence or absence of L-cysteine. When CDO was reduced and complexed with L-cysteine prior to reaction with nitric oxide, a distinct signal at $g = 4.0$ corresponding to coordination of the metal center by nitric oxide was observed. Integration of the signal at $g = 4.0$ reveals that reduced CDO pre-incubated with L-cysteine coordinates approximately 90% more nitric oxide than CDO in the absence of the cysteine substrate. This provides evidence that resting CDO is not poised to react with nitric oxide and supports the previously determined ferric state of the resting enzyme.

The results reported herein suggest that the resting iron of CDO is not in the correct oxidation state for catalysis, and that adding exogenous ferrous iron to the assay leads to falsely inflated catalytic measurements. Although previous studies have suggested that CDO is in the ferrous state following purification, these studies utilized purification and assay conditions that could lead to incorrect interpretation of the spectroscopic data or in non-enzymatic oxidation of L-cysteine (*6,8,51,52*). Therefore, the oxidation of the metal center combined with substoichiometric iron incorporation likely accounts for the less than optimal activity observed for CDO. Currently proposed catalytic mechanisms for CDO are based on the mechanism determined for the extradiol dioxygenases (*6,53,54*). Extradiol dioxygenases coordinate their mononuclear ferrous active site metals using a 2-His/1-carboxylate facial, and the electron-donating quality of

the carboxylate ligand and catechol substrates allows them to maintain the ferrous state of the enzyme (*5,12,54*). The metal center of CDO is coordinated by a facial triad composed of three histidine residues. The lack of a carboxylate-donating ligand and the demonstrated susceptibility of the metal center in CDO to oxidation implies that the reduction potential of the metal center likely differs between the 3-His and 2-His/1-carboxylate facial traids. The substoichiometric amount of iron bound to CDO following purification has never been fully addressed, and may be due to an instability of the iron center in an oxidizing environment. Another 3-His ferrous enzyme belonging to the cupin family, Dke1, was shown to be readily deactivated in the presence of dioxygen (*75*). It was shown that the inactivation was due to the oxidation of Fe(II) to Fe(III) followed by the release of Fe(III) from the enzyme. Therefore, enzyme deactivation in the presence of an oxidizing environment may be a common feature in the 3-His cupin enzymes. These results suggest that oxygen toxicity of CDO needs to be minimized during purification, and provides the foundation on which the mechanistic properties of the enzyme can be studied.

Chapter Three

Determining the Effects of the Cys-Tyr Crosslink on Catalysis in Cysteine Dioxygenase

3.1 Introduction

Cysteine dioxygenase (CDO) is a mononuclear, non-heme iron enzyme that catalyzes the conversion of L-cysteine to cysteine sulfinic acid (*44*). Cysteine sulfinic acid is the precursor for two separate pathways that synthesize pyruvate and inorganic sulfur or taurine. CDO plays a crucial role in maintaining cellular cysteine, sulfate, and taurine levels, and an imbalance in the equilibrium of these sulfur-containing molecules has been implicated in a variety of immune, cardiac, and neurological disorders (*38,40*).

Although CDO shows low amino acid sequence identity to other proteins, it is a member of the Cupin superfamily and has been identified in both prokaryotic and eukaryotic organisms (*91*). The superfamily contains two conserved sequence motifs that coordinate the metal center: $G(X)_5HXH(X)_{3,4}E(X)_6G$ and $G(X)_5PXG(X)_2H(X)_3N$. The metal of most Cupin proteins is typically coordinated by the glutamate and two histidine residues from the first sequence and the histidine residue in the second sequence. The metal center of CDO is coordinated by the three conserved histidine residues with the glutamate residue from the first motif replaced by Cys93. Interestingly, the reported

three-dimensional structures reveal an unusual thioether linkage between Cys93 and Tyr157 located near the metal center within the active site. While the Tyr157 residue is conserved in all known forms of CDO, Cys93 is replaced by a glycine residue in yeast and prokaryotic organisms, disabling crosslink formation (*91*).

The Cys-Tyr linkage in CDO is structurally analogous to the active site crosslink identified in galactose oxidase where the linkage serves as a redox-active cofactor in catalysis (*69*). The crosslinked and non-crosslinked isoforms of galactose oxidase resolve as species of apparently differing molecular weight on SDS-PAGE, and this difference in migration behavior has also been observed for the crosslinked and non-crosslinked isoforms of CDO. Mass-spectroscopic analysis of the two bands observed for CDO indicates that the species of apparently higher molecular weight is the non-crosslinked isoform, and early characterization of the enzyme indicated that this isoform was responsible for all catalytic activity. Interestingly, removal of the crosslink in CDO by site-directed mutagenesis does not abolish the catalytic ability of the enzyme. Despite reports that a single isoform is responsible for activity and that C93S and Y157F CDO enzymes are catalytically competent, the thioether linkage repeatedly has been proposed to be relevant to the catalytic efficiency of CDO. The covalent linkage between Cys93 and Tyr157 has been contended to increase the catalytic efficiency of CDO by positioning the tyrosine hydroxyl group for optimal catalytic base interactions (*6,8,59*). Alternatively, the linkage has been hypothesized to protect this area of the active site from oxidation during catalytic turnover (*8*).

In order to ascertain if the thioether linkage in CDO leads to a catalytic or structural advantage, populations of CDO homogenously containing the crosslink were isolated and assayed for activity. Surprisingly, the resulting species was found to be catalytically inactive suggesting that the thioether linkage adversely affects the structural and catalytic properties of the enzyme. This result was further confirmed by the lack of crosslinked isoform present in cell lysate where CDO displays considerable catalytic ability. In order to probe the inactivation of CDO by crosslink formation, a two-fold approach was taken. Initially, preparations of homogenously crosslinked CDO were probed spectroscopically to study the effects of thioether bond formation on the metal coordination environment, substrate binding, and structural stability of the enzyme. Finally, formation of the thioether linkage was disrupted by generating C93S and Y157F substitutions to probe the structural and catalytic relevance of these residues in the absence of the crosslink. These results provide insight into the instability and decreased iron incorporation reported for recombinant CDO and, because crosslinked CDO is catalytically inactive, provide evidence for the importance of isolation of CDO in the non-crosslinked isoform for future characterization of the enzyme.

3.2 Material and Methods

3.2.1 Materials

Potassium phosphate (monobasic anhydrous and dibasic anhydrous), 4-(2-hydroxyethyl)-1-piperazineethanesulfonic acid (HEPES), 2-(*N*-morpholino)ethanesulfonic acid (MES), 3-(*N*-morpholino)propanesulfonic acid (MOPS, sodium chloride, ampicillin, diethylamine nitric oxide (DEANO), sodium hydrosulfite (dithionite), streptomycin sulfate, L-ascorbate, ammonium sulfate, ferrous ammonium sulfate, trifluoroacetic acid, sodium cyanide, and L-cysteine were purchased from Sigma (St. Louis, MO). Isopropyl-β-D-thiogalactoside (IPTG), glycerol, boric acid, lysozyme, acetonitrile, and sodium phosphate (monobasic anhydrous and dibasic anhydrous) were purchased from Fischer Biotech (Pittsburg, PA). Difco-brand Luria-Bertani (LB) media was purchased from VWR (West Chester, PA). Napthalene dicarboxaldehyde (NDA) was purchased from Invitrogen (Carlsbad, CA).

3.2.2 Construction of expression vectors, protein expression, and purification

Construction of the vector containing cDNA for rat CDO was performed as previously described. All mutants were constructed using the QuikChange Site-directed Mutagenesis kit from Stratagene. Primers were designed as 29 base oligonucleotides containing the appropriate substitution. Substitutions were made by replacing the wild-

type codon with the most frequently utilized codon for the variant amino acid by *E. coli*. The codons used for the substitutions were AGC (serine), TTT (phenylalanine), and GCG (alanine). Presence of the desired gene or mutation within the expression vector was confirmed by DNA sequence analysis.

Protein expression, purification, and iron binding determination were carried out as described in Chapter 2 with minor variations. An additional chromatographic step was added prior to dialysis to increase protein purity. Fractions pooled from the anionic exchange column were treated with 20% ammonium sulfate and applied to a hydrophobic Phenyl Sepharose 6 Fast Flow column (GE Healthcare Bio-Sciences, Uppsala, Sweden). Protein was eluted from the hydrophobicity column using a linear gradient from 20 – 0% ammonium sulfate buffer in 25 mM potassium phosphate, pH 7.5 with 10% glycerol. The purity of fractions was determined by SDS-PAGE, and the purest fractions were pooled, resuspended in 25 mM HEPES, pH 7.5 with 100 mM sodium chloride and 10% glycerol, iron loaded, and dialyzed as previously described.

3.2.3 Crosslinking reactions

Formation of the thioether linkage was accomplished by two separate methods. Homogenously crosslinked CDO used in activity assays was prepared by incubating 50 μL of protein ranging from 10 – 70 μM in 25 mM HEPES buffer, pH 7.5, 100 mM L-cysteine, and 1 mM ferrous ammonium sulfate in a total volume of 100 μL for twelve to fourteen hours at room temperature. Homogenously crosslinked CDO used in EPR experiments was prepared by incubating 25 μL of protein ranging from 80 – 200 μM in

50 mM MES buffer, pH 6.1, 200 mM L-cysteine, and 2 mM ferrous ammonium sulfate in a total volume of 100 μL for two hours at room temperature. Subsequent to crosslink formation, excess iron and cysteine were removed from protein samples using a HiTrap™ desalting column (Amersham Biosciences, United Kingdom) equilibrated with 25 mM HEPES, pH 7.5, with 100 mM sodium chloride and 10% glycerol. Completion of each crosslinking reaction was confirmed by SDS-PAGE. The final protein concentration was determined by measuring the absorbance at 280 nm and iron incorporation determined by ICP-AES. To determine if the iron bound to homogenously crosslinked CDO after gel filtration was stable over time, samples were dialyzed twice against 2 L of 25 mM HEPES buffer, pH 7.5 with 100 mM sodium chloride and 10% glycerol for three hours and then analyzed for iron incorporation using ICP-AES.

3.2.4 Assays

Activity assays were conducted using a Clark-type oxygen electrode (Hansatech, Inc., Norfolk, United Kingdom). Reactions were initiated by the addition of 2.0 nmol CDO to a mixture of 10 mM L-cysteine, 1 mM L-ascorbate, and 25 mM HEPES buffer, pH 7.5, at 37 °C in a total volume of 1 mL. The initial rate was determined by monitoring the decrease in oxygen concentration within 30 s. When measuring the activity of cell lysate, the cell lysate was obtained as described in Chapter 2 and a total protein concentration of 2 μM was used in the assay. The total protein concentration of the cell lysate was measured using a Bio-Rad protein assay and determined using a calibration curve from 0 – 10 mg/mL constructed with bovine serum albumin as a

standard. Steady-state kinetic assays were performed as described in Chapter 2. Dioxygen consumption was correlated with product formation by fluorescence labeling of cysteine sulfinic acid and resolution by HPLC as previously described in Chapter 2.

3.2.5 EPR measurements

EPR experiments were performed on wild-type (100 μM), C93S (100 μM), Y157F (100 μM), and homogenously crosslinked wild-type (70 μM) CDO proteins in 25 mM HEPES buffer, pH 7.5 with 10% glycerol and 100 mM sodium chloride at 4 – 8 K. Spectra were collected using a Bruker EMX spectrometer (Bruker Biospin Corp., Billerica, MA) at 9 GHz with a field modulation frequency of 100 kHz and amplitude of 0.6 mT. Cooling was performed with an Oxford Instruments ESR 900 flow cryostat and an ITC4 temperature controller. The EPR spectra were normalized by subtracting out the buffer spectrum and obtained as the sum of 4 scans. Spectra of variant and homogenously crosslinked CDO proteins with L-cysteine and nitric oxide were obtained as previously described in Chapter 2. Quantitation of each signal was determined by double integration using the WinEPR software (Bruker Biospin Corp., Billerica, MA) and normalizing for the amount of iron incorporated by each sample.

3.3 Results

3.3.1 Vector construction and protein purification

In order to study the roles of the crosslinked residues in the absence of the thioether linkage and to provide controls for crosslinking experiments, site-directed mutagenesis was performed to disrupt crosslink formation. Single-variant constructs were made to replace Cys93 and Tyr157 with the conservative substitutions serine and phenylalanine, respectively. In addition, two of the three histidine metal ligands (His86 and His88) were substituted with alanine residues to assess the role of the metal center in crosslink formation. Successful mutation of the desired residues was confirmed by DNA sequence analysis. The variant constructs yielded soluble proteins and were purified using a modification of the protocol described for wild-type CDO. The resulting yield was 10 – 20 $mg \cdot mL^{-1}$, similar to the amount of protein obtained with wild-type CDO. Consistent with previous reports, C93S and Y157F CDO resolved as single molecular weight species corresponding to the non-crosslinked isoform of CDO (*42*). Additionally, H86,88A CDO resolved only as a single molecular weight species indicating there was no apparent crosslink formation with this variant.

The activity of CDO is dependent on the presence of iron in the active site, so the amount of iron bound to the variant and wild-type CDO proteins was determined by ICP-AES. Samples from each protein purification were analyzed and these values were utilized to correct for the iron bound enzyme concentration in activity and EPR measurements. Wild-type CDO was found to contain 25 – 35% iron incorporation. Both C93S CDO and Y157F CDO contained comparable amounts of iron at 24 – 47% and 7 – 27%, respectively. H86,88A CDO was found to incorporate 2.4 ± 0.1% moles of iron per mole of enzyme, verifying that these residues are essential for proper coordination of the iron in CDO.

3.3.2 Preparation of homogenously crosslinked CDO

All previous kinetic assays for CDO have utilized a mixture of crosslinked and non-crosslinked isoforms (*6,8,51,52*). To determine the catalytic and spectroscopic properties of wild-type CDO in the homogenously crosslinked isoform, a method for isolating crosslinked CDO was developed. A previous report indicated that crosslink formation is pH-dependent and can be induced by incubating protein samples with L-cysteine (*59*). This previous study used a pH of 6.1 and yielded complete crosslink formation in 10 minutes. To determine conditions that would yield homogenously crosslinked CDO stable enough for spectroscopic and activity analyses, several incubation times were investigated at different pH values. Both crosslink formation and non-enzymatic L-cysteine oxidation have been shown to increase at pH values below 6.8. For activity analysis, crosslinking was accomplished by incubating wild-type CDO with

excess L-cysteine and ferrous iron overnight at pH 7.5 to minimize side reactions between cysteine and iron with dioxygen. Incubation overnight was necessary to ensure complete crosslink formation at the elevated pH. For spectroscopic analysis of crosslinked CDO, crosslinking was carried out at pH 6.1 and could be accomplished in two hours. This shorter incubation time resulted in increased protein stability than the overnight incubation used for activity measurements and yielded concentrations of crosslinked CDO adequate for spectroscopic measurements. Both preparation methods used for activity and spectroscopic analysis yielded homogenous populations of approximately 23 kDa as observed by SDS-PAGE, consistent with homogenously crosslinked CDO (Figure 3.1 lane 2). To probe the effects of the crosslinking reaction on the spectroscopic and catalytic properties of CDO, C93S CDO was used as a catalytically active variant incapable of forming the thioether linkage. H86,88A CDO was used to determine the effects of proper iron coordination on crosslink formation. Each variant was incubated with free L-cysteine and ferrous iron overnight at pH 7.5, and both resulting protein samples resolved as single molecular weight species consistent with the approximately 25 kDa band observed for wild-type CDO by SDS-PAGE (Figure 3.1 lanes 4 and 6). This indicates that both the thiol of Cys93 and proper coordination of the metal center by the 3-His facial triad in CDO are critical elements in crosslink formation.

Because free cysteine and iron are redox-active molecules that could interfere with activity or spectroscopic measurements, precautions were taken to remove these small molcules from protein samples subsequent to crosslink formation. Crosslinked protein samples used for activity and spectroscopic measurements were purified from low

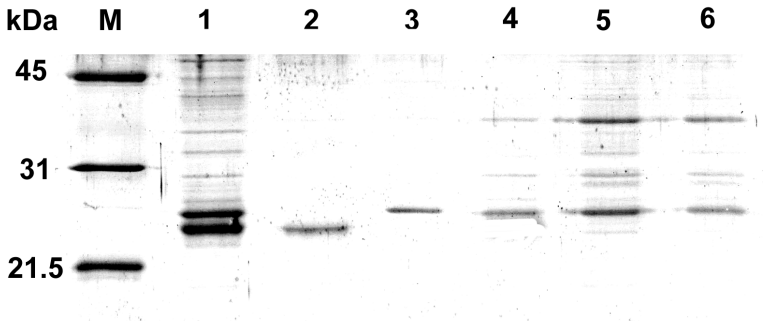

Figure 3.1 Analysis of crosslinked CDO samples by SDS-PAGE. (*M*) Molecular weight marker. (*1*) Wild-type CDO, (*2*) Wild-type CDO after overnight incubation with 100 mM L-cysteine and 1 mM ferrous ammonium sulfate, (*3*) C93S CDO, (*4*) C93S CDO after overnight incubation with 100 mM L-cysteine and 1 mM ferrous ammonium sulfate, (*5*) H86,88A CDO, (*6*) H86,88A CDO after overnight incubation with 100 mM L-cysteine and 1 mM ferrous ammonium sulfate. Samples were resolved on a 15% acrylamide gel after boiling at 90 °C in the presence of SDS and β-mercaptoethanol.

molecular weight compounds using gel filtration chromatagraphy, and the resulting protein concentrations were determined using UV spectroscopy with a molar extinction coefficient of 25,440 $M^{-1} \cdot cm^{-1}$ at 280 nm (*80*). Although some protein loss resulted from overnight incubation of variant and wild-type CDO enzymes with L-cysteine and free ferrous iron, samples of C93S and H86,88A retained more protein stability than wild-type CDO under the same conditions. This indicates that the crosslinked isoform is less stable than the non-crosslinked isoform of the enzyme. The metal-binding affinity of crosslinked CDO was analyzed by ICP-AES. Subsequent to gel filtration chromatography, crosslinked CDO contained 13.5 ± 0.7% iron per active site. To probe the stability of this iron in the active site, samples were dialyzed to determine whether or not the bound iron was released over time. Dialysis of crosslinked CDO decreased the iron incorporation of the enzyme to 4.1 ± 0.1% suggesting that the presence of the thioether linkage results in a highly unstable metal center.

3.3.3 Activity analysis of homogenously crosslinked CDO

CDO activity has been attributed to a single isoform of the enzyme, although no studies have definitively shown which isoform represents the active enzyme. To determine if crosslinked CDO is catalytically active, samples of homogenously crosslinked CDO were assayed for activity. When homogenously crosslinked CDO was assayed, no consumption of dioxygen could be detected indicating that the protein sample was catalytically inactive. Because free cysteine and iron are both redox-active molecules that can induce protein damage, stringent controls were necessary to ensure

that the crosslinking reaction conditions or gel filtration process did not inactivate the enzyme. Control reactions were performed by incubating wild-type CDO with either L-cysteine or ferrous iron to determine the effects that these molecules had on protein stability and activity. Samples that were incubated with either L-cysteine or ferrous iron showed considerable specific activity, consuming 466 ± 130 nmol·min^{-1}·mg^{-1} and 167 ± 84 nmol·min^{-1}·mg^{-1} of oxygen, respectively compared with the specific activity of untreated wild-type (535 ± 100 nmol·min^{-1}·mg^{-1}). Analysis of the control reactions by SDS-PAGE confirmed that both isoforms were present, indicating that the non-crosslinked isoform was likely responsible for the observed activity.

To further determine if the conditions used to induce crosslink formation led to protein damage, C93S CDO was used as a catalytically competent protein that would be unable to form the crosslink under the reaction conditions used for wild-type CDO. Samples of C93S CDO were incubated with cysteine, iron, or both cysteine and iron overnight, and then assayed for activity by the same protocol described for wild-type CDO. All three reaction conditions produced protein samples that retained similar specific activities (cysteine, 109 ± 81; iron, 150 ± 29; iron and cysteine, 113 ± 30 nmol/min·mg). These combined results indicate that the crosslinking reaction conditions did not lead to the inactivation of CDO. As a final control, H86,88A CDO was used to ensure that free cysteine and iron were completely removed by gel filtration chromatography and would not interfere with activity assays. Incubation of H86,88A CDO with both crosslinking reagents failed to induce abhorrent crosslink formation (Figure 4, lane 6) and no activity was detected. These combined results suggest that the

thioether crosslink formed in wild-type CDO is not relevant to catalysis, and may actually be detrimental to the enzyme.

3.3.4 SDS-PAGE and activity analysis of CDO present in cell lysate and supernatant

Because formation of the thioether linkage leads to inactivation of the enzyme, experiments were performed to determine which isoform was the predominant enzyme under cellular conditions. In order to track the progression of crosslink formation, samples of wild-type CDO were taken throughout the expression and purification process and resolved on SDS-PAGE. Resolution of all cell lysates resulted in a single-molecular-weight species consistent with the non-crosslinked isoform (Figure 3.2 lane 2). All samples taken after the insoluble cellular components were removed resolved as the same two molecular weight species observed for the purified wild-type protein (Figure 3.2 lane 3). In order to make a comparison between the activity of purified CDO and CDO in cell lysate, specific activity measurements of the lysate were made in the absence of L-ascorbate. The specific activity of lysate containing expressed CDO was 3,700 ± 500 $nmol \cdot (min \cdot mg)^{-1}$, approximately twice the specific activity as purified CDO. Vector-only cells showed negligible activity, indicating the observed activity was due to CDO. As visualized by SDS-PAGE, CDO in cell lysate exists in the homogenously non-crosslinked isoform, suggesting that activity can be attributed solely to the non-crosslinked species (Figure 3.2 lane 2). To correlate the formation of the crosslink results in decreased activity, the specific activity of cell supernatant containing both crosslinked and non-crosslinked

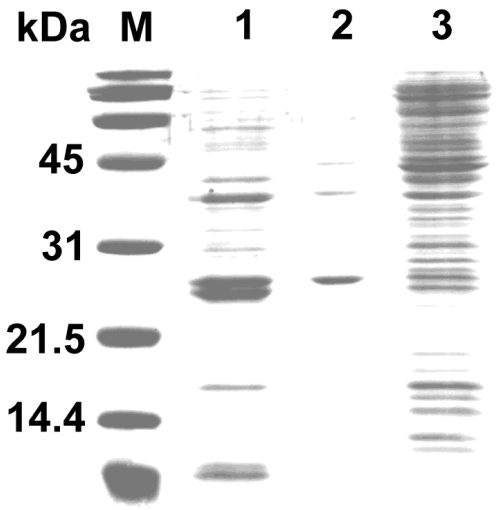

Figure 3.2 Analysis of cellular lysate and supernatant containing expressed CDO by SDS-PAGE. (*M*) Molecular weight marker, (*1*) Purified wild-type CDO, (*2*) Cell lysate containing expressed CDO, (*3*) Cell supernatant resulting from the removal of insoluble cellular components by centrifugation. Samples were resolved on a 15% acrylamide gel after boiling at 90 °C in the presence of SDS and β-mercaptoethanol.

isoforms of CDO following the removal of insoluble cellular components was assayed in the presence and absence of L-ascorbate (Figure 3.2 lane 3). L-ascorbate was used to determine if there was a specific insoluble component in cell lysate that might contribute to any decreased activity observed for CDO in cellular supernatant. The supernatant containing expressed CDO displayed approximately half the activity observed for lysate containing only non-crosslinked CDO (2,100 ± 600 nmol·(min·mg)$^{-1}$). Additionally, the lost activity could not be recovered by the addition of L-ascorbate to the assay, indicating that the loss of activity was not due to oxidation of the metal center to an inactive form.

3.3.5 Activity analysis of variant CDO proteins.

Because crosslink formation leads to inactivation of CDO, the catalytic properties of C93S and Y157F CDO were evaluated to probe how these residues contribute to the catalytic efficiency of CDO in the absence of the crosslink. Wild-type CDO consumes 1.21 moles of dioxygen per mole of cysteine sulfinic acid produced. To determine the effects of removal of the thieother linkage on the catalytic coupling of the enzyme, the specific activities of C93S and Y157F CDO proteins were determined by measuring the consumption of dioxygen and then correlating this activity with production of cysteine sulfinic acid. Interestingly, removal of the crosslink by site-directed mutagenesis resulted in nearly a one-to-one ratio of dioxygen consumption to cysteine sulfinic acid formation (1.06 and 1.07 for C93S and Y157F CDO proteins, respectively), suggesting that Cys93 and Tyr157 do not play a direct role to the catalytic mechanism of CDO.

Table 3.1 Catalytic properties for variant CDO proteins. Assays measured consumption of the dioxygen substrate by CDO (2 μM) with 10 mM L-cysteine in 25 mM HEPES, pH 7.5 and L-ascorbate (1 mM) at 37 °C. The catalytic coupling is defined as the moles of dioxygen consumed per mole of cysteine sulfinic acid produced. Product formation was detected subsequently by fluorescence labeling and HPLC analysis. Steady-state kinetic assays measured the consumption of dioxygen by CDO (2 μM) in the presence of L-ascorbate and varying concentrations of L-cysteine (50 μM – 10 mM). Apparent kinetic parameters were obtained directly from these fits and corrected parameters (in parentheses) were determined by refitting the data using the concentration of iron-bound enzyme as determined by ICP-AES. Each data point obtained is the average of three separate experiments. (ND* – No activity detected)

	k_{cat} (min^{-1})	K_m (mM)	k_{cat}/K_m ($mM^{-1} \cdot min^{-1}$)	catalytic coupling
wild-type CDO	8.48 ± 0.40	0.107 ± 0.030	88.56 ± 25 (253.8 ± 72)	1.21
C93S CDO	6.17 ± 0.15	0.068 ± 0.009	90.74 ± 12 (193.5 ± 26)	1.06
Y157F CDO	4.98 ± 0.14	0.039 ± 0.008	127.69 ± 27 (458.3 ± 95)	1.07
H86,88A CDO	ND*	ND*	ND*	ND*

To assess the catalytic efficiency of C93S and Y157F CDO enzymes, steady-state kinetic assays were performed. Steady-state kinetic parameters were determined for C93S and Y157F CDO proteins by measuring the continuous consumption of dioxygen and these results were compared with wild-type. Wild-type CDO was found to have a k_{cat} value of 9.48 ± 0.40 min^{-1} and a K_m value of 107 ± 30 μM, with a k_{cat}/K_m value of 88.6 ± 25 $mM^{-1} \cdot min^{-1}$. The k_{cat}/K_m values for both variants were comparable to wild-type before and after correcting for iron concentration, which further confirms that these residues do not play a direct role in the catalytic mechanism of CDO (Table 3.1). There was no detectable activity beyond the background rate of cysteine autooxidation for H86,88A CDO.

3.3.6 Spectroscopic analysis of variant CDO proteins and crosslinked CDO.

The location of Cys93 and Tyr157 in the active site suggests that they may be involved in maintaining the proper coordination environment of the metal center. To determine if substitution of either residue results in alteration of the metal coordination environment, EPR spectra of the resting state of C93S and Y157F CDO enzymes were obtained. Although the spectra of each variant enzyme differed in intensity proportional to the amount of iron bound, both signals were high-spin Fe^{3+} (S = 5/2) observed at g = 4.3 (Figure 3.3b and 3.3c), consistent with the spectrum observed for wild-type CDO in the resting state (Figure 3.3a). The iron coordinated by wild-type CDO has been shown to exist almost entirely in the ferric state (greater than 99% of the total bound iron). To determine what fraction of the iron bound to C93S and Y157F CDO contributed to the

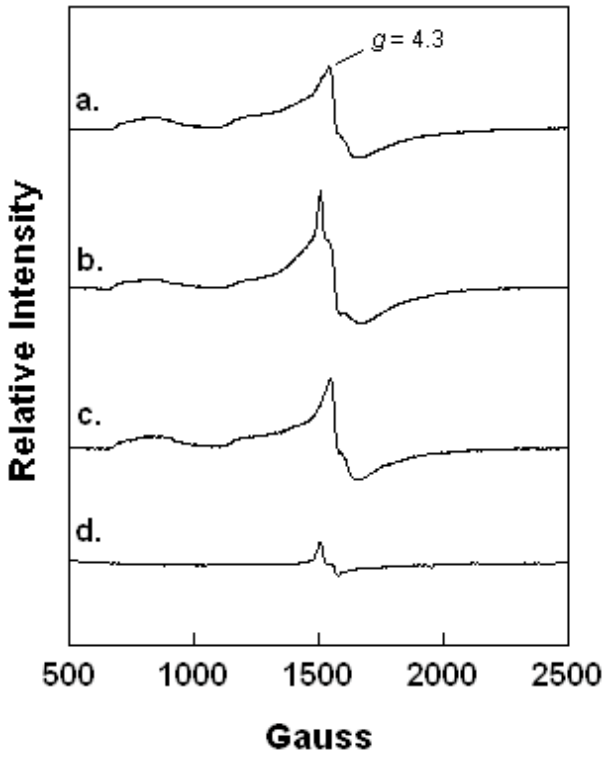

Figure 3.3 EPR spectra of variant and homogenously crosslinked CDO proteins. *(a)* EPR spectrum of wild-type CDO. *(b)* EPR spectrum of C93S CDO. *(c)* EPR spectrum of Y157F CDO. *(d)* EPR spectrum of homogenously crosslinked CDO. EPR spectra of wild-type and variant CDO proteins were obtained using approximately 100 μM protein and the spectrum of homogenously crosslinked CDO was obtained using 70 μM. All protein samples were in 25 mM HEPES buffer, pH 7.5, 100 mM sodium chloride, and 10% glycerol at 6 K. Each spectrum was obtained by averaging the signal from four accumulations.

observed ferric signal, the signal at g = 4.3 of each variant protein was integrated and quantitated using the signal of wild-type CDO as a standard. The iron bound to C93S and Y157F CDO enzymes existed almost entirely in the ferric state (greater than 98% for both enzymes). Formation of the thioether linkage has been shown to destabilize the metal center of CDO. To determine if this corresponds to an alteration in the metal coordination environment, the EPR spectrum of the resting state of homogenously crosslinked CDO was obtained. In contrast to the EPR spectra of C93S and Y157F CDO enzymes, the spectrum of homogenously crosslinked CDO deviated from that observed for wild-type CDO following purification (Figure 3.3d). This indicates that crosslink formation does alter the metal-binding environment. Integration of the signal at g = 4.3 suggests that the iron bound to homogenously crosslinked CDO also exists in the ferric state (greater than 99%).

EPR has been used to monitor the binding of L-cysteine and nitric oxide in CDO. The binding of L-cysteine to the resting form of wild-type CDO results in alteration of the coordination environment of the resting metal center, leading to a change in the ferric signal observed at g = 4.3. Consistent with the catalytic ability of C93S and Y157F CDO enyzymes, the EPR spectra of each variant enzyme incubated with L-cysteine showed a distinct signal sharpening, indicating that both variants are capable of binding the substrate (data not shown). Incubation of homogenously crosslinked CDO with L-cysteine did not alter the EPR spectra obtained for the resting enzyme, indicating either that the enzyme is incapable of coordinating L-cysteine or that gel filtration failed to remove excess L-cysteine used in the crosslinking reaction. Nitric oxide has been used as

a spectrally active yet catalytically inactive analog of dioxygen to study dioxygen binding in wild-type CDO. Complexation of nitric oxide with the iron center has been shown to result in the formation of a high spin S = 3/2 species observable at g = 4.0 (Figure 3.4a) and is dependent on both the oxidation state of the metal center and pre-complexation of the enzyme with L-cysteine (*37*). To probe the ability of each variant and homogenously crosslinked CDO to properly coordinate nitric oxide, samples were anaerobically reduced and incubated with L-cysteine prior to reaction with nitric oxide. The spectra of C93S CDO showed a distinct signal at g = 4.0 consistent with binding of nitric oxide to the metal center (Figure 3.4b). Double integration of the signal at g = 4.0 showed that each signal was proportional to the amount of iron bound by each variant. The spectrum of Y157F with L-cysteine and nitric oxide showed a decreased affinity for nitric oxide with approximately 90% less spin count per metal ion than wild-type or C93S CDO enzymes (represented by a decrease in signal intensity at g = 4.0 from 20.02 to 2.00 after correction for the iron incorporated by each sample). To determine if the altered metal binding coordination observed in the resting state spectrum for homogenously crosslinked CDO disables the enzyme from coordinating either substrate, the EPR spectrum of reduced crosslinked CDO in the presence of L-cysteine and nitric oxide was obtained. The spectrum of homogenously crosslinked CDO incubated with L-cysteine and nitric oxide showed a distinct signal at g = 4.0 (Figure 3.4d). It has been shown that the metal center of CDO is unreactive with nitric oxide prior to complexation with L-cysteine. The appearance of a signal at g = 4.0 indicates that crosslinked CDO is capable of binding both L-cysteine and nitric oxide.

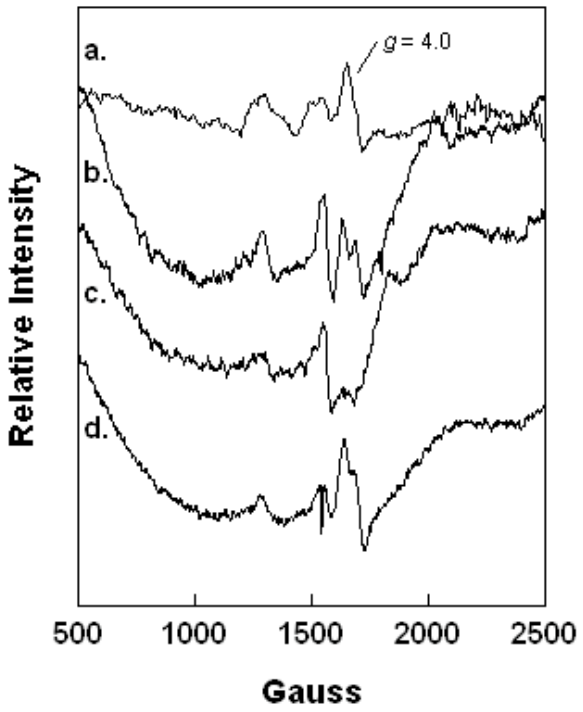

Figure 3.4 EPR spectra of variant and homogenously crosslinked CDO proteins incubated with L-cysteine and nitric oxide. *(a)* The spectrum of wild-type CDO. *(b)* The spectrum of C93S CDO. *(c)* The spectrum of Y157F CDO. *(d)* The spectrum of homogenously crosslinked CDO. All EPR spectra were obtained using approximately 80 μM protein, 6 mM L-cysteine, and 100 μM DEANO in 25 mM HEPES, pH 7.5, 100 mM sodium chloride, and 10% glycerol at 8 K.

3.4 Discussion

An active site thioether linkage analogous to the one found in CDO previously has been idendified in the copper-dependent enzyme galactose oxidase. This linkage has been shown to be necessary for catalysis through site-directed mutagenesis studies and serves to stabilize a tyrosyl radical generated during catalytic turnover (*69*). The thioether linkage in CDO has been proposed to enhance the catalytic and structural integrity of the enzyme despite reports of the catalytic competence of variant CDO enzymes incapable of forming the thioether linkage. Previously determined three-dimensional structures, kinetic parameters, and spectroscopic characteristics of CDO have utilized a mixture of the crosslinked and non-crosslinked isoforms, yet studies indicate that a single isoform is responsible for catalytic activity. CDO present in cell lysate displays considerable activity and resolves as a single isoform on SDS-PAGE consistent with the non-crosslinked species. Removal of insoluble components of the cell lysate results in conversion of approximately half the expressed protein to the crosslinked isoform and the activity of the enzyme in supernatant is approximately half that of the enzyme in cell lysate. The lost activity cannot be recovered by the addition of L-ascorbate indicating that the loss of activity is likely due to conversion of some of the enzyme to the crosslinked isoform.

To better elucidate the effects of the thioether linkage on catalysis, a method was developed to isolate the enzyme in the homogenously crosslinked isoform and the resulting protein was assayed for activity. Samples of wild-type CDO where crosslinking has been induced resolve as an approximately 23 kDa species indicating that the reaction conditions utilized yield completion of the crosslinking reaction. To ensure that crosslinking conditions do not lead to adventitious inactivation of the enzyme, a catalytically competent variant of CDO incapable of forming the covalent linkage (C93S CDO) was treated in the same manner as wild-type. The crosslinking reaction and gel filtration purification used to isolate wild-type CDO in the crosslinked isoform fail to reduce the catalytic activity of the C93S CDO; however, homogenously crosslinked CDO displays no measureable activity. This lack of activity by CDO homogenously containing the thioether linkage is consistent with the loss of activity observed for CDO in supernatant compared with CDO in cell lysate. These results also explain the apparent substrate inhibition reported for wild-type CDO when the enzyme is assayed under conditions known to rapidly induce crosslink formation (*59*). These same studies report that protein variants incapable of forming the crosslink do not display inhibition at high concentrations of L-cysteine.

CDO in cell lysate exists predominantly in the non-crosslinked isoform and has been shown to bind more iron and display considerably more activity than the purified enzyme. Purified CDO contains both crosslinked and non-crosslinked isoforms. Inactivation of oxygen-activating metalloproteins by site-specific oxidative events has been reported for several enzymes (*92-94*). To probe how the presence of the thioether

linkage in the active site causes inactivation of the CDO, wild-type CDO was isolated in the homogenously crosslinked isoform and analyzed spectroscopically. A potential role for the thioether linkage found in CDO may be targeting the enzyme for degradation. CDO is regulated through post-translational modification by the 26S ubiquitin-proteasome system (*58*). Enzymes that are targeted by the ubiquitin-proteasome system often undergo minor structural changes that signal ubiquitination. Formation of the rigid bond between Cys93 and Tyr157 may induce a conformational change in CDO and increase the susceptibility of the enzyme to ubiquitination. Interestingly, prokaryotic systems do not target proteins for protealytic degradation through the ubiquitin-proteasome system, and prokaryotic CDO replaces Cys93 with a glycine residue. Following incubation with excess L-cysteine and ferrous iron, C93S CDO has increased stability compared with wild-type CDO, indicating that formation of the crosslink decreases the structural integrity of the enzyme. The EPR spectrum of homogenously crosslinked CDO indicates that the enzyme has an altered metal coordination environment that may be induced by a minor conformational change in the active site. This altered metal binding coordination may lead to improper coordination of L-cysteine in the active site of homogenously crosslinked CDO and results in destabilization of the metal center. The inability of crosslinked CDO to tightly bind the metal cofactor partially explains the substoichiometric amount of iron bound to purified recombinant CDO.

To probe the characteristics of CDO lacking the thioether linkage, site-directed protein variants incapable of forming the crosslink were characterized catalytically and

spectroscopically. Cys93 and Tyr157 were replaced with serine and phenylalanine, respectively, in order to probe the role of the covalent linkage in cysteine oxidation. To determine if iron coordination plays a role in formation of the thioether bond, two of the three histidine metal binding ligands were replaced with alanine residues to disable the enzyme from binding iron. All variant CDO proteins yield approximately 25-kDa species when resolved on SDS-PAGE, indicating that crosslink formation is disrupted by removal of each substituted amino acid. Additionally, incubation of H86,88A CDO with excess L-cysteine and ferrous iron does not result in conversion of the enzyme to the crosslinked isoform. The facial triad composed of three histidine residues that coordinates the metal center of CDO represents a departure from what was previously thought to be a ubiquitous metal binding motif in non-heme ferrous oxygenases. The inability of H86,88A CDO to form the crosslink in the presence of free ferrous iron and L-cysteine indicates that this structural feature plays a critical role in biogenesis of the thioether linkage and suggests that crosslink formation is highly specific to the active site of eukaryotic CDO.

The Cys-Tyr crosslink in CDO is located approximately 3 Å from the iron center (*6*-*8*), and the three-dimensional structure of resting CDO indicates that the hydroxyl group of Tyr157 is involved in hydrogen bonding with a water ligand coordinated to the metal center. Alternative positioning of Tyr157 induced by rigid covalent bond formation with Cys93 may hinder the hydrogen bonding interaction of this residue with the resting-state water ligand contributing to the decreased iron incorporation observed for homogenously crosslinked CDO. Metal-binding analysis indicates that preparations

of wild-type CDO containing both isoforms incorporates only 25 – 35% iron in the active site, and greater than 99% of the bound iron is in the catalytically inactive ferric state. Removal of the tyrosine hydroxyl group by site-directed mutagenesis does not eliminate the ability of CDO to coordinate iron, although Y157F CDO has decreased affinity for the metal center compared with wild-type (7 – 27%). The depleted iron binding affinity of Y157F CDO supports the role of the hydroxyl group of this residue in metal center stabilization. The EPR spectra of C93S and Y157F CDO enzymes indicate that the iron present is in the same coordination environment as observed for wild-type CDO and the iron exists in the ferric state. Because the EPR spectra of variant CDO enzymes is consistent with that observed for wild-type and homogenously crosslinked CDO does not bind a significant amount of iron, these results suggest that the EPR spectrum of wild-type CDO is representative of the spectrum of the non-crosslinked enzyme. Incubation of C93S CDO with L-cysteine and nitric oxide results in formation of an EPR signal at g = 4.0, consistent with the signal observed for complexation of nitric oxide with the metal center of wild-type CDO, indicating that this residue is uninvolved in substrate binding. Interestingly, although Y157F CDO is capable of binding L-cysteine, little signal at g = 4.0 is produced when the enzyme is incubated with nitric oxide, suggesting that this residue may be involved in the binding of dioxygen in the active site of CDO.

The proposed catalytic mechanism of CDO is based on the mechanism of the extradiol dioxygenases (*6*). This family of enzymes uses an active-site histidine residue to stabilize the orientation of dioxygen needed for proper activation and insertion into the non-oxygen substrate. Recently, the three-dimensional structure of CDO has been

determined with L-cysteine and an analog of dioxygen (carbon monoxide) bound in the active site (*10, 16*). This structure indicates that the hydroxyl group of Tyr157 is also involved in hydrogen bonding with dioxygen in a similar manner to the histidine residues of the extradiol dioxygenases. The inability of Y157F CDO to stabilize nitric oxide in the active site suggests that the residue may fulfill the role of hydrogen bond donor during catalysis. Mutation of the histidine residues found in the active sites of the extradiol dioxygenases results in enzyme inactivation, yet Y157F CDO is reported to be catalytically competent. To determine the extent to which the tyrosine hydroxyl group in CDO participates in catalysis, steady-state kinetic parameters were determined and related to the catalytic coupling between dioxygen consumption and cysteine sulfinic acid formation by CDO. Although the measured k_{cat}/K_m value of Y157F CDO is lower than that observed for wild-type, the k_{cat}/K_m values for wild-type and Y157F CDO are proportional to the amount of iron bound by each enzyme, indicating that the lower activity is not the result of the tyrosine hydroxyl group acting in catalysis. The catalytic competence of Y157F CDO also suggests that nitric oxide may only be a suitable surrogate for studying the reactivity of dioxygen with the metal center rather than the interaction of dioxygen with active site residues. Removal of the thioether linkage by site-directed mutagenesis has a positive affect on the catalytic coupling of CDO; catalysis by C93S and Y157F CDO enzymes is nearly completely coupled (1.06 and 1.07, respectively, moles of dioxygen consumped per mole of cysteine sulfinic acid produced) in contrast to wild-type CDO which consumes 1.21 moles of dioxygen per mole of

cysteine sulfinic acid produced. The tight catalytic coupling of C93S and Y157F CDO enzymes is further evidence that neither residue plays a direct role in catalysis.

In conclusion, the presence of the thioether linkage identified in the three-dimensional structure of CDO is not necessary for catalysis and results in complete inactivation of the enzyme. This inactivation is likely the result of a minor conformational change induced from rigid covalent bond formation between Cys93 and Tyr157 in the active site that results in release of the metal center from the active site. Tyr157 does not play a direct role in catalysis and is involved only in stabilization of the metal coordination environment, while Cys93 appears to be needed for regulation of enzyme activity through crosslink formation. It has been shown that the metal center of CDO is sensitive to redox changes in the environment, and formation of the crosslink occurs primarily when the enzyme is removed from reducing cellular conditions. The inability of free ferrous iron to compensate for the lack of the 3-His facial triad in formation of the thioether linkage suggests that the crosslink in CDO may be dependent on the unusual metal coordination environment. The evolutionary implications of the redox tunable 3-His facial triad and the conservation of two residues capable of abolishing catalytic competence is confounding and may represent an additional mechanism by which the cellular flux of cysteine is regulated.

Chapter Four

Summary

Sufficient concentrations of cysteine have been shown to be paramount in mediating the redox potential of the cell in eukaryotic organisms. Not only is the primary cellular antioxidant agent (glutathione) synthesized from cysteine, but redox-sensitive thiols deriving from cysteine in proteins and transcription factors signal secondary cellular response to oxidative threats. Taurine has also been shown to be crucial in a variety of cellular processes in eukaryotic organisms, including maintaining the ionic potential of the cell membrane by controlling the concentration of sodium and calcium ions in the cell. Additionally, taurine fulfills the role of a cellular antioxidant by reacting with hypochlorous acid produced during the immune response.

The equilibrium between cellular concentrations of cysteine and taurine in eukaryotic organisms is regulated by the enzyme cysteine dioxygenase (CDO). CDO depends on the presence of a mononuclear non-heme iron center to catalyze the oxidation of L-cysteine to cysteine sulfinic acid using both atoms of molecular dioxygen. Publication of the three-dimensional structures of several mammalian CDO proteins revealed two unusual structural attributes of the enzyme that had previously not been

identified in other non-heme, ferrous-dependent enzymes. Typical non-heme mononuclear ferrous enzymes utilize a metal binding motif composed of two histidine ligands and either a glutamate or aspartate residue arranged in a facial triad (known as the 2-His/1-carboxylate facial triad). CDO was the first mononuclear ferrous iron enzyme identified to bind its metal center using a facial triad composed entirely of histidine residues. Crosslinkages formed between non-adjacent amino acids have been identified in several heme-dependent and copper-dependent enzymes. In addition to coordinating its metal center with an unusual binding motif, CDO was the first mononuclear ferrous-dependent enzyme shown to have a covalent linkage between two non-adjacent active site residues (Cys93 and Tyr157) within angstroms of the metal center. Despite the medical significance of eukaryotic CDO, little is known about how these structural features affect the catalytic efficiency of the enzyme.

4.1 Determination of appropriate assaying conditions for recombinant CDO

CDO present in lysate is reported to display considerable activity; however, early isolation of the enzyme from liver homogenate indicated that purified CDO is catalytically inactive. Further attempts at characterizing the recombinant enzyme have yielded steady-state kinetic parameters that vary by orders of magnitude. In order to accurately probe the effects of the 3-His facial triad and Cys-Tyr crosslink on catalysis, a reliable assay was needed to explore the potential inactivation of CDO occurring during purification of the enzyme as well as to understand the cause for discrepancy in the reported kinetic parameters.

Studies of recombinant CDO have utilized a variety of reaction conditions. To elucidate the source of the discrepencies in reported kinetic parameters, a method of assay was developed that measured the continuous consumption of dioxygen by CDO and this was directly correlated with end-point analysis of cysteine sulfinic acid production. All recombinant CDO enzymes have been reported to bind substoichiometric amounts of iron. To compensate for the decreased concentration of iron-bound enzyme in assays, some assays include exogenous ferrous iron. In order to determine the effect of exogenous iron on non-enzymatic product formation, exogenous ferrous iron was incubated with L-cysteine in the absence of CDO. Incubation of ferrous iron with L-cysteine consumed over 10,000 $nmol \cdot min^{-1}$ of dioxygen that corresponded to the production of 34 ± 6 $nmol \cdot min^{-1}$ of cysteine sulfinic acid. Because of the ability of exogenous ferrous iron to generate product non-enzymatically, exogenous iron was not included in subsequent assays.

Assays that do not include exogenous ferrous iron utilize extended incubation times to yield sufficient product for accurate detection. L-cysteine is unstable in buffer and oxidizes to form cystine, cysteine sulfinic acid, and cysteine sulfonic acids. Additionally, two different pH optima (6.1 and 7.5) have been reported for CDO. To probe the non-enzymatic oxidation of L-cysteine with differing buffer conditions over time, L-cysteine was incubated in a range of buffers at pH values from 6.1 to 8.5. Significant consumption of dioxygen corresponding to non-enzymatic oxidation of L-cysteine was observed with all buffers at pH values below 6.8; however, no consumption of dioxygen was observed in any buffer at pH values exceeding 6.8. These results

indicated that an optimum pH value observed for CDO at pH 6.1 is the result of increased autooxidation of L-cysteine rather than an increase in enzymatic turnover. HEPES buffer at pH 7.5 was used for all subsequent assays because this buffer and pH did not affect the non-enzymatic oxidation of L-cysteine. The removal of exogenous ferrous iron in assays and the use of a buffer and pH that do not inhibit the enzyme or produce cysteine sulfinic acid non-enzymatically yielded an accurate assay that could be used to probe the inactivation of CDO occurring during purification.

4.2 Evaluation of the stability of the iron center bound by the 3-His facial triad

Prior to determination of the three-dimensional structure of CDO, all known mononuclear ferrous enzymes had been shown to bind their metal center using two histidine residues and a carboxylate donating residue. Replacement of the carboxylate ligand with a histidine in several 2-His/1-carboxylate containing enzymes completely eliminates dioxygenase activity. Including CDO, three enzymes have been identified that bind their metal centers using a facial triad composed entirely of histidine residues. One of these enzymes (Dke1) has been studied using site-directed mutagenesis to replace a histidine metal binding ligand with a carboxylate donating ligand. Conversion of the 3-His facial triad to a 2-His/1-carboxylate facial triad resulted in an inability of the enzyme to bind iron. Both studies of 3-His and 2-His/1-carboxylate metal binding motifs imply that a difference in reactivity exists between the two facial triads that aids in the chemistry of their respective enzymes.

In many 2-His/1-carboxylate containing enzymes, the ferrous metal center is protected by the electron-donating ability of the carboxylate ligand, electron-donating

substrates, or an external source of electrons provided by a cofactor or co-substrate. Both CDO and Dke1 are involved in metabolic pathways that aid in mediating oxidative stress in their physiological environments. Studies of Dke1 show that the enzyme is inactivated under oxidative conditions. This inactivation was determined to be caused by a change in the Fe(II) center to Fe(III) followed by release of the metal center of the enzyme. The susceptibility of the metal center of Dke1 to oxidation may indicate that the 3-His facial triad is more redox-sensitive than 2-His/1-carboxylate facial triads, and this tunability may aid in the role of the enzyme in mediating oxidative conditions in the cell.

Purified recombinant CDO displays no activity beyond the background rate of L-cysteine oxidation, while cell lysate containing expressed recombinant CDO displayed considerable catalytic ability. To determine if this apparent inactivation of CDO corresponded to oxidation of the metal center, the EPR spectra of CDO in cell lysate and following purification were obtained. The spectrum of CDO in cell lysate displayed no signal at g = 4.3, indicating that the metal center of the enzyme in cellular conditions exists in the EPR-silent Fe(II) state. CDO in cell lysate was incubated with the oxidant ferricyanide, and the resulting spectrum showed a distinct signal at g = 4.3, confirming that the resting state observed for the enzyme in cell lysate is Fe(II). The spectrum of purified CDO also showed a distinct signal at g = 4.3, indicating that some of the metal center had been oxidized during removal of CDO from the cellular environment. Quantification of the signal at g = 4.3 indicates that greater than 99% of the iron in CDO exists in the inactive Fe(III) oxidation state following purification.

To correlate oxidation of the metal center with a decrease in activity, L-ascorbate was included in assays as an external reductant for the metal center. Addition of L-ascorbate increased the activity of the purified enzyme to 535 ± 100 nmol·(min·mg)$^{-1}$. When the concentration of iron-bound enzyme present in assays was accounted for, the specific activity of purified CDO was 1,900 ± 400 nmol·(min·mg)$^{-1}$, approximately half the activity of CDO present in cell lysate. This suggests that the lack of activity observed for purified CDO is not only due to oxidation of the metal center but an instability of the metal center resulting from this oxidation, and this behavior is consistent with the stability of the metal center bound by Dke1.

4.3 Analysis of non-crosslinked CDO

The amino acid crosslink found in CDO is formed from two active site residues (Cys93 and Tyr157) located within angstroms of the metal center. Tyr157 is conserved in all known CDO proteins, suggesting that this residue plays a key role in maintaining the structural or catalytic efficiency of the enzyme. Cys93 is only conserved in mammalian CDO proteins, indicating that this residue imparts an evolutionary advantage to the enzyme. The presence of the crosslink causes a shift in resolution of the enzyme on SDS-PAGE and this change in migration is characteristic of many other crosslinked enzymes. Typical purification of CDO yields both crosslinked and non-crosslinked isoforms of the enzyme as observed by SDS-PAGE. Previously, separation of the two isoforms was accomplished and the resulting species were assayed for activity. These studies reported that all activity could be attributed to a single isoform; however, no

studies have been conducted to determine which isoform represents the physiologically active enzyme.

The thioether linkage in CDO is analogous to the crosslink found in the copper-dependent enzyme galactose oxidase. Site-directed mutagenesis studies have been performed on galactose oxidase to disrupt crosslink formation and indicate that the thioether linkage is a cofactor in catalysis. To determine if the thioether linkage in CDO fulfills the same catalytic role as the crosslink in galactose oxidase, variant constructs were made to replace Cys93 and Tyr157 with serine and phenylalanine, respectively. Tyr157 has been suggested to be involved in hydrogen bonding interactions with a water ligand for the metal center in the resting-state enzyme and with dioxygen during catalytic turnover. The decreased metal-binding affinity of Y157F CDO confirms the role of this residue in metal center stabilization. Y157F CDO is capable of properly coordinating both L-cysteine, although not an analog of dioxygen, and the variant enzyme displays a catalytic efficiency comparable to wild-type CDO. This suggests that the hydroxyl group of Tyr157 does not act as a general base during catalysis. C93S CDO was also capable of binding substrates and turning over catalytically in a manner consistent with wild-type. These results suggest that non-crosslinked CDO represents the physiologically active enzyme.

4.4 Effects of crosslink formation on the metal center and activity of CDO

Variant CDO enzymes incapable of forming the crosslink display catalytic competence suggesting that crosslink formation in the active site leads to inactivation of the enzyme. To determine if crosslinked CDO is catalytically inactive, a method was

developed to isolate the enzyme in the homogenously crosslinked isoform. Crosslink formation in CDO was accomplished by incubating the enzyme with excess L-cysteine and exogenous ferrous iron followed by removal of small molecules from the sample by gel filration. Crosslinking reactions carried out at pH 7.5 were incubated overnight to ensure complete formation of the thioether linakge; however, reactions carried out at lower pH could be completed withing two hours. Completion of each reaction was verified by SDS-PAGE. Homogenously crosslinked CDO displayed no activity beyond the background rate of cysteine oxidation, confirming that crosslink formation results in inactivation of the enzyme. Spectroscopic analysis of homogenously crosslinked CDO indicates that the enzyme is capable of binding both substrates, but has a depleted affinity for iron and the iron readily diffuses out of the active site.

The effect of crosslink formation on proper coordination of the metal center in CDO may result from a conformational change. The hydroxyl group of Tyr157 has been implicated in stabilization of the metal center by hydrogen bonding with a water ligand in the resting-state enzyme. Rigid bond formation with Cys93 could prevent positioning of the tyrosine residue for optimal hydrogen bonding. Additionally, the EPR spectrum of homogenously crosslinked CDO differs from that observed for wild-type, C93S, and Y157F CDO enzymes, confirming that crosslink formation results in an altered metal coordination environment. Formation of the rigid thioether bond in the active site may also result in a conformational change that could distort the 3-His facial triad and result in release of the metal center. Cys93 is replaced with a glycine residue in yeast and prokaryotic organisms, suggesting that the ability of CDO to form the thioether linkage

imparts an evolutionary advantage. The metabolic significance of CDO suggests that inactivation of CDO by crosslink formation may work to regulate enzyme activity. CDO is known to be regulated post-translationally through ubiquitination. Attachment of ubiquitin to target molcules signals them for proteolytic degradation, and ubiquitination is often triggered by a conformational change in the target molecule. Additionally, prokaryotic organisms do not use a ubiquitin proteasome system and prokaryotic CDO replaces Cys93 with a glycine, and so cannot form the thioether linkage.

Formation of the thioether linkage in CDO depends on the presence of the substrate L-cysteine, which further suggests that crosslink formation in the active site of CDO is a highly specific process. The redox dependence of crosslink formation may be linked to the redox susceptibility of the metal center. An additional variant of CDO was made to replace two of the three histidine metal-binding ligands (His86 and His88) with alanine residues to probe the involvement of the 3-His facial triad in crosslink formation. H86,88A CDO yields a single-molecular-weight band when the enzyme is resolved on SDS-PAGE and the enzyme is incapable of stabilizing iron within the active site. This implicates proper incorporation of the active site iron in crosslink formation. To determine if the inability of H86,88A CDO to bind iron could be compensated by the addition of exogenous ferrous iron, crosslinking reactions were performed on the variant enzyme. Incubation of H86,88A CDO with excess ferrous iron and L-cysteine failed to induce crosslink formation, confirming that coordination of the metal center by the 3-His facial triad is key for the formation of the thioether linkage. The lack of crosslinked amino acids in other mononuclear ferrous enzymes indicates that the 3-His facial triad

and the Cys-Tyr crosslink may be linked physiologically. Inactivation of CDO by oxidation of the metal center and by formation of the thioether linkage in the active site provides a platform for tight regulation of the enzyme.

References

1. Giustarini, D., Dalle-Donne, I., Milzani, A., and Rossi, R. (2009) Oxidative stress induces a reversible flux of cysteine from tissues to blood *in vivo* in the rat, *FEBS Journal 276*, 4946-4958.
2. Winterbourn, C. C., and Hampton, M. B. (2008) Thiol chemistry and specificity in redox signaling, *Free Radical Biology & Medicine 45*, 549-561.
3. Schnackenberg, L. K., Chen, M., Sun, J., Holland, R. D., Dragan, Y., Tong, W., Welsh, W., and Beger, R. D. (2009) Evaluations of the trans-sulfuration pathway in multiple liver toxicity studies, *Toxicology and Applied Pharmacology 235*, 25-32.
4. Swiss Institute of Bioinformatics, www.expasy.ch
5. Que, L., and Ho, R. Y. N. (1996) Dioxygen activation by enzymes with mononuclear non-heme iron active sites, *Chem. Rev. 96*, 2607-2624.
6. McCoy, J. G., Bailey, L. J., Bitto, E., Bingman, C. A., Aceti, D. J., Fox, B. G., and Phillips, G. N. (2006) Structure and mechanism of mouse cysteine dioxygenase, *Proc. Nat. Acad. Science 103*, 3084-3089.
7. Simmons, C. R., Liu, Q., Huang, Q., Hao, Q., Begley, T. P., Karplus, P. A., and Stipanuk, M. H. (2006) Crystal structure of mammalian cysteine dioxygenase: a

novel mononuclear iron center for cysteine thiol oxidation, *J. Biol. Chem. 281*, 18723-18733.

8. Ye, S., Wu, X., Wei, L., Tang, D., Sun, P., Bartlam, M., and Rao, Z. (2007) An insight into the mechanism of human cysteine dioxygenase: key roles of the thioether-bonded tyrosine-cysteine cofactor, *J. Biol. Chem. 282*, 3391-3402.

9. Arciero, D. M., Lipscomb, J. D., Huynh, B. H., Kent. T. A., and Munck, E. (1983) EPR and Mossbauer studies of protocatechuate 4,5-dioxygenase. Characterization of a new Fe^{2+} environment, *J. Biol. Chem. 258*, 14981-14991.

10. Solomon, E. I., Decker, A., and Lehnert, N. (2003) Non-heme iron enzymes: contrasts to heme catalysis, *Proc. Natl. Acad. Sci. USA 100*, 3589-3594.

11. Sunderson, W. A., Zatsman, A. I., Emerson, J. P., Farquhar, E. R., Que, L. Jr., Lipscomb, J. D., and Hendrich, M. P. (2008) Electron paramagnetic resonance detection of intermediates in the enzymatic cycle of an extradiol dioxygenase, *J. Am. Chem. Soc. 130*, 14465-14467.

12. Costas, M., Mehn, M. P., Jensen, M. P., and Que, L. J. (2004) Dioxygen activation at mononuclear nonheme iron active sites: enzymes, models, and intermediates, *Chem. Rev. 104*, 939-986.

13. Kovaleva, E. G., and Lipscomb, J. D. (2008) Versatility of biological non-heme Fe(II) centers in oxygen activation reactions, *Nat. Chem. Biol. 4*, 186-193.

14. Zhang, Z., Barlo, N. N., Baldwin, J. E., and Schofield, C. J. (1997) Metal-catalyzed oxidation and mutagenesis studies on the iron(II) binding site of 1-aminocyclopropane-1-carboxylate oxidase, *Biochemistry 36*, 15999-16007.

15. Thrower, J., Mirica, L. M., McCusker, K. P., and Klinman, J. P. (2006) Mechanistic investigations of 1-aminocyclopropane-1-carboxylic acid oxidase with alternate cyclic and acyclic substrates, *Biochemistry 45*, 13108-13117.

16. Kreisberg-Zakarin, R., Borovok, I., Yanko, M., Aharonowitz, Y., and Cohen, G. (1999) Recent advances in the structure and function of isopenicillin N synthase, *Anotnie van Leeuwenhoek 75*, 33-39.

17. Fitzpatrick, P. F. (1999) Tetrahydropterin-dependend amino acid hydroxylases, *Annu. Rev. Biochem. 68*, 355-381.

18. Orville, A. M., and Lipscomb, J. D. (1993) Simultaneous binding of nitric oxide and isotopically labeled substrates or inhibitors by reduced protocatechuate 3,4-dioxygenase, *J. Biol. Chem. 268*, 8596-8607.

19. Kovaleva, E. G., Neibergall, M. B., Chakrabarty S., and Lipscomb, J. D. (2007) Finding intermediates in the O_2 activation pathways of non-heme iron oxygenases, *Acc. Chem. Res. 40*, 475-483.

20. Lipscomb, J. D. (2008) Mechanism of extradiol aromatic ring-cleaving dioxygenases, *Curr. Opin. Struct. Biol. 18*, 644-649.

21. Brosnan, J. T., and Brosnan, M. E. (2006) The sulfur-containing amino acids: and overview, *J. of Nutr. 5*, 1636-1640.

22. Singh, S., Padovani, D., Leslie, R. A., Chiku, T., and Banerjee, R. (2009) Relative contributions of cystathionine beta-synthase and gamma-cystathionase to H_2S biogenesis *via* alternative trans-sulfuration reactions, *J. Biol. Chem. 284*, 22457-22466.

23. Roche Applied Sciences “Biochemical Pathways”, ExPASy proteomics server, www.expasy.ch

24. D’Autreaux, B., and Toledano, M. B. (2007) ROS as signaling molecules: mechanisms that generate specificity in ROS homeostasis, *Nat. Rev. Mol. Cell. Biol. 8*, 813-824.

25. Kalinina, E. V., Chernov, N. N., and Saprin, A. N. (2008) Involvement of thio-, peroxi-, and glutaredoxins in cellular redox-dependent processes, *Biochemistry (Moscow) 73*, 1493-1510.

26. Kearney, E. B., and Kenney, W. C. (1974) Covalently bound flavin coenzymes, *Horizons Biochem. Biophys. 1*, 62-98.

27. Norberg, J., and Arner, E. S. J. (2001) *Free Radic. Biol. Med. 31*, 1287-1312.

28. Powis, G., and Montfort, W. R. (2001) Properties and biological activities of thioredoxins, *Annu. Rev. Pharmacol. Toxicol. 41*, 261-295.

29. Zhong, L., Arner, E. S. J., and Holmgren, A. (2000) Essential role of selenium in the catalytic activities of mammalian thioredoxin reductase revealed by characterization of recombinant enzymes with selenocysteine mutations, *Proc. Natl. Acad. Sci. USA 97*, 5854-5859.

30. Arscott, L. D., Gromer, S., Schirmer, R. H., Becker, K., and Williams, C. H. (1992) *Proc. Natl. Acad. Sci. USA 94*, 3621-3626.

31. Williams, C. H. (1992) *Chemistry and Biochemistry of Flavoensymes 3*, 121-211.

32. Menshchikova, E. B., Lankin, V. Z., Zenkov, N. K., Bondar, I. A., Krugovykh, N. F., and Trufakin, V. A. (2006) *Oxidative Stress. Prooxidants and Antioxidants*

33. May, J. M., Mendiratta, S., Hill, K. E., and Burk, R. F. (1997) Reduction of dehydroascorbate to ascorbate by the selenoenzyme thioredoxin reductase, *J. Biol. Chem. 272*, 22607-22610.

34. Fernandes, A. P., and Holmgren, A. (2004) Glutaredoxins: glutathione-dependent redox enzymes with functions far beyond a simple thioredoxin backup system, *Antioxid. Redox Rignal. 6*, 63-74.

35. Daily, D. Vlamis-Gardikas, A., Offen, D., Mittelmann, L., Melamed, E., Holmgren, A., and Barzilai, A. (2001) Glutaredoxin protects cerebellar granule neurons from dopamine-induced apoptosis by dual activation of the ras-phophoinositide 3-kinase and jun n-terminal kinase pathways, *J. Biol. Chem. 276*, 21628-21626.

36. Klatt, P. Pineda-Molina, E., DeLacoba, M. G., Padilla, A. C., Martinez-Galisteo, E. Barzena, J. A., and Lamas, S. (1999) Redox regulation of C-Jun DNA binding by reversible S-glutathiolation, *FASEB J. 13*, 1481-1490.

37. Hall, A., Karplus, P. A., and Poole, L. B. (2009) Typical 2-Cys peroxiredoxins: structures, mechanisms, and functions, *FEBS Journal 276*, 2469-2477.

38. Stipanuk, M. H., Dominey, J. E., Lee, J.-I., and Coloso, R. M. (2006) Mammalian cysteine metabolism: new insights into regulation of cysteine metabolism, *J. Nutr. 136*, 1652-1659.

39. Redmond, H. P., Stapleton, P. P., Neary, P., and Bouchier-Hayes, D. (1998) Immunonutrition: the role of taurine, *Nutrition 14*, 599-604.

40. Schuller-Levis, G. B, and Park, E. (2003) Taurine: new implcations for an old amino acid, *FEMS Micr. Biol. Lett. 226*, 195-202.

41. Han, X., Patters, A. B., Jones, D. P., Zelikovic, I., and Chesney, R. W. (2006) The taurine transporter: mechanisms of regulation, *Acta Physiol. 187*, 61-73.

42. Mann, K., Kiefer, F., Spanagel, R, and Littleton, J. (2008) Acamprosate: recent findings and future research directions, *Alcohol Clin. Exp. Res. 32*, 1105-1110.

43. Schuller-Levis, G. B., and Park, E. (2004) Taurine and its chloramine: modulators of immunity, *Neurochem. Res. 29*, 117-126.

44. Sorbo, B., and Ewetz L. (1965) The enzymatic oxidation of cysteine to cysteine sulfinate in rat liver, *Biochem. Biophys. Res. Commun. 3*, 359-363.

45. Lombardini, J. B., and Singer, T. P. (1969) Cysteine oxygenase. II. Studies on the mechanism of the reaction with ^{18}oxygen, *J. Biol. Chem. 225*, 1172-1175.

46. Stipanuk, M. H. (1986) Metabolism of sulfur-containing amino acids, *Annu. Rev. Nutr. 6*, 179-209.

47. Hirschberger, L. L., Daval, S., Stover, P. J., and Stipanuk, M. H. (2001) Murine cysteine diosygenase gene: structural organization, tissue-specific expression and promoter identification, *Gene 277*, 153-161.

48. Yamaguchi K., Hosokawa Y., Kohashi N., Kori Y., Sakakibara S., and Ueda I. (1978) Rat liver cysteine dioxygenase (cysteine oxidase), *J. Biochem. 83*, 479-491.

49. Parsons, R. B., Ramsden, D. B., Waring, R. H., Barber, P. C., and Williams, A. C. (1998) Hepatic localization of rat cysteine dioxygenase, *J. Hepatology 29*, 595-602.

50. Stipanuk, M. H., Londono, M., Hirschberger, L. L., Hickey, C., Thiel, D. J., and Wang, L. (2004) Evidence for expression of a single distinct form of mammalian cysteine dioxygenase, *Amino Acids 26*, 99-106.

51. Chai, S. C., Jerkins, A. A., Banik, J. J., Shalev, I., Pinkham, J. L., Uden, P. C., and Maroney, M. J. (2005) Heterologous expression, purification, and characterization of recombinant rat cysteine dioxygenase, *J. Biol. Chem. 280*, 9865-9869.

52. Simmons, C. R., Hirschberger, L. L., Machi, M. S., and Stipanuk, M. H. (2006) Expression, purification, and kinetic characterization of recombinant rat cysteine dioxygenase, a non-heme metalloenzyme necessary for regulation of cellular cysteine levels, *Protein Expr. Purif. 47*, 74-81.

53. Chai, S. C., Bruyere, J. R., and Maroney, M. J. (2006) Probes of the catalytic site of cysteine dioxygenase, *J. Biol. Chem. 281*, 15774-15779.

54. Pierce, B. S., Gardner, J. D., Bailey, L. J., Brunold, T. C., and Fox, B. G. (2007) Characterization of the nitrosyl adduct of substrate-bound mouse cysteine dioxygenase by electron paramagnetic resonance: electronic structure of the active site and mechanistic implications, *Biochemistry 46*, 8569-8578.

55. Bagley, P. J., Hirschberger, L. L., and Stipanuk, M. H. (1995) Evaluation and modification of an assay procedure for cysteine dioxygenase activity: high-

performance liquid chromatography method for measurement of cysteine sulfinate and demonstration of physiological relevance of cysteine dioxygenase activity in cysteine catabolism, *Anal. Biochem. 227*, 40-48.

56. Simmons, C. R., Krishnamoorthy, K., Grannett, P. L., Schuller, D. J., Dominey, J. E., Begley, T. P., Stipanuk, M. H., and Karplus, P. A. (2008) Putative Fe^{2+}-bound persulfenate intermediate in cysteine dioxygenase, *Biochemistry 47*, 11390-11392.

57. Lee, J. I., Londono, M., Hirschberger, L. L., and Stipanuk, M. H. (2004) Regulation of cysteine dioxygenase and gamma-glutamylcysteine synthetase is associated with hepatic cysteine level, *J. Nutr. Biochem. 15*, 112-122.

58. Dominy, J. E., Hirschberger, L. L., Coloso, R. M., and Stipanuk, M. H. (2006) *In vivo* regulation of cysteine dioxygenase *via* the ubiquitin-26S proteasome system, *Adv. Exp. Med. Biol. 583*, 37-47.

59. Dominy, J. E., Hwang, J., Guo, S., Hirschberger, L. L., Zhang, S., and Stipanuk, M. H. (2008) Synthesis of amino acid cofactor in cysteine dioxygenase is regulated by substrate and represents a novel post-translational regulation of activity, *J. Biol. Chem. 18*, 12188-12201.

60. Robbins, S. P., (2007) Biochemistry and functional significance of collagen cross-linking, *Biochem. Soc. Trans. 35*, 849-852.

61. Smulevich, G., Jakopitsch, C., Droghetti, E., and Obinger, C. (2006) Probing the structure and bifunctionality of catalase-peroxidase (KatG), *J. Inorg. Biochem. 100*, 568-585.

62. Jakopitsch, C., Ivancich, A., Schmuckenschlager, F., Wanasinghe, A., Poltl, G., Furtmuller, P. G., Ruker, F., and Obinger, C. (2004) Influence of the unusual covalent adduct on the kinetics and formation of radical intermediates in Synechocystic catalase peroxidase, *J. Biol. Chem. 279*, 46082-46095.

63. Ghiladi, R. A., Medzihradszky, K. F., and Ortiz de Montellano, P. R. (2005) Role of the Met-Tyr-Trp cross-link in *Mycobacterium tuberculosis* catalase-peroxidase (KatG) as revealed by KatG(M255I), *Biochemistry 44*, 15093-15105.

64. Ghiladi, R. A., Knudsen, G. M., Medzihradszky, K. R., and Ortiz de Montellano, P. R. (2005) The Met-Tyr-Trp cross-link in *Mycobacterium tuberculosis* catalase-peroxidase (KatG), *J. Biol. Chem. 280*, 22651-22663.

65. Klinman, J. P. (2003) The multi-functional topa-quinone copper amine oxidases, *Biochim. Biophys. Acta 1647*, 131-137.

66. Bollinger, J. A., Brown, D. E., and Dooley, D. M. (2005) The formation of lysine tyrosylquinone (LTQ) is a self-processing reaction: expression and characterization of a *Drosophila* lysyl oxidase, *Biochemistry 44*, 11708-11714.

67. Klinman, J. P., (1996) New quinocofactors in eukaryotes, *J. Biol. Chem. 271*, 27189-27192.

68. Samuels, N. M., and Klinman, J. P. (2006) Investigation of Cu(I)-dependent 2,4,5-trihydroxyphenylalanine quinone biogenesis in *Hansenula polymorpha* amine oxidase, *J. Biol. Chem. 281*, 21114-21118.

69. Baron, A. J., Stevens, C., Wilmot, C., Seneviratne, K. D., Blakeley, V., Dooley, D. M., Phillips, S. E. V., Knowles, P. T., and McPherson, M. J. (1994) Structure

and mechanism of galactose oxidase: the free radical site, *J. Biol. Chem. 269*, 25095-25105.

70. Whittaker, J. W. (2003) Free radical catalysis by galactose oxidase, *Chem. Rev. 103*, 2347-2363.

71. Whittaker, M. M., and Whittaker, J. W. (2003) Cu(I)-dependent biogenesis of the galactose oxidase redox cofactor, *J. Biol. Chem. 278*, 22090-22101.

72. Firbank, S. J., Rogers, M., Hurtado-Guerrero, R., Dooley, D. M., Halcrow, M. A., Phillips, S. E. V., Knowles, P. F., and McPherson, M. J. (2003) Cofactor processing in galactose oxidase, *Biochem. Soc. Trans. 31*, 506-509.

73. Stipanuk, M. H. (1986) Metabolism of sulfur-containing amino acids, *Annu. Rev. Nutr. 6*, 179-209.

74. Straganz, G. D., and Nidetzky, B. (2008) Structural and functional comparison o 2-His-1-carboxylate and 3-His metallocenter in non-heme iron(III)-dependent enzymes, *Biochem. Soc. Trans. 36*, 1180-1186.

75. Leitgeb, S., Straganz, G. D., and Nidetzky, B. (2009) Biochemical characterization and mutational analysis of the mononuclear non-heme Fe^{2+} site in Dke1, a cupin-type dioxygenase from *Acinetobacter johnsonii, Biochem. J. 418*, 403-411.

76. Gryska, P. K., Muller, T. A., Campbell, M. G., and Hausinger, R. P. (2007) Metal ligand substitution and evidence for quinone formation in taurine/alpha-ketoglutarate dioxygenase, *J. Inorg. Biochem. 101*, 797-808.

77. Kreisburg-Zakarin, R., Borovok, I., Yanko, M., Frolow, F., Aharonowitz, Y., and Cohen, G. (2000) Structure-function studies of the non-heme iron active site of isopenicillin N synthase: some implications for catalysis, *Biophys. Chem. 86*, 109-118.

78. Shaw, J. F., Chou, Y. S., Chang, R. C., and Yang, S. F. (1996) Characterization of the ferrous ion binding sites of apple 1-aminocyclopropane-1-carboxylate oxidase by site-directed mutagenesis, *Biophys. Res. Commun. 225*, 697-700.

79. Bantan-Polak, T., Kassai, M., and Grant, K. B. (2001) A comparison of fluorescamine and naphthalene-2,3-dicarboxaldehyde fluorogenic reagents for microplate-based detection of amino acids, *Anal. Biochem. 297*, 128-136.

80. Gasteiger E., Hoogland, C. Gattiker, A., Duvaud, S., Wilkins, M. R., Appel, R. D., and Bairoch, A. (2005) The Proteomics Protocols Handbook, Humana Press, 571-607.

81. Hillas, P. J., and Fitzpatrick, P. F. (1996) A mechanism for hydroxylation by tyrosine hydroxylase based on partitioning of substituted phenylalanines, *Biochemistry 35*, 6969-6975.

82. Keefer, L. K., Nims, R. W., Davies, K. M., and Wink, D. A. (1996) "NONOates" (1-substituted diazen-1-ium-1,2diolates) as nitric oxide donors: convenient nitric oxide dosage forms, *Methods Enzymol. 268*, 281-293.

83. Wang, X., and Stanbury, D. M. (2008) Direct oxidation of L-cysteine by $[FeIII(bpy)_2(CN)_2]^+$ and $[FeIII(bpy)(CN)_4]^{-1}$, *Inorg. Chem. 47*, 1224-1236.

84. Russell, W. R., Scobbie, L., Duthie, G. G., and Chesson, A. (2008) Inhibition of 15-lipoxygenase-catalysed oxygenastion of arachidonic acid by substituted benzoic acids, *Bioorg. Med. Chem. 16*, 4589-4593.

85. Dubus, A., Sami, M., Brown, T. J. N., Schofield, C. J., Baldwin, J. E., and Frere, J. (2000) Studies of isopenicillin N synthase enzymatic properties using a continuous spectrophotometric assay, *FEBS Lett. 485*, 142-146.

86. Straganz, G. D., and Nidetzky, B. (2005) Reaction coordinate analysis for beta-diketone cleavage by the non-heme Fe^{2+}-dependent dioxygenase Dke1, *J. Am. Chem. Soc. 127*, 12306-12314.

87. Helling, S., Vogt, S., Rhiel, A., Ramzan, R., Wen, L., Marcus, K., and Kadenback, B. (2008) Phosphorylation and kinetics of mammalian cytochrome c oxidase, *Mol. Cell Proteomics 7*, 1714-1724.

88. Solomon, E. I., Decker, A., and Lehnert, N. (2003) Non-heme iron enzymes: contrasts to heme catalysis, *Proc. Natl. Acad. Sci. U. S. A. 100*, 3589-3594.

89. Arciero, D. M., Lipscomb, J. D., Huynh, B. H., Kent, T. A., and Munck, E. (1983) EPR and Mossbauer studies of protocatechuate 4,5-dioxygenase: characterization of a new Fe^{2+} environment, *J. Biol. Chem. 258*, 14981-14991.

90. Boese, M., Mordvintec, P. I., Vanin, A. F., Busse, R., and Mulsch, A. (1995) *S*-nitrosation of serum albumin by dinitrosyl-iron complex, *J. Biol. Chem. 270*, 29244-29249.

91. Dominy, J. E., Simmons, C. R., Karplus, P. A., Gehring, A. M., and Stipanuk, M. H. (2006) Identification and characterization of bacterial cysteine dioxygenases: a new route of cysteine degradation for eubacteria, *J. Bacteriol. 188*, 5561-5569.

92. Levine, R. L., Oliver, C. N., Fulks, R. M., and Stadtman, E. R. (1981) Turnover o bacterial glutamine synthetase: oxidative inactivation precedes proteolysis, *Proc. Natl. Acad. Sci. U. S. A. 78,* 2120-2124.

93. Zhang, Z., Barlow, J. N., Baldwin, J. E., and Schofield, C. J. (1997) Metal-catalyzed oxidation and mutagenesis studies on the iron(II) binding site of 1-aminocyclopropane-1-carboxylate oxidase, *Biochemistry 36*, 15999-16007.

94. Grune, T., Merker, K., Sandig, G., and Davies, K. J. A. (2003) Selective degradation of oxidatively modified protein substrates by the proteasome, *Biochem. Biophys. Res. Commun. 305*, 709-718.